Acta Universitatis Sapientiae

Informatica

Volume 14, Number 1, 2022

Sapientia Hungarian University of Transylvania
Scientia Publishing House

Acta Universitatis Sapientiae, Informatica
is covered by the following services:

DOAJ (Directory of Open Access Journals)
EBSCO (relevant databases)
EBSCO Discovery Service
io-port.net
Japan Science and Technology Agency (JST)
Micosoft Academic
Ulrich's Periodicals Directory/ulrichsweb
Web of Science – Emerging Sources Citation Index
Zentralblatt für Mathematik

Contents

Acta Univ. Sapientiae Informatica **14,** 1 (2022) 1–21

DOI: 10.2478/ausi-2022-0001

Using the Bag-of-Audio-Words approach for emotion recognition

Mercedes VETRÁB
University of Szeged, Institute of Informatics
Hungary, Szeged, Árpád tér 2.
ELKH-SZTE Research Group on Artificial Intelligence
Hungary, Szeged, Tisza Lajos körút 103.
orcid=0000-0001-7511-2910
email: vetrabm@inf.u-szeged.hu

Gábor GOSZTOLYA
University of Szeged, Institute of Informatics
Hungary, Szeged, Árpád tér 2.
ELKH-SZTE Research Group on Artificial Intelligence
Hungary, Szeged, Tisza Lajos körút 103.
orcid=0000-0002-2864-6466
email: ggabor@inf.u-szeged.hu

Abstract. The problem of varying length recordings is a well-known issue in paralinguistics. We investigated how to resolve this problem using the bag-of-audio-words feature extraction approach. The steps of this technique involve preprocessing, clustering, quantization and normalization. The bag-of-audio-words technique is competitive in the area of speech emotion recognition, but the method has several parameters that need to be precisely tuned for good efficiency. The main aim of our study was to analyse the effectiveness of bag-of-audio-words method and try to find the best parameter values for emotion recognition. We optimized the parameters one-by-one, but built on the results of each other. We performed the feature extraction, using openSMILE. Next we transformed our features into same-sized vectors with openXBOW, and finally trained and evaluated SVM models with 10-fold-crossvalidation and UAR. In our experiments, we worked with a Hungarian emotion database. According to our results, the emotion classification performance improves with the bag-of-audio-words feature representation. Not all the BoAW parameters have the optimal settings but later we can make clear recommendations on how to set bag-of-audio-words parameters for emotion detection tasks.

Computing Classification System 1998: H.3.1, I.2.7.
Mathematics Subject Classification 2010: 68R15
Key words and phrases: bag-of-audio-words, emotion detection, human voice, sound processing

1 Introduction

Human speech is not only used for encoding the words uttered, but it also contains other information about the speakers. For example, about their physical and mental state. These include the emotional state, signs of illness, depression, joy and so on. This extra information can be used in various ways by computer science and engineering information technology. Nowadays emotion detection from audio data (speech emotion recognition or SER) is an active area of research with a wide range of possible applications. It can be used in the human-computer interfaces, like that for monitoring human communication [12] and detecting the gender of the speaker, or their emotional state, or how confident they are. We can also use paralinguistics in dialogue systems [3] where we can detect the problematic dialogue phrases or adapt the dialogue to help the speaker. Besides this, it may be useful in healthcare systems [10, 26] to monitor the patient's mental state. Last, but not least we can utilize emotion detection in call centres [26]. For instance if the client get angry, we can automatically inform a boss about this. Using machines for emotion recognition and monitoring systems is a currently evolving area. In the future with good emotion recognition systems, we will be able to create more human-oriented and friendlier systems. For example we can create intelligent tutorial systems that can adapt to the student's mental state and give them more constructive advice. In addition, we can use it for lie detection to improve law enforcement. Emotion detection is also useful in a call centre or a banking software monitoring application, where we can monitor how patient members of the staff are. Furthermore we can also use it for the support diagnostics of therapists, create more empathic healthcare robots, and in computer games use it to set the difficulty of the game by the emotion of the user [13]. There are other interesting applications in paralinguistics. Human computer interfaces and user adaptation systems could be used to recognizing the age and the gender of the speaker from their voice. For instance here are some electronic systems that can use these human features: an automatic dialogue system can adapt to the speaker by speaking slower and louder for an older user or use a different corpus for younger and older customers; an interactive voice response system can choose the background music by guessing the age and the gender of the user; smart home systems can adapt to the age of the speaker because an older customer needs more automation while a younger customer need a more collaborative system; a police call analysis system can identify the age and the gender of a suspect from a telephone call [17].

Since the beginning of research in this area, many feature extraction and classification techniques have been used along with different datasets to get the best results. The variable length of recordings has always been a big problem here. This is due to the fact that our recordings have different lengths, but our classifiers expect a fixed length input. So one of the most difficult problems in speech emotion recognition and in other paralinguistics areas is feature extraction, because as we mentioned our recordings are different in length, but the classification techniques requires fixed-sized feature vectors. Several methods have already been developed to tackle the problem of varying length and to make the features extracted from the recordings the same length. For example x-vectors [18], i-vectors [27], Fisher vectors [8], neural networks [9] and the Bag-of-Audio-Words (i.e: BoAW [15]) approach that we investigate here. Our experiments were performed on a Hungarian database and our final results indicated that the BoAW technique can be used effectively. However, we should also add that creating any BoAW feature representation is sensitive to the parameter settings and working with bigger codebooks for better classification result requires more CPU time.

Our baseline comes from a Hungarian emotion speech database. Previous studies (i.e.: [25], [23], [8]) using this database produced accuracy scores of 66–70%. Previous results in speech emotion recognition with another databases are came between 60–80% [24, 11, 20]. Our results give us an unweighted average recall (UAR) score of 66–71%.

2 Bag-of-audio-words method

Using the bag-of-audio-words feature representation, we can overcome the above-mentioned problem of varying length. This feature extraction method is similar to the bag-of-visual-words [5] and the bag-of-words [28] techniques, which are used in image and speech preprocessing. Now we will present the BoAW workflow.

BoAW first performs an analysis on the entire audio database and then, based on the results obtained, generates statistics for each file separately that represent their relationship to the entire database. Figure 1 shows the general workflow for generating a BoAW representation from a dataset. The two columns belong to the training and the test set extraction steps. As we can see, the extraction of the test set depends on the train set extraction workflow, but it mostly contains the same steps, so let us discuss the training set.

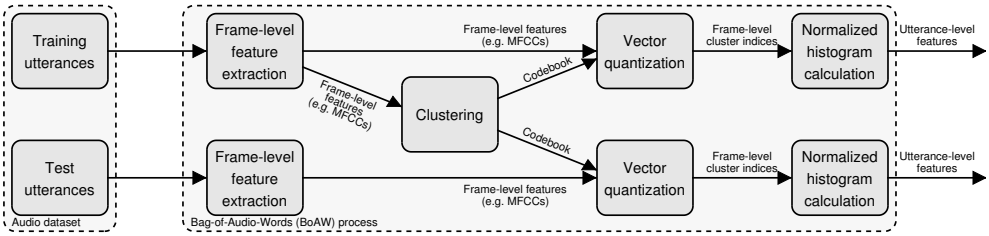

Figure 1: Workflow for the bag-of-audio-words technique.

In the first step, we have to extract the frame-level feature vectors per recording. In this step we get a different number of feature vectors for each recording, because the number of vectors depends on the original length of the evaluated recording and the frame's windowing size. In the next step, we work with all the feature vectors from all the recordings, collect them into one big "bag" and perform clustering on it. The purpose of this is to break down the vectors of the "bag" into meaningful subsets such that vectors in the same groups are more similar to other vectors in the same group than those in other groups. The number of clusters to be produced is determined by us. This cluster size parameter N is one of the parameters of the BoAW method. The centres of the created clusters will be called "codewords". The group of these "codewords" will be the "codebook". The N parameter is called the codebook size. The vector dimension of the classification will depend on the codebook size.

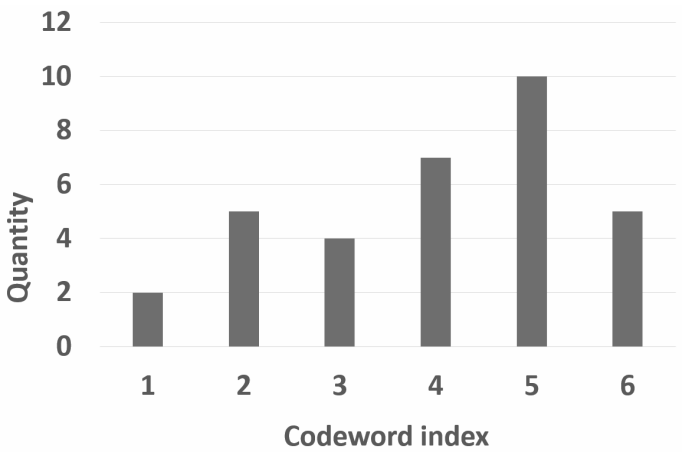

Figure 2: A bag-of-audio-words histogram of the recording.

After the clustering process, in the vector quantization step, we again work with individual recordings and create a histogram for each recording. We replace the original feature vectors by the index of the closest codeword. We then find the nearest neighbours using the minimum Euclidean distance. We can also specify how many closest vectors we are looking for (this is also a parameter of the BoAW method). So this produced, same-sized (i.e. N) histograms for each recording. The x-axis of the histogram lists the index of each codeword, and the y-axis shows quantities which represent how many of the feature vectors of the recording were mapped into a particular codeword. After quantization, each file's feature becomes independent of the length of the particular audio recording. For example, Figure 2 shows a histogram for one recording. In this case the codewords are represented by their indices (i.e. $1, 2, 3$ and so on). This recording has 43 frames, and every frame gets mapped into 1 codeword.

In the last step, we normalize the histogram, so the given frequencies are divided by the number of frames of the speech recording. We notice that each histogram can be represented by a codebook-sized vector. These histograms will be our new feature vectors that have an independent length from the recording sizes. We will call this set of histograms "Bag-of-Audio-Words" and use it as features for our classifier.

Figure 1 shows how the clustering step can be omitted for the test set. This can be done because the openXBOW software allows us to save two important things: the parameter settings applied to the training set and the computed codebook. Then we use these later in the test set, so that the quantization step can be performed on the cluster centres generated during the training set recordings without re-clustering. This operation is easy to implement, since the test file has frame-level feature vectors. They are the same as those produced with a set of features like the vectors of the training set, so we can classify them into each cluster based on their distance from the previously defined codewords.

2.1 Parameters of the BoAW method

The BoAW method has many adjustable parameters that can influence the process of codebook creation. In our study, we tested the effect of the preprocessing method, clustering method, the codebook size N, and the quantization neighbour number parameters on the learning algorithm performance. For the codebook building, we used an open-source program called openXBOW [21].

Preprocessing techniques: with openXBOW we can do some preprocessing for the frame level descriptors, before the clustering step. If some of the features have extremely high or low values compared to the others, they may dominate the Euclidean distance during the BoAW vector quantization step. We tested to see how preprocessing improves the performance, so we tried out three different solutions for it. The first one was without any preprocessing, the second one was normalizing the feature vectors and the third one was by standardizing the vectors before clustering.

Clustering method: One important factor is the clustering procedure used to create the codebook. Pancoast and Akbacak used k-means in their original study [16]; however, due to the large number of frames to be clustered, the runtime of this approach is very high. Rawat et al offer simple random sampling [19]; its runtime is marginally better than the k-means, and it does not really affect the performance. Later, Arthur et al. applied k-means++ clustering [1], a cluster center initialization procedure, which was used instead of completely random sampling, hence the distribution of cluster centers became more balanced. Compared to k-means, cluster centers are not selected at random during initialization, but selected via a uniform distribution. We tested the effect of applying the k-means and k-means++ methods on our data.

Histogram neighbour number: Instead of looking for just the closest codeword, each vector may also be assigned to a certain number of the closest codewords. Pancoast and Akbacak assume that instead of just using the closest cluster to each frame, we can assign a set of closest neighbours [16]. This leads to a more precise description of the recordings with the same feature vector size. This is why we experimented with two different settings (5 and 10).

Codebook size: As we said earlier, we can control how many clusters we wish to create, and how long we want the feature vectors to be. In each experiment we tested the effect of the following lengths: 32, 64, 128, 256, 512, 1 024, 2 048, 4 096, 8 192.

Derivatives: In speech processing, it is common practice to subtract the first and second derivatives of the feature vectors extracted from the sound recordings. These are the so-called deltas and delta-deltas, from which the dynamics of speech can be deduced [6]. With the help of the openXBOW program, we can create separate codebooks for the original low-level descriptors and another for the Δs.

3 Data and methods

Next, we will present our experimental setup and environment: the database, the classification method and its parameters, the evaluation metric, and the feature set we used.

3.1 Hungarian emotion database

In each experiment, we created and evaluated our classification model on the Hungarian emotion database. It contains utterances of 97 native Hungarian and Hungarian-speaking speakers [25]. The voice samples were recorded during television shows. The vast majority of segments were recorded from an emotion-rich, continuous, spontaneous programme with actors. The other part came from an improvisation entertainment show. In the first case due to the acting performance, the samples are vivid, and the emotions are clearer. The samples from the second case due to the improvisation, are closer to real-life emotions. The database contains 1111 sentences, which were separated into an 831 sample training set and a 280 sample test set. We had to detect four emotions, namely neutral, joy, anger, sad. The distribution of the emotions however was not uniform. The training set sample distribution was: $\approx$ 57% neutral, $\approx$ 6% sad, $\approx$ 9% joy and $\approx$ 27% anger. The test set sample distribution was: $\approx$ 62% neutral, $\approx$ 4% sad $\approx$ 7% joy and $\approx$ 27% anger. The training set contains approximately 20 minutes of recordings and the test set contains approximately 7 minutes of recordings. The sampling frequency of the samples is 16 kHz. Earlier studies working with the same database were able to achieve a classification accuracy score of 66–70% [23, 25, 8].

3.2 Feature set

The feature set employed in the study came from the INTERSPEECH 2013 Paralinguistic Challenge [22]. It contains 65 frame-level features: 55 spectral; 6 voicing related low-level descriptors; 4 energy-related. 60 ms frame (Gaussian window function) and a sigma value of 0.4 was used for the speech-related features; and a 25 ms frame (Hamming window function with a step size of 10 ms) for the others.

For feature extraction we used the open-source openSMILE software package [7] with the `IS13 ComParE` config file. The final feature set we used contained not only the basic features, but also their derivatives. We used deltas because we wanted to get information about the dynamics of the speech samples over time.

3.3 Evaluation method

The classification was performed using the LIBSVM library [4], which is an SVM (Support Vector Machine [2]) implementation written in C++; here we used the Python extension. The SVM C complexity parameter was tested in the range 10^{-5} to 10^{0}. In the evaluated configurations the following powers of 10 used were: -5; -4; -3; -2; -1 and 0. We applied a Python implemented standardization on the input BoAW feature representations before each model was trained.

In the optimization part of our experiments, we worked with the training set, based on 10-fold cross-validation. We split the data into roughly 10 equal folds, where each speaker is shown in only one fold, so each fold became absolute speaker independent. Afterwards, we trained on the 9/10 part and evaluated on the 1/10 part for each possible combination. Consequently, when evaluating one part as a test set, we got predictions for a specific part of the entire database which did not overlap with the other parts, so after running all possible combinations, we had exactly one prediction for each element of the entire database. UAR metrics could then be easily derived from this. After the 10th evaluation, we collected the predicted percentage scores from all the test cases (one score for each sample) and calculated the UAR metrics. The unweighted average recall was used as an indicator to see how good the actual feature set was for emotion recognition.

In the test scenario, we trained a model on the whole training set with the optimal C parameter value found above and evaluated it on the test set with the Unweighted Average Recall (UAR) metrics [14]. The reason we use this metric, because we have imbalanced classes. Accuracy and UAR metrics are related, but the accuracy gives a more optimistic value because it gives higher scores to classes with more samples, but the UAR gives the correct expectation on each class predictions.

In the last part, we describe our experimental procedure and the evaluation of our results. We extracted 2×65 features (65 frame-level features and their derivatives) in a frame-level window. Therefore we created two codebooks in parallel (one for 65 frame-level features and one for their derivatives). Because of this, the codebook sizes given in this section have to be multiplied by 2 to get the number of features currently used. The results of each test cases are shown below and the best results are given in tabular form for better transparency. In each figure, the x-axis shows the size of the codebook (which has to be multiplied), and the y-axis shows the UAR of the SVM. The legends of our figures contains abbreviations: “a1” means 1 neighbour during quantization; “a5”

Feature-preprocessing	**Maximum UAR**	**Codebook size**
No preprocessing	36.32%	8 192
Normalization	46.73%	4 096
Standardization	45.42%	1 024

Table 1: Preprocessing: The best results got without preprocessing, with normalization and standardization, when we evaluated our technique with cross-validation.

means 5 neighbours during quantization; "a10" means 10 neighbours during quantization; "standardized" and "stand" both means standardization during preprocessing; "normalized" and "norm" both means normalization during preprocessing; "k-means" means k-means clustering technique, "k-means++" means k-means++ clustering technique.

4 Tests and results

4.1 Preprocessing

In the first case, we compared preprocessing techniques before clustering. Preprocessing is always a good choice because databases contains outliers, which have a detrimental effect on learning effectiveness.

From our results (see Figure 3 and Table 1), it is apparent that the data without preprocessing proved to be the weakest in all cases. By comparison, normalization and standardization gave performance improvements that were nearly the same. Another advantage of normalizing or standardizing the input is that significantly fewer clusters are required for optimal performance than leaving the input unchanged (8 192). When we applied normalization, we got 46.35% for 1 024 codewords, so we found that in both normalization and standardization, a size of 1 024 was big enough to achieve the best performance. This lower codebook size also helps the performance of the SVM, because in a smaller feature space the speed and success of the learning will also increase.

The best result of the cross-validation (i.e. 46.73%) was achieved with normalization and a codebook size of 4 096. Otherwise there is no significant difference between the best standardization and normalization results. In addition, it is not clear that normalization or standardization will produce a better result with the feature set. Here, further tests were performed in parallel, with normalization and standardization to ascertain the benefits.

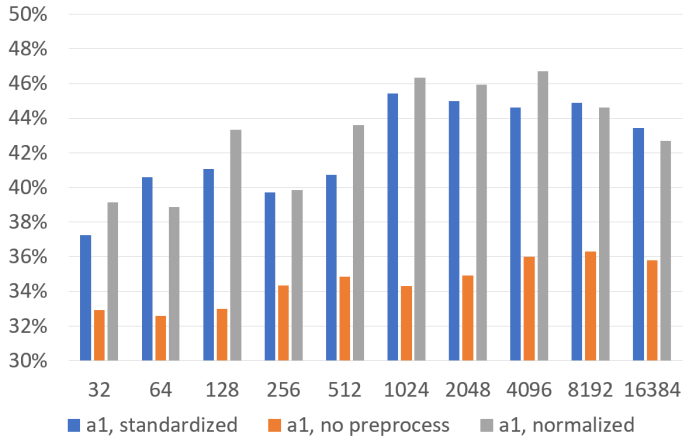

Figure 3: Preprocessing: The results obtained for different codebook sizes and preprocessing techniques.

Feature-preprocessing	**a**	**Maximum UAR**	**Codebook size**
Normalization	1	46.73%	4 096
	5	48.93%	4 096
	10	49.14%	16 384
Standardization	1	45.42%	1 024
	5	46.16%	8 192
	10	47.37%	8 192

Table 2: Number of neighbours: The best results obtained for 1, 5, 10 neighbours with normalization and standardization.

4.2 Number of neighbours assigned during quantization

In the next comparison, we investigate how many closest codewords have to be assigned to a frame-level feature vector when creating a histogram, to achieve the optimal performance. In our experiments, we tested three options, where we used the closest 1/5/10 neighbours. Based on the results of our previous optimization, all three quantatization options were also evaluated with normalization and standardization.

From our new results (see Table 2, Figure 5 and Figure 4), we may conclude that more than one neighbour gives better results in the majority of cases. This can be seen for both preprocessing techniques (normalization and standardization). As regards the performance of the classification algorithm, we

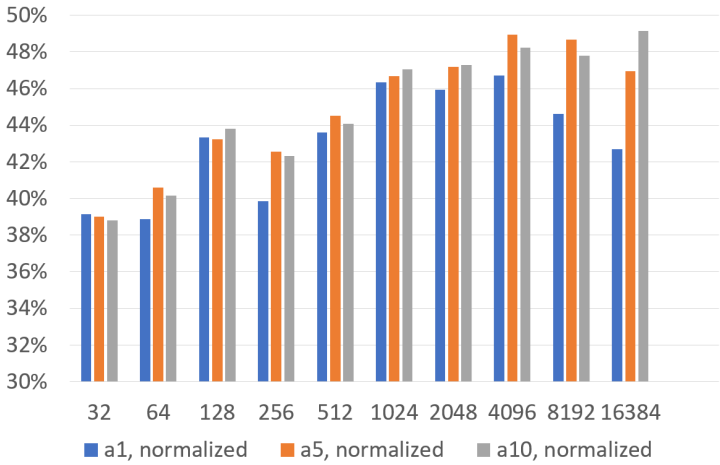

Figure 4: Number of neighbours: The results obtained for $1, 5, 10$ neighbours and normalization.

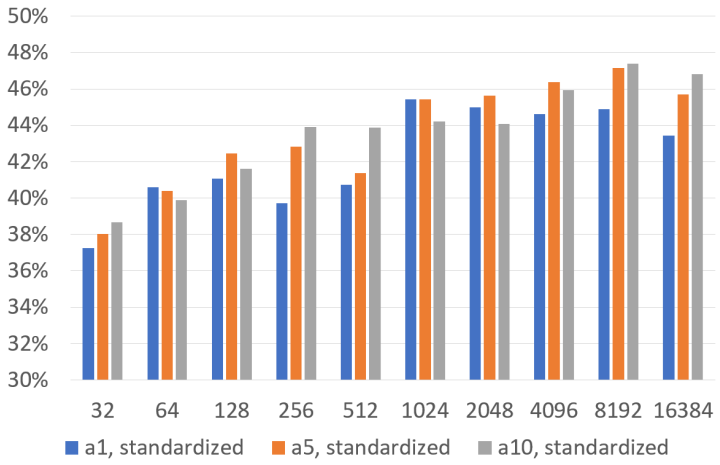

Figure 5: Number of neighbours: The results obtained for $1, 5, 10$ neighbours and standardization.

did not find any significant difference between the $a = 5$ and $a = 10$ values. As can be seen, above the codebook size of 512 we got significantly better results with applied preprocessing, so any kind of preprocessing is always a good choice if we want better results. With larger codebook sizes there is only a small difference (1%–3%) between the results got using standardization and normalization. Hence we need to investigate them further.

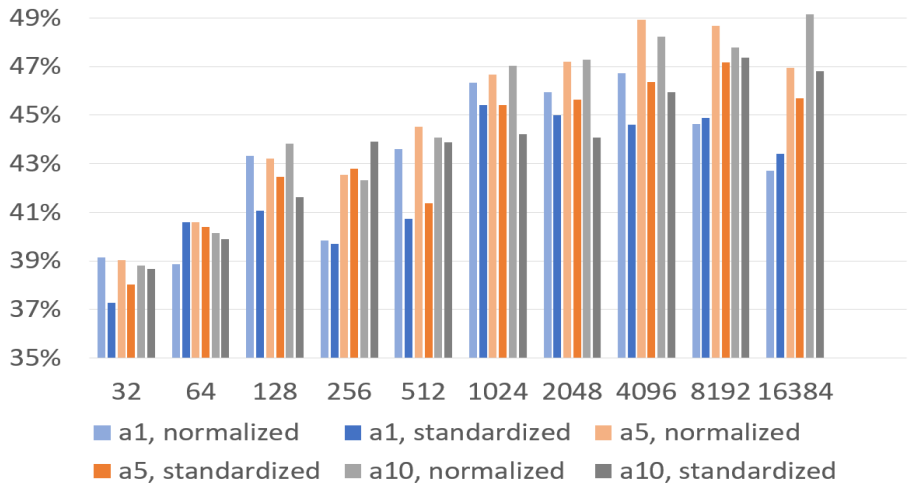

Figure 6: Number of neighbours: The results got using different codebook sizes, preprocessing techniques and neighbour counts.

Table 2 shows the best results for the different cases. We notice that 5 and 10 closest codewords give the same improvement, compared to the 1 neighbour version. Although not significant, the $a = 10$ option gives slightly better results in both preprocessing cases. Here we think that the multi-neighbour technique needs more clusters to achieve the best results. However it can be seen in Figure 6 that with standardization and normalization, the codebook size of 1 024 is already capable of giving results as good as the best single-neighbour variation. Based on our results, we decided in later test cases to test the 5 and 10 options in order to draw a more precise conclusion.

4.3 Clustering algorithm

The third parameter we investigated was the clustering algorithm, where we tested two techniques: k-means and k-means++. Based on our earlier results we decided to test them with normalization and standardization, and with 5 and 10 neighbours in the quantification step.
So our test cases were:

- 5 neighbours and standardization
- 5 neighbours and normalization
- 10 neighbours and standardization
- 10 neighbours and normalization

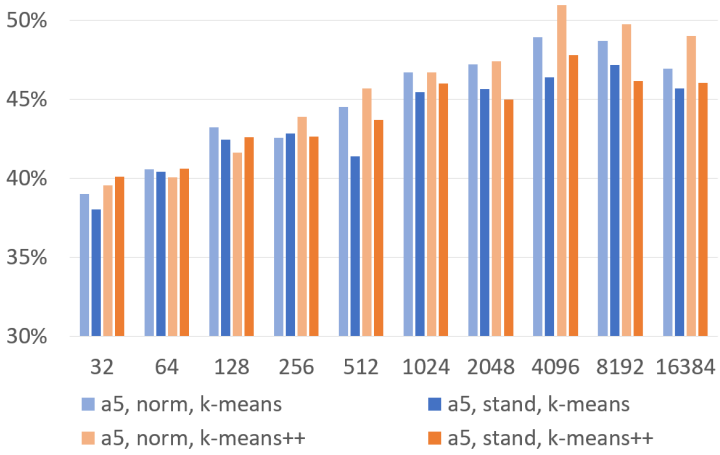

Figure 7: Clustering algorithm: The results obtained for k-means and k-means++ algorithms with 5 neighbours.

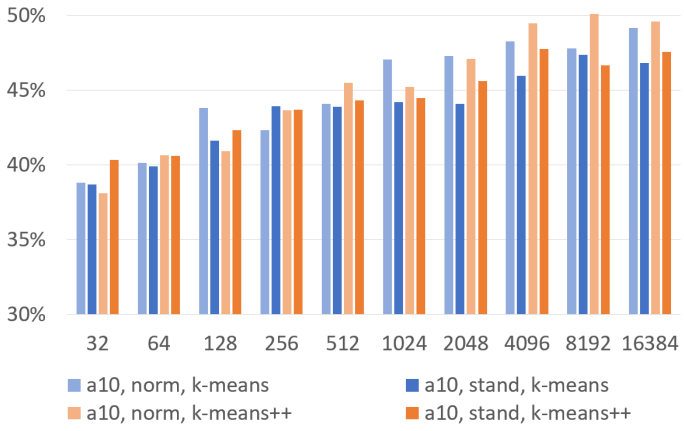

Figure 8: Clustering algorithm: The results obtained for k-means and k-means++ algorithms with 10 neighbours.

Based on the results (see Table 3, Figure 7, Figure 8, and Figure 9), we can say that both clustering methods have the same trend. Once again we get higher scores than 46% above a codebook size of 512. Also, we notice that normalization begins to perform better than the standardized case as the codebook size increases. The accuracy values are best with a codebook size of 4 096, which means that we need higher spatial dimensions to get better results. Since we did not find any significant difference between the trends of

Clustering-algorithm	Feature preprocessing	a	Maximum UAR	Codebook size
k-means	Normalization	5	48.93%	4 096
		10	49.14%	16 384
k-means	Standardization	5	46.16%	8 192
		10	47.37%	8 192
k-means++	Normalization	5	50.94%	4 096
		10	47.77%	4 096
k-means++	Standardization	5	50.08%	8 192
		10	47.74%	4 096

Table 3: Clustering algorithm: The best results for k-means and k-means++ algorithms with cross-validation.

k-means and k-means++, we decided to take the codebook sizes and settings that proved promising in our previous experiment (1 024 codebook size and normalization). Then, other tests were performed using the k-means algorithm.

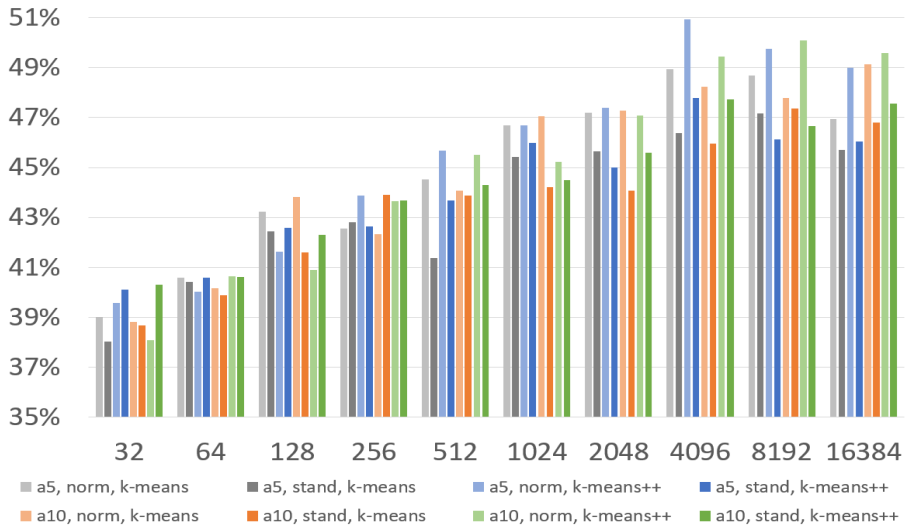

Figure 9: Clustering algorithm: The results got using different codebook sizes, preprocessing techniques, neighbour counts and quantatization algorithms.

4.4 Upsampling

Upsampling for smaller datasets and downsampling for large ones are common techniques when we have a very unbalanced dataset for labels. Because

Feature-preprocessing	**a**	**Maximum UAR**	**Codebook size**
Normalization	5	58.88%	2 048
	10	60.42%	256
Standardization	5	55.93%	128
	10	58.59%	1 024

Table 4: Upsampling: The best results obtained with upsampling in cross-validation training.

our Hungarian emotion database is smaller and not a balanced one (57–61% of the dataset has the label "neutral"), we decided to use upsampling on our BoAW features before SVM learning. In this scenario, we tested how upsampling affects our results. We carried out tests with 5 and 10 neighbours, standardization and normalization, as previously and we utilized the k-means clustering algorithm.

Based on the results (see Table 4 and Figure 10), we can state that upsampling gave an improvement of about 10% compared to all of our previous results. In addition, perhaps the biggest advantage is that we were able to further reduce the optimal codebook size, which is good in terms of the speed and degree of difficulty of the learning process. It has only one disadvantage, namely our training curve is not as stable as before. There are two peaks here instead of one and it leads to less predictable learning. Because of this, we applied upsampling in our next experiment.

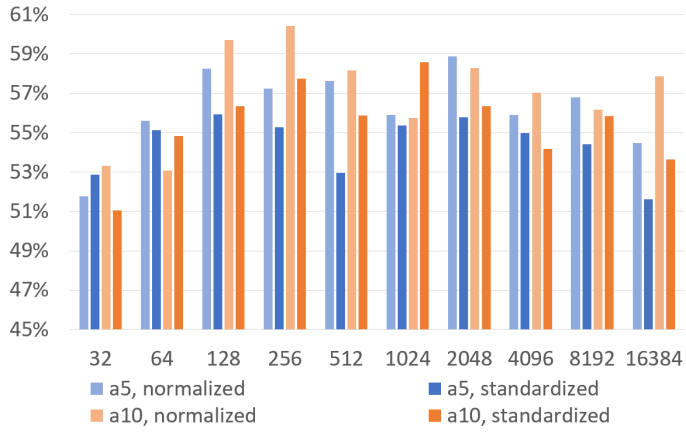

Figure 10: Upsampling: The results obtained with upsampling in cross-validation training.

Feature-preprocessing	a	Maximum UAR	Codebook size
Normalization	5	58.63%	512
	10	57.48%	512
Standardization	5	56.08%	512
	10	59.00%	512

Table 5: Deltas: The best results of cross-validation using deltas.

4.5 Derivatives

As we mentioned previously, using derivatives is a frequently used technique in speech processing to get information about the speaker's change of voice over time. In the last optimizing scenario we tested the effect of using these deltas. Our experiments so far have shown that the 16 384-sized codebooks always give a lower performance, and working with big dimensions slows down the training process. Because of the low performance we no longer need to run cross-validation and test with this huge 16 384 size. It should be added that the codebook sizes on Figure 11 had to be doubled, because we created two unit-sized codebooks; one for the original features and one for deltas and we used both of them while training.

From our results (see Table 5 and Figure 11), by using deltas we managed to reduce the number of necessary and sufficient codewords to a moderate size. Another advantage is that training trends are less random than before and much more predictable. So owing to this positive result, the final evaluation with the test database was performed with deltas.

4.6 Final tests

All of our previous decisions were made based on the optimal results got by the cross-validation performed on the teaching set, so our final set of BoAW parameters are the following:

- 5 neighbours, normalization, upsampling and using deltas
- 10 neighbours, normalization, upsampling and using deltas
- 5 neighbours, standardization, upsampling and using deltas
- 10 neighbours, standardization, upsampling and using deltas

All of our previous results indicate that above a codebook size of 64 the results display consistently increasing trends. Because of this, we decided to

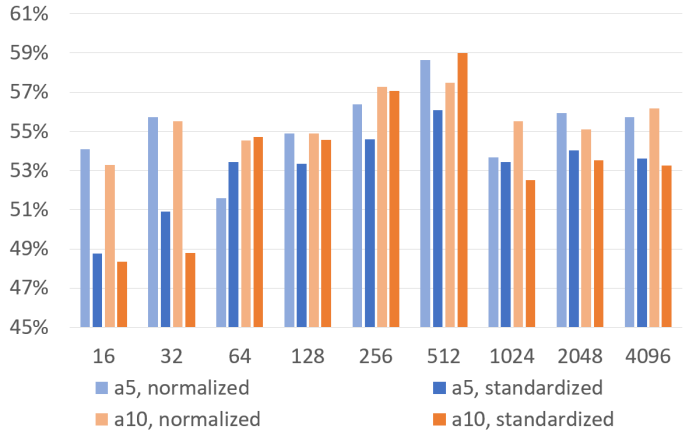

Figure 11: Deltas: The results of cross-validation using deltas.

Feature-preprocessing	**a**	**Maximum UAR**	**Codebook size**
Normalization	5	68.68%	64
	10	67.77%	128
Standardization	5	71.15%	64
	10	65.42%	64

Table 6: Final tests: The best results of the final tests without cross-validation.

run our tests with a size of 128 (the codebook size is 64 on the test diagrams, because we have to double the size when using deltas).

Based on our final results (see Table 6 and Figure 12), we may conclude that the bag-of-audio-words representation can be utilized for speech emotion recognition. It can be seen that with the right parameter settings we were able to reduce the dimension of the best result. However the trends of the test results are not clear, and the connection between increasing codeword quantities and decreasing evaluation results also seems to suggest that the larger the codebook size we choose, the greater the chance of over-fitting and our classifier will lose its ability to generalize.

The best results on the test set are close to 70%, which is at least as good as the other published paper results. Our final percentage scores cannot be compared directly to previous published results for this database because they used accuracy instead of UAR and had no upsampling. However we can still state that BoAW is as good representation as any other if we carefully optimize the parameter values of the algorithm.

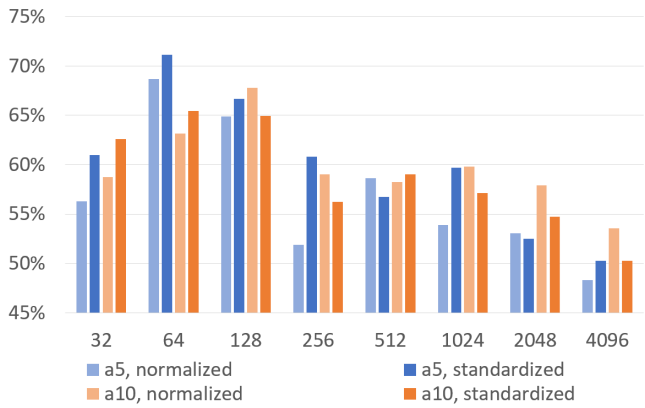

Figure 12: Final tests: The results of the final tests without cross-validation.

5 Conclusions

In this study, the bag-of-audio-words feature representation method was used for speech emotion recognition with a Hungarian emotional database. Because the BoAW method has many adjustable parameters, we had to train a lot of machine learning models with different parameter value combinations, so the training runtimes was an important consideration. Although each model building and evaluation did not take a long time, due to the many combinations and possible correction runs, the whole experiment took far too far.

From our results, we offer some useful suggestions that might be helpful when using openXBOW. These are:

- Transform the input sample set to the same scale by normalization or standardization. This is always a good choice.
- For greater generalization ability, it is worth including more neighbours in the quantizing step, such as 5 or 10.
- It is worth choosing the size of codebook from a medium-large range (e.g. between 128 and 4 096). If possible, try to keep the codebook size low to get a better generalization.
- Clustering the k-means and k-means++ algorithms are worth exploring.
- By balancing the frequency of classes seen during learning (in this case with upsampling), we can improve our generalization ability.
- We should calculate and use the deltas.

Now we see that the bag-of-audio-words technique is competitive in the area of speech emotion recognition, but this method has several parameter values that need to be precisely tuned for optimal efficiency.

There are several directions we can pursue in the future. Firstly, we would like to see if we can use other database codebooks to extract BoAW features from different databases. In another words, we wish to know whether codebooks are portable and what the best codebooks are for different purposes. We could also test other frame-level feature sets to see if there are any practical benefits of using them.

Acknowledgements

This study was partially funded by the National Research, Development and Innovation Office of Hungary via contract NKFIH FK-124413, by grant NKFIH-1279-2/2020 of the Hungarian Ministry of Innovation and Technology, and by the Ministry of Innovation and Technology NRDI Office within the framework of the Artificial Intelligence National Laboratory Programme. Gábor Gosztolya was supported by the János Bolyai Research Scholarship of the Hungarian Academy of Sciences, and by the ÚNKP-21-5 New National Excellence Program by the Hungarian Ministry of Innovation and Technology.

References

[1] D. Arthur, S. Vassilvitskii, k-means++: the advantages of careful seeding. *Proceedings of SODA*. **8** (2007) pp. 1027–1035, https://dl.acm.org/doi/10.5555/1283383.1283494 ⇒6

[2] S. Bernhard, C. John, S. John, J. Alexander, C. Robert, Estimating the support of a high-dimensional distribution. *Neural Computation* **13** (2001) 1443–1471, https://doi.org/10.1162/089976601750264965 ⇒8

[3] F. Burkhardt, M. Ballegooy, K. Engelbrecht, T. Polzehl, J. Stegmann, Emotion detection in dialog systems: Applications, strategies and challenges, *Proceedings Of ACII*. 2009, pp. 985–989. ⇒2

[4] C. Chang, C. Lin, LIBSVM: A library for support vector machines, *ACM Transactions On Intelligent Systems And Technology* **2**, 3 (2011) 1–27, https://doi.org/10.1145/1961189.1961199 ⇒8

[5] G. Csurka, F. Perronnin, Fisher Vectors: Beyond bag-of-visual-words image representations, *Computer Vision, Imaging And Computer Graphics, Theory And Applications* **229** (2011) 28–42, http://dx.doi.org/10.1007/978-3-642-25382-9_2 ⇒3

[6] L. Deng, J. Droppo, A. Acero, A Bayesian approach to speech feature enhancement using the dynamic cepstral prior, *2002 IEEE International Conference on Acoustics, Speech, and Signal Processing* **1** (2002) 829–832, http://dx.doi.org/10.1109/ICASSP.2002.5743867 ⇒6

[7] F. Eyben, M. Wöllmer, B. Schuller, Opensmile: The Munich Versatile and Fast Open-source Audio Feature Extractor. *Proceedings Of ACM Multimedia.* (2010) pp. 1459–1462, http://doi.acm.org/10.1145/1873951.1874246 ⇒7

[8] G. Gosztolya, Using the Fisher vector representation for audio-based emotion recognition. *Acta Polytechnica Hungarica.* **17** (2020) 7–23, http://dx.doi.org/10.12700/APH.17.6.2020.6.1 ⇒3, 7

[9] T. Grósz, L. Tóth, A comparison of deep neural network training methods for large vocabulary speech recognition. *Proceedings Of TSD*, 2013, pp. 36–43, http://dx.doi.org/10.1007/978-3-642-40585-3_6 ⇒3

[10] M. Hossain, G. Muhammad, Cloud-assisted speech and face recognition framework for health monitoring. *Mobile Networks And Applications.* **20** (2015) 391–399, https://doi.org/10.1007/s11036-015-0586-3 ⇒2

[11] D. Issa, M. F. Demirci, A. Yazici, Speech emotion recognition with deep convolutional neural networks, *Biomedical Signal Processing and Control*, **59** (2020) 101894, http://dx.doi.org/10.1016/j.bspc.2020.101894 ⇒3

[12] J. James, L. Tian, C. Inez Watson, An open source emotional speech corpus for human robot interaction applications, *Proceedings Of Interspeech* (2018) pp. 2768–2772, https://doi.org/10.21437/Interspeech.2018-1349 ⇒2

[13] C. Jones, J. Sutherland, Acoustic emotion recognition for affective computer gaming. **1** (2008), https://doi.org/10.1007/978-3-540-85099-1 ⇒2

[14] F. Metze, A. Batliner, F. Eyben, T. Polzehl, B. Schuller, S. Steidl, Emotion recognition using imperfect speech recognition. *Proceedings Of Interspeech*, 2010, pp. 478–481, http://dx.doi.org/10.21437/Interspeech.2010-202 ⇒8

[15] S. Pancoast, M. Akbacak, Bag-of-audio-words approach for multimedia event classification. *Proceedings Of Interspeech*, 2012, pp. 2105–2108. ⇒3

[16] S. Pancoast, M. Akbacak, Softening quantization in bag-of-audio-words. *Proceedings Of ICASSP*, 2014, pp. 1370–1374, https://doi.org/10.1109/ICASSP.2014.6853821 ⇒6

[17] J. Přibil, A. Přibilová, J. Matoušek, GMM-based speaker age and gender classification in Czech and Slovak. *Journal Of Electrical Engineering*, **68** (2017) 3–12, http://dx.doi.org/10.1515/jee-2017-0001 ⇒2

[18] P. Raghavendra, W. Tianzi, V. Jesus, C. Nanxin, D. Najim, X-vectors meet emotions: A study on dependencies between emotion and speaker recognition, *ICASSP 2020 – 2020 IEEE International Conference on Acoustics, Speech and Signal Processing (ICASSP)*, 2020, pp. 7169–7173, http://dx.doi.org/10.1109/ICASSP40776.2020.9054317 ⇒3

[19] S. Rawat, P. Schulam, S. Burger, D. Ding, Y. Wang, F. Metze, Robust audio-codebooks for large-scale event detection in consumer videos, *Proceedings Of Interspeech*, 2013, pp. 2929–2933 ⇒6

[20] M. Schmitt, F. Ringeval, B. Schuller, At the border of acoustics and linguistics: Bag-of-audio-words for the cecognition of emotions in speech, *Proceedings Of Interspeech*, 2016, pp. 495-499, http://dx.doi.org/10.21437/Interspeech.2016-1124 ⇒3

[21] M. Schmitt, B. Schuller, openXBOW – Introducing the Passau open-source crossmodal bag-of-words toolkit. *Journal Of Machine Learning Research* **18** (2017) 1–5, http://jmlr.org/papers/v18/17-113.html ⇒5

[22] B. Schuller, S. Steidl, A. Batliner, A. Vinciarelli, K. Scherer, F. Ringeval, et al., The INTERSPEECH 2013 computational paralinguistics challenge: Social signals, conflict, emotion, autism, *Proceedings Of Interspeech*, 2013, pp. 148–152. ⇒7

[23] D. Sztahó, V. Imre, K. Vicsi, Automatic classification of emotions in spontaneous speech, *Proceedings Of COST 2102*, 2011, pp. 229–239, http://dx.doi.org/10.1007/978-3-642-25775-9_23 ⇒3, 7

[24] M. Swain, A. Routray, P. Kabisatpathy, Databases, features and classifiers for speech emotion recognition: a review, *Int J Speech Technol* **21** (2018) 93–120, https://link.springer.com/article/10.1007/s10772-018-9491-z ⇒3

[25] K. Vicsi, D. Sztahó, Recognition of emotions on the basis of different levels of speech segments. *Journal Of Advanced Computational Intelligence And Intelligent Informatics* **16** (2012) 335–340, http://dx.doi.org/10.20965/jaciii.2012.p0335 ⇒3, 7

[26] L. Vidrascu, L. Devillers, Detection of real-life emotions in call centers, *Proceedings Of Interspeech*, 2005, pp. 1841–1844, http://dx.doi.org/10.21437/Interspeech.2005-582 ⇒2

[27] T. Zhang, J. Wu, Speech emotion recognition with i-vector feature and RNN model, *2015 IEEE China Summit and International Conference on Signal and Information Processing (ChinaSIP)*, 2015, pp. 524-528, http://dx.doi.org/10.1109/ChinaSIP.2015.7230458 ⇒3

[28] Y. Zhang, R. Jin, Z. Zhou, Understanding bag-of-words model: A statistical framework. *International Journal Of Machine Learning And Cybernetics* **1** (2010) 43–52, http://dx.doi.org/10.1007/s13042-010-0001-0 ⇒3

Received: November 23, 2021 • Revised: February 1, 2022

Acta Univ. Sapientiae Informatica **14,** 1 (2022) 22–34

DOI: 10.2478/ausi-2022-0002

Signless Laplacian energy of a first KCD matrix

Keerthi G. MIRAJKAR
Department of Mathematics,
Karnatak University's Karnatak Arts College, Dharwad - 580001,
Karnataka, India
email: keerthi.mirajkar@gmail.com

Akshata MORAJKAR
Department of Mathematics,
Karnatak University's Karnatak Arts College, Dharwad - 580001,
Karnataka, India
email: akmorajkar@gmail.com

Abstract. The concept of first KCD signless Laplacian energy is initiated in this article. Moreover, we determine first KCD signless Laplacian spectrum and first KCD signless Laplacian energy for some class of graphs and their complement.

1 Introduction

In this article, a connected, simple and undirected graph G having n vertices and m edges is considered. The degree of vertex v_i is represented as d_i. The complement $\overline{G}$ of G has two vertices adjacent if they are not adjacent in G [12]. The regular graph G has degree r. For undefined terminologies refer [12].

The idea of energy of a graph G was outlined by Gutman [11]. It defines energy of G as the sum of absolute eigenvalues of G. Tremendous work on this concept is available in the literature [11, 16]. Recently various graph-energy-like quantities: Laplacian [10], signless Laplacian [1, 8], distance [13] etc. are studied. Further, two non-isomorphic graphs having same spectra are cospectral otherwise noncospectral. Various energies are available in the literature

Computing Classification System 1998: G.2.2
Mathematics Subject Classification 2010: 05C07, 05C50
Key words and phrases: First KCD signless Laplacian matrix, first KCD signless Laplacian eigenvalues, first KCD signless Laplacian energy.

defined using the degree of a vertex. The vertex degree and edge degree together makes the concept more fascinating and opens new areas of research. With this urge a new matrix using vertex and edge degree together was defined by Mirajkar et al. in [14].

The first Karnatak College Dharwad matrix i.e., first KCD matrix [14] $KCD_1(G)$ is defined as

$$kcd_{1_{ij}} = \begin{cases} (d_i + d_j) + d_{ij} & \text{if } v_i \text{ is adjacent to } v_j \ , \\ 0 & \text{otherwise,} \end{cases}$$

with d_i and d_j representing vertex degrees v_i and v_j respectively, the edge degree is $d_{ij} = d_i + d_j - 2$.

$\beta_1 \geqslant \beta_2 \geqslant ... \geqslant \beta_n$ represents the first KCD eigenvalues of G. The first KCD energy $E_{KCD_1}(G)$ [14] is

$$E_{KCD_1}(G) = \sum_{i=1}^{n} |\beta_i|. \tag{1}$$

If $D(G)$ and $KCD_1(G)$ are the diagonal matrix and first KCD matrix respectively, then for a (n, m) graph G, the first Karnatak College Dharwad Laplacian matrix [15] $L_{KCD_1}(G)$ is

$$L_{KCD_1}(G) = D(G) - KCD_1(G).$$

It has first KCD Laplacian eigenvalues $\eta_1 \geqslant \eta_2 \geqslant ... \geqslant \eta_n$ in the non-increasing order. The corresponding first Karnatak College Dharwad Laplacian energy [15] $LE_{KCD_1}(G)$ is

$$LE_{KCD_1}(G) = \sum_{i=1}^{n} \left| \eta_i - \frac{2m}{n} \right|, \tag{2}$$

where $\eta_i, i = 1, 2, ..., n$ represents the first KCD Laplacian eigenvalues of G.

If $D(G)$ and $A(G)$ are the diagonal matrix and adjacency matrix respectively, then the signless Laplacian matrix [1] of G is

$$SL(G) = D(G) + A(G).$$

It has $\mu_1^+ \geqslant \mu_2^+ \geqslant ... \geqslant \mu_n^+$ as the signless Laplacian eigenvalues of G.
The signless Lapalcian energy [1] of G is

$$SLE(G) = \sum_{i=1}^{n} \left| \mu_i^+ - \frac{2m}{n} \right|.$$

Analogous to energy of a graph G the concept of $SLE(G)$ also has numerous chemical applications. For some of the spectral properties of $SL(G)$ refer [1, 3, 5, 6, 7]. Further more, the concept of $SL(G)$and $SLE(G)$ has motivated us to develop the idea of the first KCD signless Laplacian matrix and first KCD signless Laplacian energy of G.

With this motivation, in the second section, we introduce the first KCD signless Laplacian matrix and first KCD signless Laplacian energy of G, followed by general basic results on them. Further, in third section we determine first KCD signless Laplacian spectrum and first KCD signless Laplacian energy for some class of graphs and their complements.

2 First *KCD* signless Laplacian energy

Definition 1 *If* $D(G)$ *and* $KCD_1(G)$ *are the diagonal matrix and first* KCD *matrix respectively, then for a* (n, m) *graph* G*, the first Karnatak College Dharwad signless Laplacian matrix* $SL_{KCD_1}(G)$ *is defined as*

$$SL_{KCD_1}(G) = D(G) + KCD_1(G).$$

It has first KCD *signless Laplacian eigenvalues* $\eta_1^+ \geqslant \eta_2^+ \geqslant ... \geqslant \eta_n^+$ *in the non-increasing order, where* η_1^+ *and* η_n^+ *are the highest and lowest first* KCD *signless Laplacian eigenvalues of* G *respectively.*

The corresponding first Karnatak College Dharwad signless Laplacian energy $SLE_{KCD_1}(G)$ *is defined as*

$$SLE_{KCD_1}(G) = \sum_{i=1}^{n} \left| \eta_i^+ - \frac{2m}{n} \right|, \tag{3}$$

where $\eta_i^+, i = 1, 2, ..., n$ *are the first* KCD *signless Laplacian eigenvalues of* G.

Lemma 2 *If* G *is a regular graph, then*

$$SLE_{KCD_1}(G) = E_{KCD_1}(G). \tag{4}$$

Proof. The regular graph G satisfies

$$\eta_i^+ - \frac{2m}{n} = \beta_i, \quad i = 1, 2, ..., n \tag{5}$$

Making an appeal to Eq. (5) in (3), we get

$$SLE_{KCD_1}(G) = \sum_{i=1}^{n} |\beta_i| = E_{KCD_1}(G).$$

□

Corollary 3 *If* G *is a regular graph, then*

$$SLE_{KCD_1}(G) = LE_{KCD_1}(G) = E_{KCD_1}(G).$$

Proof. From Eq. (4), we have

$$SLE_{KCD_1}(G) = E_{KCD_1}(G). \tag{6}$$

Further, from [15], we consider

$$LE_{KCD_1}(G) = E_{KCD_1}(G) \tag{7}$$

Finally, from Eqs. (6) and (7), we obtain the required result.

□

3 Estimation of first *KCD* signless Laplacian energy for some class of graphs and their complements

This section considers first $SLE_{KCD_1}(G)$ for few class of graphs and respective complements.
If $\eta_1^+ \geqslant \eta_2^+ \geqslant ... \geqslant \eta_k^+$ are the distinct first KCD signless Laplacian eigenvalues of G having the multiplicities $t_1, t_2, ..., t_k$ then, the first KCD signless Laplacian spectrum of G is denoted as

$$SL_{Spec_{KCD_1}}(G) = \begin{pmatrix} \eta_1^+ & \eta_2^+ & ... & \eta_k^+ \\ t_1 & t_2 & ... & t_k \end{pmatrix},$$

where $t_1 + t_2 + ... + t_k = n$.

Further calculations are based on the following

Lemma 4 [13] If

$$M = \begin{pmatrix} M_0 & M_1 \\ M_1 & M_0 \end{pmatrix}$$

represents a symmetric matrix with block partition, then the eigenvalues of M are the eigenvalues of the matrices $M_0 + M_1$ and $M_0 - M_1$.

Theorem 5 *If* $K_{\frac{n}{2},\frac{n}{2}}$ *has* $|V(K_{\frac{n}{2},\frac{n}{2}})| = n = \{2l; l = 3, 4, ...\}$, *then*

$$SL_{Spec_{KCD_1}}\left(K_{\frac{n}{2},\frac{n}{2}}\right) = \begin{pmatrix} \frac{n}{2} & \left(\frac{3-2n}{2}\right)n & \left(\frac{2n-1}{2}\right)n \\ n-2 & 1 & 1 \end{pmatrix}$$

and

$$SLE_{KCD_1}\left(K_{\frac{n}{2},\frac{n}{2}}\right) = 2n^2 - 2n.$$

Proof. For $K_{\frac{n}{2},\frac{n}{2}}$ of order n, we have

$$SL_{KCD_1}\left(K_{\frac{n}{2},\frac{n}{2}}\right) = \begin{pmatrix} \frac{n}{2}I_{\frac{n}{2}} & (2n-2)J_{\frac{n}{2}} \\ (2n-2)J_{\frac{n}{2}} & \frac{n}{2}I_{\frac{n}{2}} \end{pmatrix}.$$

Here $I_{\frac{n}{2}}$ is the identity matrix having order $\frac{n}{2}$ and $J_{\frac{n}{2}}$ is the $\frac{n}{2} \times \frac{n}{2}$ matrix with all entries as 1.
Further, above matrix can be expressed as

$$SL_{KCD_1}\left(K_{\frac{n}{2},\frac{n}{2}}\right) = \begin{pmatrix} M_0 & M_1 \\ M_1 & M_0 \end{pmatrix},$$

where $M_0 = \frac{n}{2}I_{\frac{n}{2}}$ and $M_1 = (2n-2)J_{\frac{n}{2}}$.
Now,

$$M_0 + M_1 = \frac{n}{2}I_{\frac{n}{2}} + (2n-2)J_{\frac{n}{2}}$$

and

$$M_0 - M_1 = \frac{n}{2}I_{\frac{n}{2}} - (2n-2)J_{\frac{n}{2}}.$$

By using ***Lemma* 4**, the spectrum of $SL_{KCD_1}\left(K_{\frac{n}{2},\frac{n}{2}}\right)$ is

$$SL_{Spec_{KCD_1}}\left(K_{\frac{n}{2},\frac{n}{2}}\right) = \begin{pmatrix} \frac{n}{2} & \left(\frac{3-2n}{2}\right)n & \left(\frac{2n-1}{2}\right)n \\ n-2 & 1 & 1 \end{pmatrix}.$$

Further, employing the Eq. (3), we derive

$$\begin{aligned} SLE_{KCD_1}\left(K_{\frac{n}{2},\frac{n}{2}}\right) &= \sum_{i=1}^{n}\left|\eta_i^+ - \frac{2m}{n}\right| \\ &= \sum_{i=1}^{n}\left|\eta_i^+ - \frac{n}{2}\right| \\ &= (n-2)\left|\frac{n}{2}-\frac{n}{2}\right| + \left|\left(\frac{3-2n}{2}\right)n - \frac{n}{2}\right| \\ &\quad + \left|\left(\frac{2n-1}{2}\right)n - \frac{n}{2}\right| \\ &= 2n^2 - 2n. \end{aligned}$$

□

Definition 6 [9] The crown graph $CR(c)$ for an integer $c \geqslant 3$ represents the graph with vertex set $\{u_1, u_2, ..., u_c, v_1, v_2, ..., v_c\}$ and edge set $\{u_i v_j, 1 \leqslant i, j \leqslant c, i \neq j\}$.

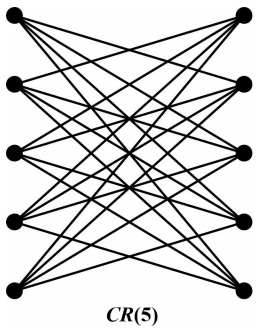

Figure 1: Crown graph

Theorem 7 *For* $CR(c)$ *with an integer* $c \geqslant 3$,

$$SL_{Spec_{KCD_1}}(CR(c)) = \begin{pmatrix} 5-3c & 5c-7 & 11c-7-4c^2 & 4c^2-9c+5 \\ c-1 & c-1 & 1 & 1 \end{pmatrix}$$

and

$$SLE_{KCD_1}(CR(c)) = 8(2c^2-5c+3).$$

Proof. For $CR(c)$ of order $n = 2c$, we have

$$SL_{KCD_1}(CR(c)) = \begin{pmatrix} (c-1)I_c & (4c-6)(J_c - I_c) \\ (4c-6)(J_c - I_c) & (c-1)I_c \end{pmatrix}.$$

Here I_c is the identity matrix having order c and J_c is the square matrix having order c with all entries equal to 1.
Further, above matrix can be expressed as

$$SL_{KCD_1}(CR(c)) = \begin{pmatrix} M_0 & M_1 \\ M_1 & M_0 \end{pmatrix},$$

where $M_0 = (c-1)I_c$ and $M_1 = (4c-6)(J_c - I_c)$.
Now,

$$M_0 + M_1 = (5-3c)I_c + (4c-6)J_c$$

and

$$M_0 - M_1 = (5c-7)I_c - (4c-6)J_c.$$

By using ***Lemma* 4**, the spectrum of $SL_{KCD_1}(CR(c))$ is

$$SL_{Spec_{KCD_1}}(CR(c)) = \begin{pmatrix} 5-3c & 5c-7 & 11c-7-4c^2 & 4c^2-9c+5 \\ c-1 & c-1 & 1 & 1 \end{pmatrix}.$$

Further, employing the Eq. (3), we prove

$$\begin{aligned} SLE_{KCD_1}(CR(c)) &= \sum_{i=1}^{n=2c} \left|\eta_i^+ - (c-1)\right| \\ &= 8(2c^2 - 5c + 3). \end{aligned}$$

□

Definition 8 [2, 4] The cocktail party graph $CP(a)$ (for $a \geqslant 3$) is the graph consisting of two rows of paired vertices in which all vertices but the paired ones are connected with an edge.

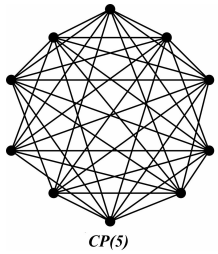

Figure 2: Cocktail party graph

Theorem 9 *For* $CP(a)$ *with an integer* $a \geqslant 3$,

$$SL_{Spec_{KCD_1}}(CP(a)) = \begin{pmatrix} 2a-2 & 18-14a & 16a^2-34a+18 \\ a & a-1 & 1 \end{pmatrix}$$

and

$$SLE_{KCD_1}(CP(a)) = 8(a-1)(4a-5).$$

Proof. For $CP(a)$ of order $n = 2a$, we have

$$SL_{KCD_1}(CP(a)) = \begin{pmatrix} (8a-10)(J_a-I_a)+(2a-2)I_a & (8a-10)(J_a-U_a) \\ (8a-10)(J_a-U_a) & (8a-10)(J_a-I_a)+(2a-2)I_a \end{pmatrix}.$$

Here I_a is the identity matrix having order a, J_a is the square matrix having order a with all entries equal to 1 and U_a is a square matrix with all entries as zeros, except the entries on the anti-diagonal being 1.
Further, above matrix can be expressed as

$$SL_{KCD_1}(CP(a)) = \begin{pmatrix} M_0 & M_1 \\ M_1 & M_0 \end{pmatrix},$$

where $M_0 = (8a-10)(J_a-I_a)+(2a-2)I_a$ and $M_1 = (8a-10)(J_a-U_a)$.
Now,

$$M_0 + M_1 = 2(8a-10)J_a - (6a-8)I_a - (8a-10)U_a$$

and

$$M_0 - M_1 = (8a-10)U_a - (6a-8)I_a.$$

By using ***Lemma* 4**, the spectrum of $SL_{KCD_1}(CP(a))$ is

$$SL_{Spec_{KCD_1}}(CP(a)) = \begin{pmatrix} 2a-2 & 18-14a & 16a^2-34a+18 \\ a & a-1 & 1 \end{pmatrix}.$$

Further, employing the Eq. (3), we prove

$$\begin{aligned} SLE_{KCD_1}(CP(a)) &= \sum_{i=1}^{n=2a} \left|\eta_i^+ - 2(a-1)\right| \\ &= 8(a-1)(4a-5). \end{aligned}$$

□

Theorem 10 *If* $\overline{K_{\frac{n}{2},\frac{n}{2}}}$ *has* $|V(\overline{K_{\frac{n}{2},\frac{n}{2}}})| = n = \{2l; l = 3, 4, ...\}$, *then*

$$SL_{Spec_{KCD_1}}\left(\overline{K_{\frac{n}{2},\frac{n}{2}}}\right) = \begin{pmatrix} 5-\frac{3n}{2} & \frac{2n^2-9n+10}{2} \\ n-2 & 2 \end{pmatrix}$$

and

$$SLE_{KCD_1}\left(\overline{K_{\frac{n}{2},\frac{n}{2}}}\right) = 4(n-2)(n-3).$$

Proof. For $\overline{K_{\frac{n}{2},\frac{n}{2}}}$ of order n, we have

$$SL_{KCD_1}\left(\overline{K_{\frac{n}{2},\frac{n}{2}}}\right) = \begin{pmatrix} (2n-6)J_{\frac{n}{2}} - \left(\frac{3n}{2}-5\right)I_{\frac{n}{2}} & O_{\frac{n}{2}} \\ O_{\frac{n}{2}} & (2n-6)J_{\frac{n}{2}} - \left(\frac{3n}{2}-5\right)I_{\frac{n}{2}} \end{pmatrix}.$$

Here $I_{\frac{n}{2}}$ is the identity matrix having order $\frac{n}{2}$, $J_{\frac{n}{2}}$ is the $\frac{n}{2} \times \frac{n}{2}$ matrix with all entries as 1 and $O_{\frac{n}{2}}$ is a zero matrix of order $n/2$.
Further, above matrix can be expressed as

$$SL_{KCD_1}\left(\overline{K_{\frac{n}{2},\frac{n}{2}}}\right) = \begin{pmatrix} M_0 & M_1 \\ M_1 & M_0 \end{pmatrix},$$

where $M_0 = (2n-6)J_{\frac{n}{2}} - \left(\frac{3n}{2}-5\right)I_{\frac{n}{2}}$ and $M_1 = O_{\frac{n}{2}}$.
Now,

$$M_0 + M_1 = (2n-6)J_{\frac{n}{2}} - \left(\frac{3n}{2}-5\right)I_{\frac{n}{2}} = M_0 - M_1.$$

By using ***Lemma* 4**, the spectrum of $SL_{KCD_1}\left(\overline{K_{\frac{n}{2},\frac{n}{2}}}\right)$ is

$$SL_{Spec_{KCD_1}}\left(\overline{K_{\frac{n}{2},\frac{n}{2}}}\right) = \begin{pmatrix} 5-\frac{3n}{2} & \frac{2n^2-9n+10}{2} \\ n-2 & 2 \end{pmatrix}.$$

Further, employing the Eq. (3), we derive

$$\begin{aligned} SLE_{KCD_1}\left(\overline{K_{\frac{n}{2},\frac{n}{2}}}\right) &= \sum_{i=1}^{n}\left|\eta_i^+ - \left(\frac{n}{2}-1\right)\right| \\ &= 4(n-2)(n-3). \end{aligned}$$

□

Theorem 11 *For* $\overline{CR(c)}$ *with an integer* $c \geqslant 3$*,*

$$SL_{Spec_{KCD_1}}\left(\overline{CR(c)}\right) = \begin{pmatrix} c & 4-7c & 4c^2-9c+4 & 4c^2-c \\ c-1 & c-1 & 1 & 1 \end{pmatrix}$$

and

$$SLE_{KCD_1}\left(\overline{CR(c)}\right) = 8(c-1)(2c-1).$$

Proof. For $\overline{CR(c)}$ of order $n = 2c$, we have

$$SL_{KCD_1}\left(\overline{CR(c)}\right) = \begin{pmatrix} (4c-2)J_c-(3c-2)I_c & (4c-2)I_c \\ (4c-2)I_c & (4c-2)J_c-(3c-2)I_c \end{pmatrix}.$$

Here I_c is the identity matrix having order c and J_c is the square matrix having order c with all entries equal to 1.
Further, above matrix can be expressed as

$$SL_{KCD_1}\left(\overline{CR(c)}\right) = \begin{pmatrix} M_0 & M_1 \\ M_1 & M_0 \end{pmatrix},$$

where $M_0 = (4c-2)J_c-(3c-2)I_c$ and $M_1 = (4c-2)I_c$.
Now,

$$M_0 + M_1 = (4c-2)J_c + cI_c$$

and

$$M_0 - M_1 = (4c-2)J_c - (7c-4)I_c.$$

By using ***Lemma* 4**, the spectrum of $SL_{KCD_1}\left(\overline{CR(c)}\right)$ is

$$SL_{Spec_{KCD_1}}\left(\overline{CR(c)}\right) = \begin{pmatrix} c & 4-7c & 4c^2-9c+4 & 4c^2-c \\ c-1 & c-1 & 1 & 1 \end{pmatrix}.$$

Further, employing the Eq. (3), we prove

$$\begin{aligned} SLE_{KCD_1}\left(\overline{CR(c)}\right) &= \sum_{i=1}^{n=2c} \left|\eta_i^+ - c\right| \\ &= 8(c-1)(2c-1). \end{aligned}$$

□

Theorem 12 *For* $\overline{CP(a)}$ *with an integer* $a \geqslant 3$*,*

$$SL_{Spec_{KCD_1}}\left(\overline{CP(a)}\right) = \begin{pmatrix} -1 & 3 \\ a & a \end{pmatrix}$$

and

$$SLE_{KCD_1}\left(\overline{CP(a)}\right) = 4a.$$

Proof. For $\overline{Cp(a)}$ of order $n = 2a$, we have

$$SL_{KCD_1}\left(\overline{Cp(a)}\right) = \begin{pmatrix} I_a & 2U_a \\ 2U_a & I_a \end{pmatrix}.$$

Here I_a is the identity matrix having order a and U_a is a square matrix with all entries as zeros, except the entries on the anti-diagonal being 1.
Further, above matrix can be expressed as

$$SL_{KCD_1}\left(\overline{Cp(a)}\right) = \begin{pmatrix} M_0 & M_1 \\ M_1 & M_0 \end{pmatrix},$$

where $M_0 = I_a$ and $M_1 = 2U_a$.
Now,

$$M_0 + M_1 = I_a + 2U_a$$

and

$$M_0 - M_1 \;=\; I_a - 2U_a.$$

By using ***Lemma* 4**, the spectrum of $SL_{KCD_1}\left(\overline{CP(a)}\right)$ is

$$SL_{Spec_{KCD_1}}\left(\overline{CP(a)}\right) \;=\; \begin{pmatrix} -1 & 3 \\ a & a \end{pmatrix}.$$

Further, employing the Eq. (3), we establish

$$\begin{aligned} SLE_{KCD_1}\left(\overline{CP(a)}\right) &= \sum_{i=1}^{n=2a} \left|\eta_i^+ - 1\right| \\ &= 4a. \end{aligned}$$

□

Acknowledgments

Authors are thankful to Karnatak University, Dharwad, Karnataka, India for the support through University Research Studentship (URS), No.KU/Sch/URS/2020-21/1103 dated: 21/12/2020.

References

[1] N. Abreu, D. M.Cardoso, I. Gutman, E. A. Martins, M. Robbiano, Bounds for the signless Laplacian energy, *Linear Algebra Appl.*, **435** (2011) 2365–2374. ⇒ 22, 23, 24

[2] N. Biggs, *Algebraic Graph Theory*, Cambridge University Press, New York, 1993. ⇒28

[3] D. Cvetković, Signless Laplacians and line graphs, *Bull. Acad. Serbe Sci. Arts Cl. Sci. Math. Natur.*, **131,** 30 (2005) 85–92. ⇒24

[4] D. Cvetković, M. Doob, H. Sachs, *Spectra of Graphs: Theory and Applications*, Academic Press, New York, USA, 1980. ⇒28

[5] D. Cvetković, P. Rowlinson, S. K. Simić, Signless Laplacians of finite graphs, *Linear Algebra Appl.*, **423,** 1 (2007) 155–171. ⇒24

[6] D. Cvetković, P. Rowlinson, S. K. Simić, Eigenvalue bounds for the signless Laplacian, *Publ. Inst. Math.*, **81,** 95 (2007) 11–27. ⇒24

[7] D. Cvetković, P. Rowlinson, S. K. Simić, *An Introduction to the Theory of Graph Spectra*, Cambridge University Press, Cambridge, UK, 2010. ⇒24

[8] D. Cvetković, S. K. Simić, Towards a spectral theory of graphs based on the signless Laplacian I, *Publ. Inst. Math.*(Beograd), **85** (2009) 19–33. ⇒22
[9] J. A. Gallian, A dynamic survey of graph labeling, *Electron. J. Comb.*, **17** (2018), #DS6. ⇒27
[10] I. Gutman, B. Zhou, Laplacian energy of a graph, *Linear Algebra Appl.*, **414** (2006) 29–37. ⇒22
[11] I. Gutman, The energy of a graph, *Ber. Math. Stat. Sekt. Forschungsz. Graz.*, **103** (1978) 1–22. ⇒22
[12] F. Harary, *Graph Theory*, Addison-Wesely, Reading, Mass, 1969. ⇒22
[13] G. Indulal, I. Gutman, A. Vijaykumar, On distance energy of graphs, *MATCH Commun. Math. Comput. Chem.*, **60** (2008) 461–472. ⇒22, 25
[14] K. G. Mirajkar, A. Morajkar, First KCD matrix and first KCD energy of a graph, Accepted for publication in *Mathematical Forum*, **28** (2020). ⇒23
[15] K. G. Mirajkar and A. Morajkar, Laplacian energy of a first KCD matrix, Communicated for publication in *Commun. Combin., Cryptogr. & Computer Sci.* ⇒ 23, 25
[16] B. Zhou, More on energy and Laplacian energy, *MATCH Commun. Math. Comput. Chem.*, **64** (2010) 75–84. ⇒22

Received: February 3, 2022 • Revised: March 23, 2022

Acta Univ. Sapientiae Informatica **14,** 1 (2022) 35–48

DOI: 10.2478/ausi-2022-0003

Limit laws for two distance-based indices in random recursive tree models

Sarkoat NADERI
Department of Statistics
Science and Research Branch
Islamic Azad University
Tehran, Iran
email: snaderi@gmail.com

Ramin KAZEMI
Department of Statistics
Faculty of Basic Sciences
Imam Khomeini International University
Qazvin, Iran
email: r.kazemi@sci.ikiu.ac.ir

Mohammad H. BEHZADI
Department of Statistics
Science and Research Branch
Islamic Azad University
Tehran, Iran
email: behzadi@srbiau.ac.ir

Abstract. In this paper, we derive several results related to total path length and Sackin index in two classes of random recursive trees. A limiting distribution of the normalized version of the Sackin index is given by the contraction method in random recursive trees. Also, we show the normalized total path length converges in L^2 and almost surely to a limiting random variable in plane-oriented recursive trees via martingales.

1 Introduction

A loopless graph G is a collection of vertices and edges connecting pairs of such vertices. The vertex set and the edge set of G are denoted by $\mathsf{V}(\mathsf{G})$ and

Computing Classification System 1998: E.1
Mathematics Subject Classification 2010: 05C05, 60F05
Key words and phrases: recursive trees, Sackin index, total path length, contraction method, martingale

$E(G)$, respectively. Trees are defined as connected graphs without cycles [2]. In a rooted tree, the depth of a vertex is the number of edges from the root to the vertex. The outdegree of vertex v is the number of tail ends adjacent to it (denoted by $d^+(v)$). The leaves of the tree are the vertices with outdegree zero. The Sackin index of a rooted tree is the sum of the depths of its leaves and the total path length is the sum of all root-to-vertex distances [17].

A tree T_n of order n labelled $1, 2, ..., n$ is a recursive tree if for each h $(2 \leq h \leq n)$ the labels of vertices in the unique path from the 1-st vertex to the h-th vertex of the tree form an increasing subsequence of set $\{1, 2, ..., h\}$. A random recursive tree (RRT) of order n is a tree picked at random from the family of all recursive trees of order n. We assume that each of all $(n-1)!$ possible choices of a tree is equiprobable. Equivalently, we may describe RRTs via the following tree evolution process, which generates RRTs of arbitrary order n. At step 1, the tee starts with the root (labeled by 1). At step $h+1$, the vertex with label $h+1$ is attached to any previous vertex v of the already grown tree T_h with probability $p_h(v) = 1/h$.

Let L_n^R be the number of leaves of the RRT of order n. Najock and Heyde [11] showed that

$$\mathbb{E}(L_n^R) = \frac{n}{2}, \qquad \mathbb{V}ar(L_n^R) = \frac{n}{12}$$

Let D_j^R be the depth of vertex j in a RRT of order n. In [12],

$$\mathbb{E}(D_j^R) = H_{j-1}, \quad \mathbb{V}ar(D_j^R) = H_{j-1} - H_{j-1}^{(2)},$$

where

$$H_n^{(p)} = \sum_{k=1}^{n} \frac{1}{k^p}, \quad H_n := H_n^{(1)}, \quad p \geq 1.$$

Assume that I_n^R is the total path length of a RRT. Then

$$\mathbb{E}(I_n^R) = n(H_n - 1),$$

which is asymptotically equivalent to $n \ln n$.

Mahmoud [9] showed that there is a random variable I^R such that

$$\frac{I_n^R - n \ln n}{n} \to I^R,$$

in quadratic mean and almost surely. Also, as $n \to \infty$,

$$\mathbb{V}ar(I_n^R) \sim \left(2 - \frac{1}{6}\pi^2\right) n^2.$$

A plane-oriented recursive tree (PORT) T_n is obtained from T_{n-1} by choosing a parent in T_{n-1} and adjoining a vertex labeled n to it. The vertex n can be adjoined at any of the insertion positions or gaps between the children of the chosen parent since insertion in each gap will give a different ordering. Similar to RRTs, we can describe the following description for this model:
Step 1: The tree starts with the root (labelled by 1).
Step $h+1$*:* The vertex with label $h+1$ is attached to any previous vertex v (with outdegree $d^+(v)$) of the already grown PORT T_h with probability

$$p_{h+1}(v) = \frac{1+d^+(v)}{2h-1}.$$

Plane-oriented recursive trees were introduced in the literature under a few different names such as heap-ordered trees, nonuniform recursive trees, scale-free trees (see [10] for main results on this tree).

The depth of node j in a random PORT of order n has been studied by Mahmoud et al. [10] and Panholzer and Prodinger [12]. They proved with different approaches that

$$\begin{aligned}\mathbb{E}(D_j^P) &= H_{2j-2} - \frac{1}{2}H_{j-1},\\ \mathbb{V}\mathrm{ar}(D_j^P) &= H_{2j-2} - \frac{1}{2}H_{j-1} - H^{(2)}_{2j-2} + \frac{1}{4}H^{(2)}_{j-1}.\end{aligned}$$

Then $\mathbb{E}(D_j^P) = \mathbb{V}\mathrm{ar}(D_j^P) = \frac{1}{2}\log j + \mathcal{O}(1)$. Let L_n^P be the number of leaves of a PORT of order n. Mahmoud and Smythe [10] showed that

$$\mathbb{E}(L_n^P) = \frac{2n-1}{3}, \qquad \mathbb{V}\mathrm{ar}(L_n^P) = \frac{n}{9} - \frac{1}{18} - \frac{1}{6(2n-1)}.$$

Assume that I_n^P is the total path length of a random PORT. Mahmoud [8] showed that

$$\mathbb{E}(I_n^P) = \left(H_{2n-3} - \frac{1}{2}H_{n-2}\right)\left(n - \frac{1}{2}\right) - \frac{1}{2}(n-1),$$

which is asymptotically equivalent to $\frac{1}{2}n\log n$.

Hwang [6] proved that the centered and normalized random variables $(I_n^P - \mathbb{E}(I_n^P))/n$ converge in distribution and with all moments to $\sqrt{\pi}I^P$, where a recurrence of the moments of I^P is given by

$$\eta_m = \mathbb{E}((I^P)^m) = \frac{\Gamma(m-1)\sum\limits_{a+b+c=m}\binom{m}{a,d,c}\eta_a\eta_b\int_0^1 x^{a-3/2}(1-x)^{b-1/2}\varphi(x)^c\,dx}{2\sqrt{\pi}\Gamma(m-1/2)},$$

for $m \geq 2$ with $\eta_0 = 1$ and $\eta_1 = 0$ ($0 \leq a, b, c \leq m$). Here

$$\varphi(x) = (x \log x + (1-x)\log(1-x) + 2x)/(2\sqrt{\pi}).$$

Note that

$$\mathbb{V}ar(I_n^P) \sim \left(\frac{3}{2} - \frac{\pi^2}{8}\right) n^2.$$

The article is organized as follows. In Section 2, we give the average Sackin index in our tree models. In Section 3, a limiting distribution of the normalized version of the Sackin index is given by the contraction method in RRTs. Also, via martingales, the normalized total path length is shown to converge in L^2 and almost surely to a limiting random variable in PORTs.

2 Average Sackin index

Let S_n^R be the Sackin index of a RRT of order n. Szymański [18] showed that $\mathbb{E}(S_n^R) = \frac{n}{2}H_n - \frac{n}{4}$. He used from conditional expectation for proving this result. First, we prove this simple result by another method.

Lemma 1 *Let $(t_n)_{n\geq 1}$ be a give sequence and define a_n by $a_0 = 0$ and*

$$a_n = \frac{2}{n-1}\sum_{k=1}^{n-1} a_k + t_n.$$

Then for $n \geq 1$,

$$a_n = 2n\sum_{k=1}^{n-1} \frac{t_k}{k(k+1)} + t_n.$$

Proof. We have

$$2\sum_{k=1}^{n-2} a_k = (a_{n-1} - t_{n-1})(n-2).$$

Then

$$\begin{aligned} a_n &= \frac{1}{n-1}\Big(2\sum_{k=1}^{n-2} a_k + 2a_{n-1}\Big) + t_n \\ &= \frac{n}{n-1}a_{n-1} - \frac{n-2}{n-1}t_{n-1} + t_n. \end{aligned}$$

By iteration, proof is completed. □

Theorem 2 *The average Sackin index S_n^R of a RRT of order n is given by*

$$\mathbb{E}(S_n^R) = \frac{n}{2}H_n - \frac{n}{4}.$$

Proof. Let J_n be the size of the subtree rooted at node 2 in a recursive tree built from labels $1, 2, ..., n$. Then J_n is distributed uniformly on $\{1, 2, ..., n-1\}$. Conditioning on J_n,

$$S_n^R \stackrel{d}{=} S_{J_n}^R + S_{n-J_n}^{R*} + L_{J_n}^R, \tag{1}$$

where $S_k^R \stackrel{d}{=} S_k^{R*}$, $S_0^R = 0$, $S_1^R = 0$ and S_k, S_k^{R*} and J_n are independent. Suppose $a_n = \mathbb{E}(S_n^R)$ and $t_n = \mathbb{E}(L_{J_n}^R)$. Then

$$a_n = \frac{2}{n-1}\sum_{k=1}^{n-1} a_k + t_n,$$

where

$$t_n = \frac{1}{n-1}\sum_{k=1}^{n-1} \mathbb{E}(L_k^R) = \frac{n}{4}.$$

From Lemma 1, proof is completed. □

Corollary 3 *We have*

$$\mathbb{E}(S_n^R) = \frac{1}{2}n\log n + \Big(\frac{\gamma}{2} - \frac{1}{4}\Big)n + \mathcal{O}(n^{-1}),$$

where γ is the Euler's constant. Then, the average total path length is asymptotically twice as much as the asymptotic average Sackin index.

Let $\mathcal{I}_n$ be the size of the first subtree of the root in a random PORT. Then

$$P(\mathcal{I}_n = j) := \pi_{n,j} = \frac{2(n-j)C_jC_{n-j}}{nC_n}, \quad 1 \le j < n$$

where $C_n = \binom{2n-2}{n-1}/n$ denotes the (shifted) Catalan numbers [4]. Also,

$$C_n \sim \pi^{-1/2}n^{-3/2}4^{n-1}.$$

Theorem 4 *The average Sackin index S_n^P of a random PORT of order n is given by*

$$\mathbb{E}(S_n^P) = \Big(n - \frac{1}{2}\Big)\Big(\frac{2}{3}H_{2n} - \frac{1}{3}H_n\Big) - \frac{2}{3}n + \frac{1}{3}, \quad n \ge 3.$$

Proof. By conditioning on the size of the first subtree of the root, J_n,

$$S_n^P \stackrel{d}{=} S_{\mathcal{I}_n}^P + S_{n-\mathcal{I}_n}^{P*} + L_{\mathcal{I}_n}^P, \qquad n \geq 3 \tag{2}$$

where $S_j^P \stackrel{d}{=} S_j^{P*}$, $S_0^P = 0$, $S_1^P = 0$ and S_j^P, S_j^{P*} are independent. Suppose $a_n = \mathbb{E}(S_n^P)$. Then

$$a_n = 2\sum_{j=1}^{n} \pi_{n,j} a_j + b_n, \tag{3}$$

where

$$b_n = \mathbb{E}(L_{J_n}^P) = \sum_{j=1}^{n-1} \mathbb{E}(L_j^P)\pi_{n,j} = \frac{4^{n-1}}{3nC_n} - \frac{1}{3}.$$

The recurrence (3) has the exact solution (assuming $a_0 = b_0 = 0$)

$$a_n = \sum_{j=1}^{n} \frac{C_j(n+1-j)C_{n+1-j}}{C_n} b_j.$$

Denote by $[z^n]f(z)$ the coefficient of z^n in the Taylor expansion of $f(z)$. Then [3],

$$[z^n]\frac{1}{\sqrt{1-z}} \log\frac{1}{1-z} = 4^{-n}\binom{2n}{n}(2H_{2n} - H_n),$$

Thus

$$\mathbb{E}(S_n^P) = -\frac{n}{3} + \frac{1}{12C_n}\binom{2n}{n}(2H_{2n} - H_n) - \frac{n}{3} + \frac{1}{3},$$

and proof is completed. □

Corollary 5 *We have*

$$\mathbb{E}(S_n^P) = \frac{1}{3} n \log n + \Big(\frac{\gamma}{3} + \frac{2}{3}\log 2 - \frac{2}{3}\Big)n + \mathcal{O}(\log n),$$

where γ is the Euler's constant. Thus, asymptotically,

$$\mathbb{E}(S_n^P) \sim \frac{2}{3}\mathbb{E}(I_n^P).$$

3 Limiting results

Contraction method introduced in [14] for studying the quicksort algorithm. This method is famous and useful in the process of achieving the limiting distribution [13, 16]. Here, we shall use the setting of Hwang and Neininger [7] and consider a subset of RRTs in which the number of leaves in subtree rooted at node 2, $L^R_{J_n}$, is known. Let us consider the normalized random variables

$$X_n = \frac{S^R_n - \mathbb{E}(S^R_n)}{n}, \qquad n \geq 2.$$

From (1),

$$X_n \stackrel{d}{=} \frac{J_n}{n} X_{J_n} + \frac{n - J_n}{n} X^*_{n-J_n} + c_n(J_n), \quad n \geq 2 \tag{4}$$

where

$$c_n(j) \;=\; \frac{\mathbb{E}(S^R_j) + \mathbb{E}(S^R_{n-j}) - \mathbb{E}(S^R_n) + L^R_j}{n}.$$

According to (1), X_n, X^*_n, and $(\frac{J_n}{n}, \frac{n-J_n}{n}, c_n)$ are independent, and $X_n \stackrel{d}{=} X^*_n$ for all $n \geq 0$. If $\frac{J_n}{n}$, $\frac{n-J_n}{n}$ and c_n stabilize as $n \to \infty$, say, to A_1, A_2, and c, respectively, and we expect that X_n converges in distribution, then the weak limit X of X_n should satisfy the following limiting equation:

$$X \stackrel{d}{=} A_1 X + A_2 X^* + c, \tag{5}$$

where X, X^*, and (A_1, A_2, c) are independent and $X \stackrel{d}{=} X^*$. We use the minimal L_2-metric ℓ_2 where ℓ_r-metrics are defined on the spaces $\mathcal{M}_r$ of probability measures on the Borel σ-algebra of $\mathbb{R}$ with finite absolute rth moment by [13]:

$$\ell_r(\mu, \nu) = \inf\{\|X - Y\|_r, \quad X \stackrel{d}{=} \mu, Y \stackrel{d}{=} \nu\}, \quad \mu, \nu \in \mathcal{M}_r, \quad r \geq 1.$$

Let $\mathcal{M}_r(0)$ be the subspace of the centered probability measures in $\mathcal{M}_r$. The metric spaces $(\mathcal{M}_r, \ell_r)$ and $(\mathcal{M}_r(0), \ell_r)$ are complete. Also, convergence is equivalent to weak convergence and convergence of the rth absolute moment. The existence of a unique fixed-point $\mathcal{L}(X)$ in $\mathcal{M}_2(0)$ for (5) and the convergence in ℓ_2 of X_n given by (4) to X holds particularly if the following properties are satisfied [15]:

(a) $\mathbb{E}(c_n) = \mathbb{E}(c) = 0, \quad \mathbb{E}(c^2) < \infty.$

(b) $\|(\frac{J_n}{n}, \frac{n-J_n}{n}, c_n) - (A_1, A_2, c)\|_2 \to 0.$

(c) $\mathbb{E}(A_1^2) + \mathbb{E}(A_2^2) < 1.$

(d) For all $n_1 \in \mathbb{N}$, $\mathbb{E}\left(\mathbb{I}_{\{J_n \leq n_1\}} \left(\frac{J_n}{n}\right)^2\right) + \mathbb{E}\left(\mathbb{I}_{\{n-J_n \leq n_1\}} \left(\frac{n-J_n}{n}\right)^2\right) \to 0.$

Lemma 6 *Assume* J_n *is distributed uniformly on* $\{1, 2, ..., n-1\}$ *and* U *is a uniform random variable over the unit interval. Then*

$$\left(\frac{J_n}{n}, \frac{L^R_{J_n}}{n}\right) \xrightarrow{L_2} \left(U, \frac{U}{2}\right).$$

Proof. It is not hard to see that J_n has, conditioned on $U = u$, the binomial $B(n-1, u)$ distribution, and U has, conditioned on $J_n = k$, the $beta(k+1, n+1)$ distribution. Thus

$$\begin{aligned}
\mathbb{E}(UJ_n) &= \mathbb{E}(\mathbb{E}(UJ_n|U)) \\
&= \frac{n-1}{3}, \\
\mathbb{E}\left(\frac{L^R_{J_n}}{n}\right)^2 &= \frac{1}{n^2(n-1)} \sum_{j=1}^{n-1} \mathbb{E}(L_j^{R2}) \\
&= \frac{1}{12}, \\
\mathbb{E}(J_n L^R_{J_n}) &= \frac{1}{n-1} \sum_{j=1}^{n-1} \mathbb{E}(jL_j^R) \\
&= \frac{n(2n-1)}{12}, \\
\mathbb{E}(UL^R_{J_n}) &= \mathbb{E}(\mathbb{E}(UL^R_{J_n}|J_n)) \\
&= \frac{1}{n+1}(\mathbb{E}(J_n L^R_{J_n}) + n/4) \\
&= \frac{n(2n-1)}{12(n+1)} + \frac{n}{4(n+1)}.
\end{aligned}$$

Hence

$$\begin{aligned}
\mathbb{E}\left(\frac{J_n}{n} - U\right)^2 &= \frac{1}{3n} - \frac{1}{6n}, \\
\mathbb{E}\left(\frac{L^R_{J_n}}{n} - \frac{U}{2}\right)^2 &= \frac{1}{6} - \frac{n^2}{6n(n+1)} - \frac{1}{6n(n+1)} - \frac{1}{4(n+1)}.
\end{aligned}$$

By the L_2-convergence definition, proof is completed.

□

From Lemma 6,

$$\left\|\frac{J_n}{n} - U\right\|_2 \to 0, \qquad \left\|\frac{n - J_n}{n} - (1-U)\right\|_2 \to 0.$$

Also,

$$c_n(J_n) \xrightarrow{L_2} c(U) = \frac{1}{2}\Big(U\log U + (1-U)\log(1-U) + U\Big).$$

This establishes the stabilization of the modified recursion (4) to the limiting equation

$$X \stackrel{d}{=} UX + (1-U)X^* + \frac{1}{2}\Big(U\log U + (1-U)\log(1-U) + U\Big). \tag{6}$$

The limiting equation (6) defines a map $S(U)$ on $\mathcal{M}_2$:

$$S_U : \mathcal{M}_2 \to \mathcal{M}_2, \quad \mu \mapsto \mathcal{L}(UZ + (1-U)Z^* + c(U)), \tag{7}$$

where Z, Z^*, U are independent and $Z \stackrel{d}{=} Z^* \stackrel{d}{=} \mu$.

Theorem 7 *Let S_n^R be the Sackin index of a RRT of order n. Then*

$$\ell_2\left(\frac{S_n^R - \mathbb{E}(S_n^R)}{n}, X_U\right) \to 0,$$

where $\mathcal{L}(X_U)$ is the unique fixed-point in $\mathcal{M}_2(0)$ of the map S_U defined in (7).

Proof. The restriction of S_U to $\mathcal{M}_2(0)$ is a map into $\mathcal{M}_2(0)$. For this, suppose that $\mu \in \mathcal{M}_2(0)$. Then $S_U(\mu)$ has a finite second moment because of the same property of the coefficients and independence. Since $\frac{L_{J_n}^R}{n} \to \frac{U}{2}$ in L_2, $\mathbb{E}(U/2) = 1/4$, and thus $\mathbb{E}(c(U)) = 0$. This implies $\mathbb{E}(S_U(\mu)) = 0$, and then $S_U(\mu) \in \mathcal{M}_2(0)$. S_U is Lipschitz continuous on $(\mathcal{M}_2(0), \ell_2)$ such that [6],

$$lip(S_U) \le (\mathbb{E}(U^2) + \mathbb{E}((1-U)^2))^{\frac{1}{2}} = \sqrt{\frac{2}{3}} < 1.$$

Thus S_U is a contraction on space $\mathcal{M}_2(0)$. From Banach's fixed-point theorem, S_U has a (unique) fixed-point $\mathcal{L}(X_U)$ in $\mathcal{M}_2(0)$. By (6),

$$X_U \stackrel{d}{=} A_1 X_U + A_2 X_U^* + c(U).$$

It remains to check the conditions (a)-(d). First, by taking expectations in (4) and (6), respectively, we obtain $\mathbb{E}(c_n) = \mathbb{E}(c) = 0$; also, $\mathbb{E}(c^2) < \infty$. Thus (a) is satisfied. It is not hard to see that condition (b) is satisfied and also condition (c) is the contraction property of S_U. Finally, condition (d) follows from $\frac{J_n}{n}, \frac{n-J_n}{n} < 1$ since

$$\begin{aligned} & \mathbb{E}\left(\mathbb{I}_{\{J_n \le n_1\}}\left(\frac{J_n}{n}\right)^2\right) + \mathbb{E}\left(\mathbb{I}_{\{n-J_n \le n_1\}}\left(\frac{n-J_n}{n}\right)^2\right) \\ \le\ & P(J_n \le n_1) + P(n - J_n \le n_1) \\ =\ & \frac{2n_1}{n} \to 0, \end{aligned}$$

for all $n_1 \in \mathbb{N}$. Proof is completed by applying Rösler's theorem [15].

□

Corollary 8 *By Theorem 7,*

$$\mathbb{V}ar(S_n^R) = n^2 \mathbb{V}ar(X_n) \sim n^2 \mathbb{E}(X_U^2).$$

Since X_U *solves* (6)*, we deduce, by taking squares and expectations, that*

$$\mathbb{E}(X_U^2) = 3\mathbb{E}(c^2(U)) = \frac{1}{2} - \frac{\pi^2}{24}.$$

Then

$$\mathbb{V}ar(S_n^R) \sim \left(\frac{1}{2} - \frac{\pi^2}{24}\right) n^2.$$

If the $L_{J_n}^R$ is unknown, there are two ways to overcome the problem but both require a much more refined study of the problem. Firstly, one can try to generalize Rösler's proof. This seems to require to first derive the asymptotic behavior of the covariance $Cov(S_n^R, L_n^R)$ since such terms will additionally appear in Rösler's estimates. Secondly, one could try to study the joint distribution of (S_n^R, L_n^R) by means of the contraction method. This would also require to estimate the covariance. The fixed-point equation then will be

$$\begin{pmatrix} X \\ Y \end{pmatrix} \stackrel{d}{=} \begin{pmatrix} U & 0 \\ 0 & \sqrt{U} \end{pmatrix} \begin{pmatrix} X \\ Y \end{pmatrix} + \begin{pmatrix} 1-U & 0 \\ 0 & \sqrt{1-U} \end{pmatrix} \begin{pmatrix} X^* \\ Y^* \end{pmatrix} + \begin{pmatrix} c(U) \\ 0 \end{pmatrix}.$$

It can be expected that in this case, too, the claim presented in Theorem 7 is hold.

Let $D(v)$ (or D_v for convenient) be the depth of vertex v. Assume that r is the root of T_n. Each vertex in $V(T_n) \setminus \{r\}$ is a child of another vertex and is counted in its outdegree. Hence

$$\bigcup_{i=1}^{n} \bigcup_{j \in N^+(i)} \{j\} = \bigcup_{i=1}^{n} N^+(i) = V(T_n) \setminus \{r\},$$

where $N^+(i)$ is the set of children of i and $\sum_{i=1}^{n} d^+(i) = n-1$. Assume that $d^+(i) = t$ and its children are $i_1, i_2, ..., i_t$. Thus, for each $j \in \{1, 2, ..., t\}$, we have $D(i_j) = D(i) + 1$. This implies that

$$\sum_{j=1}^{t} D(i_j) = t\,(D(i)+1) = d^+(i)D(i) + d^+(i).$$

Since the depth of root is zero, we have

$$\sum_{i=1}^{n} (d^+(i)D(i) + d^+(i)) = \sum_{i=1}^{n} \Big(\sum_{j \in N^+(i)} D(j) \Big) = \sum_{i=1}^{n} D(i) = I_n.$$

This implies that

$$\sum_{i=1}^{n} d^+(i)\, D(i) = I_n - \sum_{i=1}^{n} d^+(i) = I_n - (n-1).$$

Lemma 9 *Let I_n^P be the total path length of a random PORT. Then for $n \geq 4$,*

$$\mathbb{E}(I_n^P | \mathcal{F}_{n-1}) = \frac{2n-1}{2n-3} I_{n-1}^P + \frac{n-1}{2n-3}$$

Proof. Let $\mathcal{F}_n$ be the sigma-field generated by the first n stages of PORTs. Let U_n be a randomly chosen vertex belonging to a PORT of order n. By

definition, $I_n^P = I_{n-1}^P + D(U_{n-1}) + 1$. Then

$$\begin{aligned}
\mathbb{E}(I_n^P|\mathcal{F}_{n-1}) &= I_{n-1}^P + \mathbb{E}(D(U_{n-1})|\mathcal{F}_{n-1}) + 1 \\
&= I_{n-1}^P + \sum_{i=1}^{n-1} \frac{1 + d^+(i)}{2n-3} D(i) + 1 \\
&= I_{n-1}^P + \frac{1}{2n-3}\left(\sum_{i=1}^{n-1} D(i) + \sum_{i=1}^{n-1} d^+(i)D(i)\right) + 1 \\
&= I_{n-1}^P + \frac{1}{2n-3}\left(2I_{n-1}^P - (n-2)\right) + 1 \\
&= \frac{2n-1}{2n-3} I_{n-1}^P + \frac{n-1}{2n-3}.
\end{aligned}$$

□

The proof of Lemma 9 for the internal path length of RRTs has also been done by the contraction method where the dependence problem of the present paper does not occur [1]. The proof of the following theorem is similar to the proof of a closely related result in [8].

Theorem 10 *We have*

$$\frac{I_n^P - \mathbb{E}(I_n^P)}{2n} \longrightarrow I^P,$$

in L^2 *and almost surely where* I^P *is a limiting random variable.*

Proof. From lemma 9, $\{\frac{I_n^P - \mathbb{E}(I_n^P)}{2n-1}, \mathcal{F}_n\}_{n\geq 1}$ is a martingale with uniformly bounded second moments. By the existence of the mean of I_n^P for each n, absolute integrability of the sequence $(W_n)_{n\geq 1}$ is guaranteed. Hence, the $(W_n)_{n\geq 1}$ is a zero-mean martingale. We have $I_n^P = I_{n-1}^P + D_n^P$ where D_n^P is the depth of label n. Then

$$\mathbb{E}(D_n^P|\mathcal{F}_{n-1}) = \mathbb{E}(I_n^P|\mathcal{F}_{n-1}) - I_{n-1}^P = \frac{2}{2n-3} I_{n-1}^P + \frac{n-1}{2n-3}.$$

To compute the second moment of W_n, we formulate a recurrence for it as follows. We have

$$\begin{aligned}
W_n &= \frac{I_{n-1}^P + D_n^P - \mathbb{E}(I_{n-1}^P + D_n^P)}{2n-1} \\
&= \frac{2n-3}{2n-1} W_{n-1} + \frac{D_n^P - \mathbb{E}(D_n^P)}{2n-1}.
\end{aligned}$$

Squaring the above relation, then taking expectations yields:

$$\mathbb{E}(W_n^2) = \left(\frac{2n-3}{2n-1}\right)^2 \mathbb{E}(W_{n-1}^2) + \frac{\mathbb{V}ar(D_n^P)}{(2n-1)^2} = \frac{2n-3}{(2n-1)^2}\mathbb{E}(W_{n-1}(D_n^P - \mathbb{E}(D_n^P))).$$

We have $\mathbb{E}(W_{n-1}\mathbb{E}(D_n^P)) = 0$. Thus in the last term we need only to find $\mathbb{E}(W_{n-1}D_n^P)$. But

$$\begin{aligned}\mathbb{E}(W_{n-1}D_n^P) &= \mathbb{E}(W_{n-1}\mathbb{E}(D_n^P|\mathcal{F}_{n-1})) \\ &= \mathbb{E}\left(W_{n-1}\left(2W_{n-1} + \frac{2}{2n-3}\mathbb{E}(I_{n-1}^P) + \frac{n-1}{2n-3}\right)\right) \\ &= 2\mathbb{E}(W_{n-1}^2).\end{aligned}$$

Then

$$\mathbb{E}(W_n^2) = \frac{2n-3}{2n-1}\mathbb{E}(W_{n-1}^2) + \frac{\mathbb{V}ar(D_n^P)}{(2n-1)^2} = \frac{c[n]}{c[n-1]}\mathbb{E}(W_{n-1}^2) + t[n],$$

where

$$c[n] = \frac{\Gamma\left(n-\frac{1}{2}\right)}{\Gamma\left(n+\frac{1}{2}\right)}, \quad t[n] = \frac{\mathbb{V}ar(D_n^P)}{(2n-1)^2}, \quad n \geq 1.$$

The solution to the recurrence gives $\mathbb{E}(W_n^2)$ as

$$\mathbb{E}(W_n^2) = c[n]\sum_{j=1}^{n}\frac{t[j]}{c[j]}.$$

The sum in $\mathbb{E}(W_n^2)$ converges, i.e., $\mathbb{E}(W_n^2)$ is bounded uniformly in n. Convergence almost surely and in L^2 follows from the martingale convergence theorem [5]. □

Acknowledgements

We would like to express our thanks for the anonymous referees.

References

[1] R. Dobrow, J. A. Fill, Total path length for random recursive trees. Random graphs and combinatorial structures (Oberwolfach, 1997). *Combin. Probab. Comput.* **8,** 4 (1999) 317–333. ⇒46

[2] M. Drmota, *Random Trees, An Interplay Between Combinatorics and Probability*, Springer, Wien-New York, 2009. ⇒36
[3] W.-C. Chen, W.-C. Ni, On the average altitude of heap-ordered trees, *Int. J. Found. Comput. Sci.* **5,** 1 (1994) 99–109. ⇒40
[4] B. Gittenberger, The number of descendants in simply generated random trees. In: Gardy, D., Mokkadem, A. (eds) *Mathematics and Computer Science. Trends in Mathematics.* Birkhäuser, Basel. pp. 65–73. https://doi.org/10.1007/978-3-0348-8405-1_6 ⇒39
[5] P. Hall, C. C. Heyde, *Martingale Limit Theory and its Application*, Academic Press, New York, 1980. ⇒47
[6] H.-K. Hwang, Profiles of random trees: plane-oriented recursive trees. *Random Structures Algorithms.* **30,** 3 (2007) 380–413. ⇒37, 43
[7] H.-K. Hwang, R. Neininger, Phase change of limit laws in the quicksort recurrence under varying toll functions. *SIAM J. Comput.* **31** (2002) 1687–1722. ⇒41
[8] H. M. Mahmoud, Distances in random plane-oriented recursive trees, *J. Comput. Appl. Math.* **41** (1992) 237–245. ⇒37, 46
[9] H. M. Mahmoud, Limiting distributions for path lengths in recursive trees. *Probab. Eng. Inform. Sci.* **5** (1991) 53–59. ⇒36
[10] H. Mahmoud, R.T. Smythe, J. Szymański, On the structure of random plane-oriented recursive trees and their branches. *Random Structures Algorithms.* **4,** 2 (1993) 151–176. ⇒37
[11] D. Najock, C.C. Heyde, On the number of terminal vertices in certain random trees with an application to stemma construction in philology. *J. Appl. Probab.* **19,** 3 (1982) 675–680. ⇒36
[12] A. Panholzer, H. Prodinger, Level of nodes in increasing trees revisited, *Random Structures Algorithms.* **31,** 2 (2007) 203–226. ⇒36, 37
[13] S. Rachev, L. Rüschendorf, Probability metrics and recursive algorithms, *Adv. Appl. Probab.* **27** (1995) 770–799. ⇒41
[14] U. Rösler, A limit theorem for "quicksort", *RAIRO-Inform. Theor. Appl.* **25** (1991) 85–100. ⇒41
[15] U. Rösler, The analysis of stochastic divide and conquer algorithms, *Algorithmica.* **29** (2001) 238–261. ⇒41, 44
[16] U. Rösler, L. Rüschendorf, The contraction method for recursive algorithms, *Algorithmica.* **29** (2001) 3–33. ⇒41
[17] M. J. Sackin, "Good" and "bad" phenograms, *Systematic Zoology.* **21** (1972) 225–226. https://doi.org/10.1093/sysbio/21.2.225 ⇒36
[18] J. Szymański, On the complexity of algorithms on recursive trees. *Theoret. Comput. Sci.* **74,** 3 (1990) 355–361. ⇒38

Received: February 12, 2022 • Revised: April 14, 2022

Acta Univ. Sapientiae Informatica **14,** 1 (2022) 49–74

DOI: 10.2478/ausi-2022-0004

U-Net architecture variants for brain tumor segmentation of histogram corrected images

Szidónia LEFKOVITS
George Emil Palade University of Medicine, Pharmacy, Science, and Technology Târgu Mureş,
Department of Electrical Engineering and Information Technology
email: szidonia.lefkovits@umfst.ro

László LEFKOVITS
Sapientia Hungarian University of Transylvania, Cluj-Napoca
Department of Electrical Engineering, Târgu Mureş
email: lefkolaci@ms.sapientia.ro

Abstract. In this paper we propose to create an end-to-end brain tumor segmentation system that applies three variants of the well-known U-Net convolutional neural networks. In our results we obtain and analyse the detection performances of U-Net, VGG16-UNet and ResNet-UNet on the BraTS2020 training dataset. Further, we inspect the behavior of the ensemble model obtained as the weighted response of the three CNN models. We introduce essential preprocessing and post-processing steps so as to improve the detection performances. The original images were corrected and the different intensity ranges were transformed into the 8-bit grayscale domain to uniformize the tissue intensities, while preserving the original histogram shapes. For post-processing we apply region connectedness onto the whole tumor and conversion of background pixels into necrosis inside the whole tumor. As a result, we present the Dice scores of our system obtained for WT (whole tumor), TC (tumor core) and ET (enhanced tumor) on the BraTS2020 training dataset.

Computing Classification System 1998: I.4.6
Mathematics Subject Classification 2010: 68T07
Key words and phrases: brain tumor segmentation, histogram uniformization, U-Net, VGG16-UNet, ResNet50-UNet, BraTS2020

1 Introduction

The automatic processing of medical images is one of the fastest-growing domains in the field of computer assisted medical diagnosis and surgery. The automation systems concentrate on the use of various artificial intelligence methods relying mostly on supervised learning. Generally, the computing algorithms have the role of identifying different malformations in the healthy tissues. Their role is to localize them by applying a detection algorithm or to segment the image, determining the class of each pixel. These algorithms are based on an enormous amount of data on which the algorithms have to be trained in order to obtain a capability for generalization on unseen images. In this paper we concentrate on medical image segmentation, namely, on brain tumor segmentation from MRI (Magnetic Resonance Image) data. The tumors in the brain can develop into two types: LGG (Low-Grade Glioma) and HGG (High-Grade Glioma). According to the WHO, tumors can be categorized into 4 subtypes: Grade I and II are LGG and III and IV are HGG. Grade I is a benign and slow-growing tumor, while grade II presents increased hypercellulality and can develop into a HGG tumor. Grade III and IV are much more severe variants. Grade III shows a high rate of hypercellularity and a high rate of mitosis, while Grade IV is an advanced form of Grade III in which necrosis and vascular proliferation occur [10]. Early diagnosis is essential in the treatment of the disease and facilitates timely initiation of treatment or other necessary medical interventions. It is also essential to note that computerized detection is a rapid process providing a non-contact diagnosis tool for physicians. The worldwide spread of MRI equipment and the growing number of MRI records acquired should make the general screening of the population possible, thereby detecting cases in an early stage.

The bottlenecks of an automatic brain tumor segmentation are the great variety of positions, dimensions, aspects and textures of the tumor; the deformation of the normal tissues; the wide variety of MRI equipment used without a given standardized protocol; the varying resolutions and pixel value inhomogeneity produced by different MRI machines.

MRI image processing methods can be classified into two large categories: traditional image processing methods and CNN methods. The pre-deep learning era concentrates on traditional pattern recognition methods, such as thresholding, region-based and pixel classification methods or model-based techniques. Thresholding techniques include global thresholding, local thresholding or Gaussian distribution-based thresholding. Region-based methods search for common features of a given region such as homogeneity, similarity, region grow-

ing and watershed segmentation. Pixel classification methods and model-based methods are combined in various ways. According to the literature, this category comprises clustering methods, fuzzy c-means clustering, Markov Random Fields, Artificial Neural Networks, Self-organizing Maps, Random Forest [18], Boosting, Geometric Deformable Models, Level Set Methods, Charged Fluid Model and so on. Paper [12] presents a review of the above-mentioned methods.

The organization of the BraTS – Brain Tumor Segmentation World Grand Challenges represents a major leap in the development of brain tumor segmentation [29, 20, 4, 2]. This Challenge has been organized since 2012 by the MICCAI Society at the eponymous conference. From then on, the organizers, including dozens of contributors, have been gathering MRI images from hospitals and research centers. Until 2015, all methods were based on pre-deep learning models. In 2015-2016, the new deep learning technique expanded into the field of medical imaging as well. In [21] Pereira et al. propose CNNs exploring small kernels of 3×3 pixels to obtain deeper network architecture with a lower number of weights than larger kernels. In [28] the authors propose a two-step segmentation for brain tumors: first the authors train a Fully Convolutional Neural Network (FCN) and then train Conditional Random Fields as Neural Networks.

Kamnitsas et al. [16] describe a 3D 11-layered deep neural network in which they process adjacent image patches in a single pass through the networks to handle class imbalance. In order to handle local and global features, they propose a dual-pathway multi-resolution network. Xue et al. [27] introduces a novel Generative Adversarial Network (GAN) for medical image segmentation. In the GAN, the segmentor is an FCN producing segmentation label maps, while the adversarial critic is a multi-scale CNN with L1 loss. Ding et al. [11] describes the Deep Residual Dilate Network with Middle Supervision (RDM-Net) that combines the residual network with delated convolution for multi-modal brain tumor segmentation. Chen et al. [9] proposes a dual-force training scheme for the extended version of DeepMedic, leading to more accurate segmentation in the Multi-Level DeepMedic thus obtained. Wu et al. in article [26] introduces the Multi-features Refinement and Aggregation (MRA) that utilizes hierarchical features by combining features from different levels into an aggregation module passing the joined response through a second CNN. Isensee et al. [15] developed a network that configures itself automatically considering 2D and 3D U-Net and U-Net Cascade. It computes the number of downsampling/upsampling form the resolution of the data, the class ratio and the image size after cropping the background. In addition, it determines the

patch size, the batch size, the optimization function and the number of images to be augmented in order to fit into the GPU memory. This architecture has participated at the Medical Segmentation Decathlon Challenge [31] and has achieved one of the highest mean Dice scores in all segmentation challenges.

All referenced articles written after 2015 rely on the BraTS dataset collected between 2012-2020. The most up-to-date publicly available dataset was published in the TCGA-GBM [5] and TCGA-LGG collections [6].

The main contribution of this paper consists of two major steps: we apply the histogram uniformization described below as preprocessing for the image dataset and adapt the well-known U-Net architecture for the purpose of brain tumor segmentation. In addition to applying only the Vanilla-UNet, we also adapt and train VGG16-UNet, the ResNet50-UNet versions of the U-Net. We also create an ensemble model combining the probability responses of the 3 mentioned models.

The paper is organized as follows: following this first introductory section and a short literature review, our system is described, detailing the methods and models applied and going through every component of the segmentation pipeline. Finally, we present the results obtained and suggest a number of important improvements in the conclusion.

2 Materials and methods

Our proposed automated segmentation system (Figure 1) is based on different U-shaped deep convolutional neural networks. For semantic segmentation, the traditional convolutional neural networks are transformed into fully convolutional neural networks (FCNs). Our system is trained on the BraTS 2017-2020 database.

The original 3D images are preprocessed at the beginning to provide uniform tissue intensities on all the images. In the training process, the data is divided into training, validation and test sets. The training stops when the Dice score does not increase any more. After obtaining the segmentations of the 3D brains, the connectedness of the tumors is verified. Finally, our results are evaluated using the well-known measures of accuracy on the test set.

2.1 Database

The image database used in this study is a publicly available database provided by the organization committee of BraTS (Brain Tumor Segmentation World Grand Challenge). The database consists of 369 cases of 293 HGG images

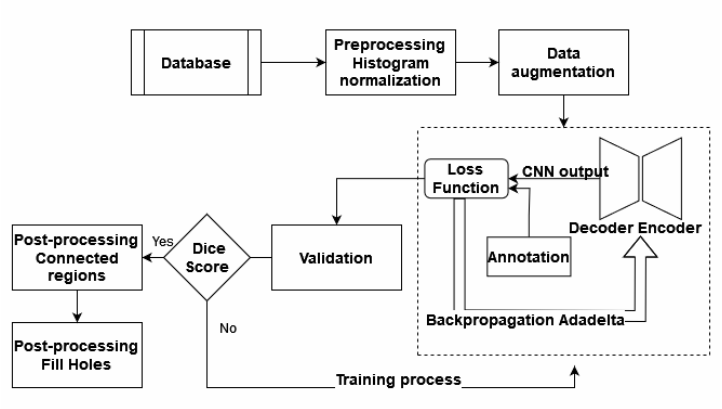

Figure 1: The proposed automatic segmentation pipeline

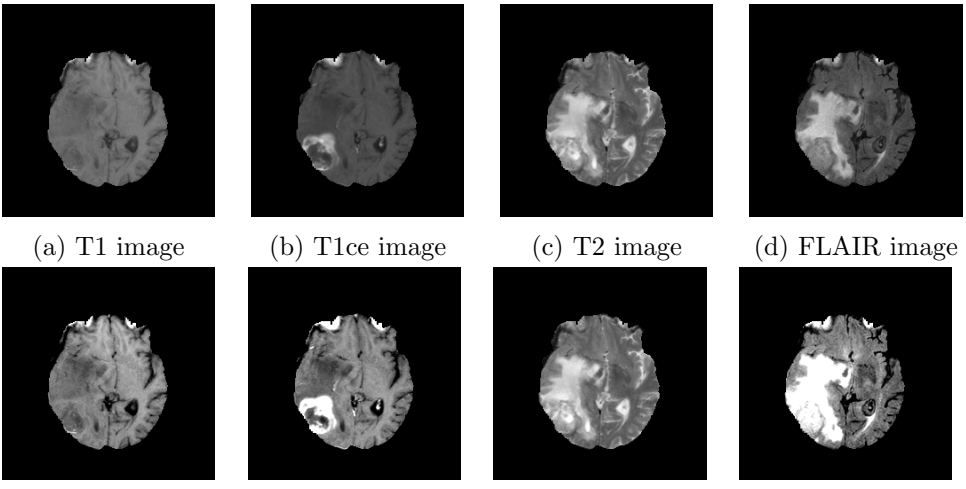

(a) T1 image (b) T1ce image (c) T2 image (d) FLAIR image

(e) corrected T1 (f) corrected T1ce (g) corrected T2 (h) corrected FLAIR

Figure 2: Histogram uniformization of the 4 modalities: 1. row: original images, 2. row: histogram unified images

and 76 LGG images. The images are of course in 3D with a resolution of $240 \times 240 \times 155$ pixels. 1 voxel corresponds to $1\ mm^3$. A human brain is about $1500\ cm^3$, represented by 1.5 million voxels. The image format is NifTI, with every image being multi-modal containing 4 modalities: T1 image (longitudinal relaxation time), T1ce image (T1ce-weigthed with contrast agent), T2 image (transverse relaxation time) and FLAIR image (T2-Fluid Attenuated Inversion Recovery) Figure 2-row1. All these images are acquired via the MRI machine with different hardware setups. Every image was annotated by experts and represents the corresponding ground truth.

The image classes are: class0 is the background and the healthy tissue; class1-necrotic tumor core (NEC, joined with the non-enhancing tumor-NET); class2-peritumoral edema (ED), class4-enhancing tumor (ET). Class3 (label3) is missing; it was initially the non-enhancing tumor (NET).

2.2 Preprocessing

The images in the original database are preprocessed applying the following steps: skull-stripping, they have the same resolution regardless of the MRI equipment and every image sets of the 4 modalities (T1, T1ce, T2, FLAIR) is co-registered to the same T1 template.

Intensity uniformization [13, 17] is an indispensable step in MRI image preprocessing. The differences in the setup and characteristics of the various equipment used to acquire images produce different intensity values for the same tissue. There is a wide range of intensity intervals that differs greatly from image to image. The same intensity grayscale value $I(x, y, z)$ can be the value of any of the possible tissue types (healthy, edema, enhanced or even necrosis) on different images. It is obvious that without obtaining the same intensity for the same tissue on different images the supervised learning cannot generalize and the segmentation results, without the preprocessing step, will be of low quality. The aim of the proposed histogram uniformization is to obtain the same intensity values for the same tissue over all images. Our uniformization method reduces the tissue intensity variance. We have chosen to transform the intensities between fist-quartile (Q_1) and third-quartile (Q_3) into a fixed experimentally defined interval $[int_1, int_2]$, because the intensity values in this range $[Q_1, Q_3]$ contain the major part of the image information. The interval $[int_1, int_2]$ is considered in the middle of the 8-bit grayscale range $[0, 255]$ (eq. 1). This histogram uniformization is a truncated linear transformation in which the values are limited into $[0, 255]$ (eq. 2). Every voxel of the

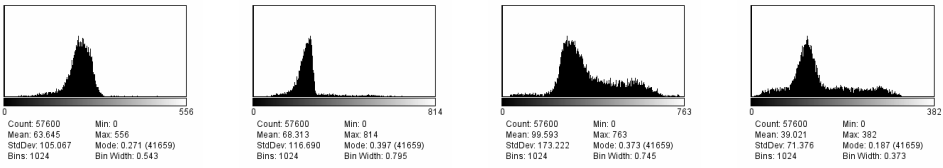

(a) T1 original histogram (b) T1ce original histogram (c) T2 original histogram (d) FLAIR original histogram

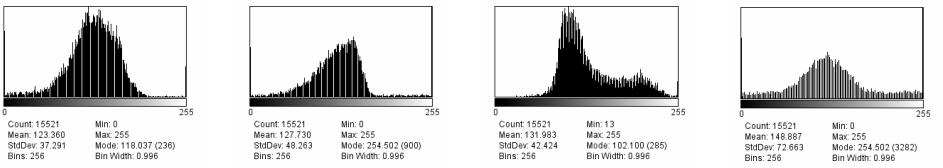

(e) T1 unified histogram (f) T1ce unified histogram (g) T2 unified histogram (h) FLAIR unified histogram

Figure 3: Original and corrected histograms of images in Figure 2

original image is transformed into the new 8-bit grayscale value by applying equations 1 and 2.

$$f(I(x,y,z)) = \frac{int_2 - int_1}{Q_3 - Q_1} \cdot I(x,y,z) + \frac{int_1 \cdot Q_3 - int_2 \cdot Q_1}{Q_3 - Q_1}, \qquad (1)$$

In this formula some values may be exceed the $[0, 255]$ interval, so the $f(I(x,y,z))$ is limited to the 8-bit grayscale value.

$$I_{new}(x,y,z) = \min\{\max\{0, f(I(x,y,z)\}, 255\} \qquad (2)$$

Thus, the histogram transformation is context-dependent and the initial wide range of values $[0, 6000]$ fits into the uint8=1byte data type (Figures 2 and 3).

2.3 CNN training

FCN is an encoder-decoder architecture (Figure 4), where the encoder obtains a convolutional code (small-sized feature) of the input image after several steps of halving and passing through the various usual layers (convolution, pooling, padding and batch normalization and dropout) in a CNN. The decoder is a symmetrical part of the encoder, built of transpose convolution, upsampling, concatenation and softmax layers. The encoder is the so-called contracting layer, since it reduces the image over a number of stages up to a given size. The output of the CNN at the end of the encoder is the code of the input

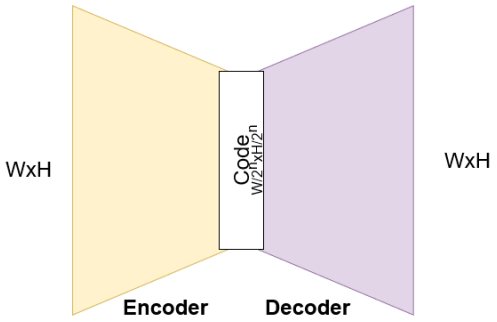

Figure 4: Encoder-decoder-type CNN

image. If the number of reductions is n, and each stage halves the input image size ($W \times H$), then after n steps the code size will be ($W/2^n \times H/2^n$). The decoder has to do the opposite operations in order to obtain a segmentation output of the same size as the original image. This is called the expending layer. The first FCN networks in the literature were SegNet [3], FCN [24] and U-Net [22].

The original U-Net [22] has 5 stages. From a grayscale input image of 572×572 pixels of resolution it obtains a code of 28×28 pixels. In the encoder part, each halving stage has the same structure: 2 convolution layers of kernel size 3×3 with a ReLU activation function (Figure 5 blue arrow), followed by a max-pooling layer with the role of halving the output of the previous convolution (Figure 5 dark red arrow). After each convolution, the input image size is reduced by 2 pixels in both width and height, due to the nature of the convolution operation applied. The inputs and outputs before and after each conv-layer are the stage-wise feature maps. At the first level of original size, the conv-layers are of depth 64 and 64; next, at a size of $1/2$, the convolutional layers are double to 128, 128, followed by two of depth 256, 256. At the size of $1/2^4$, the depth is doubled again to 512 and 512. At the end of the 5th stage, there are the last two convolutional layers of a depth of 1024, and the output of the last conv-layer is, in fact, the code of the input of size 28×28 pixels. From the code, the segmentation is obtained via the decoder part. Here, the convolutions are substituted by up-convolutions, also called transposed convolutions. These operations are the inverse-convolutions that are capable of doubling their input feature maps by padding them with zeros and passing through the kernel of the same size as the matching stage convolution kernel. In this manner they reach the $2 \times size$ (Figure 5 green arrow). The output of transposed convolutions have the same depth and size as the

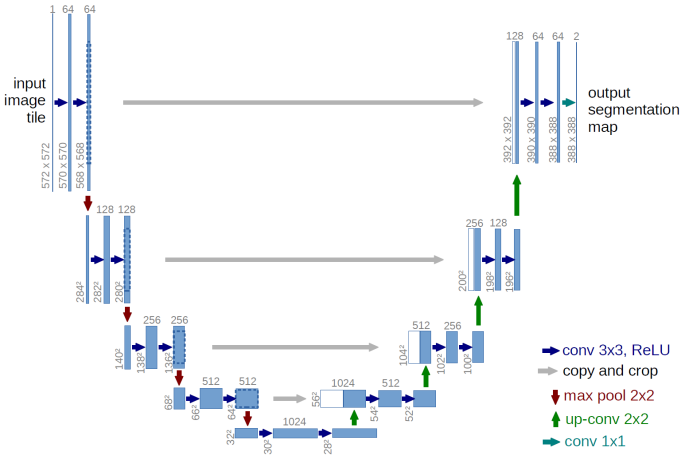

Figure 5: Original U-Net architecture [22]

corresponding convolutions. The trick here is the concatenation of the output of each encoder-stage to the first deconvolution at the same stage of the decoder (Figure 5 light gray arrow). Thus, if the input depth of the convolutions and deconvolutions were d_1 and d_1, respectively, the depth of concatenated layer will be $2d_1$. Consequently, the first deconvolution layer depth is doubled. The second deconvolution at each stage remains of the same depth d_1. The last layer is a bottleneck convolution (Figure 5 turquoise arrow) of depth 2 which obtains a segmentation map for both classes (object of interest and background.) All the details are shown in Figure 5.

In our adapted variant of U-Net, we consider 3 stages. The input image measures $240 \times 240 \times 4$ pixels. The third dimension is 4, containing the 4 image modalities (T1, T1c, T2 and FLAIR). Every stage consists of 2 convolutional layers. Each convolution is followed by batch-normalization and dropout layers. The stage-wise depth of the conv-layers is 32, 64 and 128. Halving is obtained via MaxPooling2D. The code size in our case is 60×60 pixels. The decoder part is the corresponding extending layer with the concatenation of the corresponding convolution output to the first deconvolution layer in each stage. The upsampling from a given size to its double, up to the original image size, is computed via transpose convolution with the role of Upsampling2D. The component diagram of the adapted U-Net architecture is shown in Figure 6.

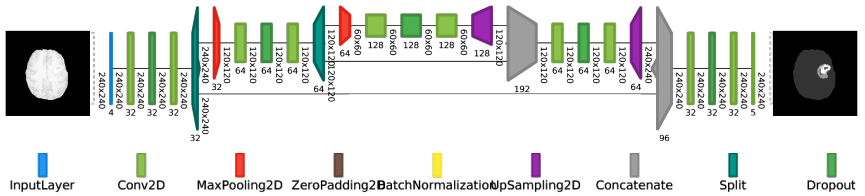

Figure 6: Adapted implementation of U-Net architecture for brain tumor segmentation

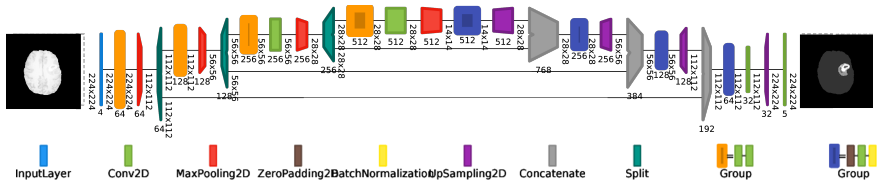

Figure 7: Adapted implementation of VGG-UNet architecture for brain tumor segmentation

The next architecture that was adapted into a U-Net-like architecture was the VGG16 [25] network. Here, the encoder part is formed based on the VGG16 architecture.

The VGG16-architecture [25] is made up of 5 stages from 224×224 pixels up to 7×7 pixels ($W/2^5 \times H/2^5$). Stages 1 and 2 contain 2 conv-layers of depth 64, 64 and 128, 128. Stages 3, 4 and 5 contain 3 conv-layers each of depth 256, 256, 256; 512, 512, 512 and 512, 512, 512. Here, the code size is 7×7 pixels. In case of classification, the code output is followed by two fully connected layers and a softmax classification layer.

The advantage of VGG16-UNet is that pretrained weights can be loaded onto this architecture. In the literature, the preloading of pretrained weights for other purposes is called transfer learning. We load the pretrained weights of ImageNet [30] into the encoder part and start the training process for the brain segmentation from those initial weight values. The ImageNet weights are weights obtained from training the VGG16 CNN network for distinguishing 1000 usual object classes, they are not related to segmentation.

The VGG16-UNet architecture, adapted for brain tumor segmentation, has the following structure: the adapted VGG16-UNet architecture. It considers the center-cropped brain images measuring 224×224 pixels. We consider 4 stages up to a size of 14×14 pixels. In one stage, we have two conv-layers padded to the same size as the stage input followed by the ReLU activation. In

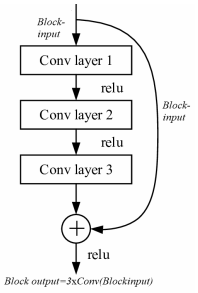

Figure 8: Residual Block with 3 conv-layers

Figure 7, a stage is denoted by the orange-colored Group. The corresponding transpose convolution is the blue group. The architectures of Figures 6 and 7 were created by the Net2Vis visualization grammar module [8].

The last architecture adapted for the purpose of multi-modal brain tumor segmentation was the ResNet50 [14]. The ResNet50 is made up of 5 convolutional blocks on the 5 consecutive sizes of the encoding part. Each block is implemented via the Residual module that learns the difference between the input and the output of the block. This residue is obtained by passing the input value through 2 or 3 convolutional layers. In our case the number of conv-layers of a residual block is 3 (Figure 8). The identity connection is in fact a skip connection.

Block1 is used once at the beginning, block2 is repeated 3 times with the 3 conv-layers $(1 \times 1, 64)$, $(3 \times 3, 64)$, $(1 \times 1, 256)$, block3 is repeated 4 times $(1 \times 1, 128)$, $(3 \times 3, 128)$, $(1 \times 1, 512)$, block4 appears 6 times $(1 \times 1, 256)$, $(3 \times 3, 256)$, $(1 \times 1, 1024)$ and the last block appears 3 times $(1 \times 1, 512)$, $(3 \times 3, 512)$, $(1 \times 1, 2048)$. The ResNet50-UNet is a network based on the ResNet architecture and combined with U-Net. The Encoder part of U-Net is substituted by the ResNet50 blocks. The architecture of ResNet50 is shown in Figure 9.

The convolution blocks represent the different stages on different input sizes. The triplets inside the conv-block represent the kernel-size $k \times k$ and the depth of the conv-layers $(k \times k, depth)$. Each conv-block is repeated a given number of times represented above the block, and the output size of every block is the resolution written under the block name.

The adapted ResNet50-UNet variant has corresponding transpose convolution layers concatenated to the outputs of the same-sized convolution block and followed by 2 convolution layer of depths (512,512); (256,256); (128,128)

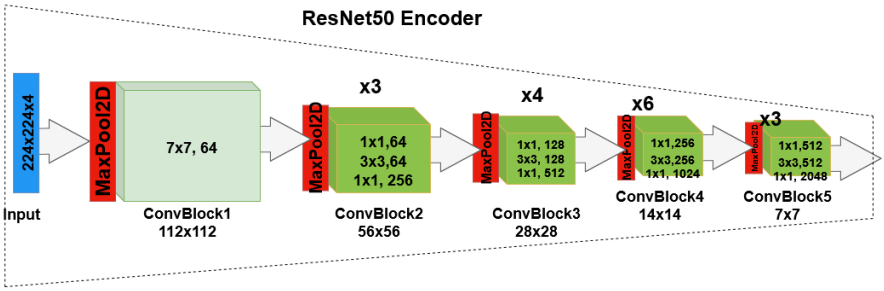

Figure 9: ResNet50 encoder: the first part of ResNet-UNet architecture

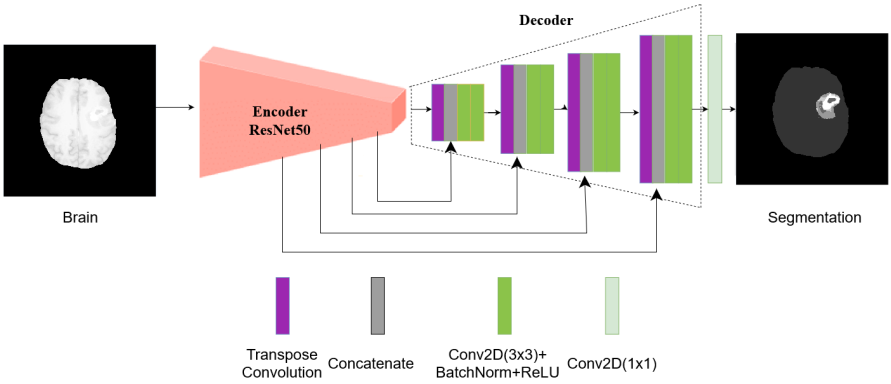

Figure 10: ResNet-UNet architecture

and (64,64). The output segmentation is obtained after a bottleneck convolution (Figure 10).

2.4 The training process

The training process is the usual training of CNN networks via the Backpropagation algorithm. The hyperparameters of the training are crucial from the perspective of the final training, validation and test scores.

Before the training starts, the preprocessed database is split into 3 parts: training (203 images=18676 slices)-60%, validation set (66 images=6006 slices)-20% and test set (66 images=10230 slices)–20%.

For the training and validation images, we only considered non-zero slices, while the test set used all slices. There were 18676 training image slices, 6006 validation images slices and 10230 test slices.

The main hyperparameters were set experimentally to obtain good validation performance. The batch size that fits into GPU memory is between 8 and 24 images. Such a batch of images is processed in parallel through the forward and backward passes of the CNN. The update to the weights is made once a batch. In every epoch, the whole training dataset is passed through the network once, in batches. The total number of training images over the batch size represents the number of iterations. Weights are adapted in every iteration. The entire process ran for 100 epochs or until a given validation Dice coefficient was met. The optimization method was AdaDelta and the loss function was the weighted mean Dice loss.

The AdaDelta optimization algorithm, instead of considering all past squared gradients, only considers those of a range with a fixed window size w. The sum of gradients is a recursive expression, an exponentially decaying average of all past squared gradients in w. It depends on the previous running average with weight γ and the current gradient with weight $(1-\gamma)$. The gradient update will be a product of the gradient and the proportion of the root-mean-square error (RMSE) of the previous update and the RMSE of the current gradient. The main advantage of AdaDelta is that the initial learning rate does not have to be set.

The loss based on which the optimization function was minimized is the weighted mean Dice-Sørensen loss (eq. 8). The Dice Similarity Coefficient (Dice) measures the similarity between two discrete pieces of data. In our case, it measures the similarity between the automatic segmentation obtained by our system and the gold standard annotations of experts. The Dice score is computed for every image in a batch, namely, for every image in the training set. It is a measure of similarity between the segmented image (Seg) and the ground truth (GT).

$$\mathrm{Dice}_I = \frac{2|Seg_I \cap GT_I|}{|Seg_I| + |GT_I| + \epsilon} \tag{3}$$

In the case of multi-class classification, the Dice score is computed class-wise, and the optimization process considers the mean-Dice loss.

$$\mathrm{mDice}_I = \sum_{c \in Classes} \mathrm{Dice}_I^c \tag{4}$$

The mean Dice score on every image or on a batch is computed by

$$\mathrm{mDice} = \sum_{\mathrm{I} \in \mathrm{Images}} \mathrm{Dice}_{\mathrm{I}} \tag{5}$$

The loss is computed from the mean Dice score of a batch.

$$\mathrm{Dice}_{\mathrm{Loss}} = 1 - \mathrm{mDice}_{\mathrm{I}} \tag{6}$$

In our training we have tried to train the CNN network not only based on the simple mean-Dice, but on the class-wise weighted Dice score ($\mathit{weight}_{\mathrm{c}}$) as well.

$$w\mathrm{mDice}_{\mathrm{I}} = \frac{2 \sum_{\mathrm{c} \in \mathrm{Classes}} \mathrm{weight}_{\mathrm{c}} |\mathrm{Seg}_{\mathrm{I}}^{\mathrm{c}} \cap \mathrm{GT}_{\mathrm{I}}^{\mathrm{c}}|}{\sum_{\mathrm{c} \in \mathrm{Classes}} \mathrm{weight}_{\mathrm{c}} \left(|\mathrm{Seg}_{\mathrm{I}}^{\mathrm{c}}| + |\mathrm{GT}_{\mathrm{I}}^{\mathrm{c}}| \right)} \tag{7}$$

$$w\mathrm{mDice} = \sum_{\mathrm{I} \in \mathrm{Images}} \mathrm{m}w\mathrm{Dice}_{\mathrm{I}} \tag{8}$$

The role of implementing the weighted mean Dice score ($w\mathrm{mDice}$) is to put more emphasis on the classes with much fewer pixels in the dataset and to overcome the problem of class imbalance. The weights were computed to be inversely proportional to the average of number of pixels in each class. The total number of pixels in an image is $240 \times 240 \times 155 \approx 9$ million. Of these, 1.5 million are brain pixels. About 2,000-90,000 pixels is tumor tissue, of which 40-80% is edema, 15-60% is enhancing tumor and 0-5% represents necrosis.

2.5 Post-processing

In the final post-processing step, we considered the formal structure of the tumors, namely, the tumor is a compact nodule. Usually, there can be 1 or sometimes 2 large nodules. Thus, we considered the 2 largest nodules, being, in volume, more than 90% of the total detected tumor regions. This way, the small false positive pixel regions could be eliminated. Another step was the elimination of false detected background pixels inside the whole tumor. These are very dark gray parts that can be easily mistaken for the background class by every autonomous system, but they are in fact necrotic regions.

3 Results and discussion

In our research we have implemented 3 variants of the U-Net [22] convolutional neural network and adapted them to be suitable for brain tumor seg-

mentation. The training of the autonomous system is based on the supervised learning method. The initial BraTS dataset is split into 3 disjoint sets: training, validation and test sets. The convolutional networks are trained on 18676 multi-modal images. The network is optimized via the AdaDelta optimization method, considering the weighted Dice loss function as optimization criteria. The weights are crucial in order to overcome the drawbacks of a class-unbalanced dataset. The weight multiplication factor for class 0 is $m_{w_0} = 1$, the weight for class 1 is $m_{w_1} = 2000$, while classes 2 and 4 are assigned $m_{w_2} = 400$ and $m_{w_4} = 800$, respectively.The factors are inversely proportional to the average size of the tumor tissue of each class. These weights are converted into the [0,1] interval.

$$weight_c = \frac{m_{w_c}}{\sum_{c \in Classes} m_{w_c}} \tag{9}$$

These weights are used only in computation of training losses. The training process stops after 100 epochs or if the mean Dice score on validation reaches 0.9915. Validation mean Dice score was determined experimentally. This value assures the sufficiently high Dice score (above 80-85%) on the whole tumor. A mean Dice score of 0.992-0.993 can be reached after running additional tens or hundreds of epochs. The further training last very long compared to the benefit of $< 1\%$ on the overall validation mean Dice score. The hyperparameters for training are batch-size between 16-24 images, and the number of iterations for an epoch is 500-1200. The weight parameter in AdaDelta is $\gamma = 0.9$. The total training time of a single CNN architecture is between 36 and 72 hours.

The hardware used for training was an NVIDIA 1080Ti GPU card with 11GB of memory. The training was done in Tensorflow Keras in the Python programming language. The visualization of the histograms and pre- and post-processing steps were done in ImageJ and Matlab.

The total number of parameters, namely, the trained and untrained weights are shown in Table 1.

Figures 11 and 12 show the comparison of the training process for the 3 convolutional neural networks.

The training process is very similar from the perspective of all 3 network types. It can be seen in Figure 11 that the simple U-Net increases the most, only after a few epochs. The mean Dice score indicates similarity as well, but the training loss for U-Net and ResNet50-UNet decreases more than for VGG-UNet.

Table 2 shows the increase in mean Dice scores throughout the training process. U-Net and ResNet50-UNet are the two best from this perspective.

CNN	Total parameters	Non-trainable parameters	Trainable parameters
U-Net	4,473,477	3,328	4,470,149
VGGUNet	13,324,667	1,920	12,322,757
ResNet50-UNet	16,375,173	32,512	16,342,661

Table 1: Trainable parameters of CNNs

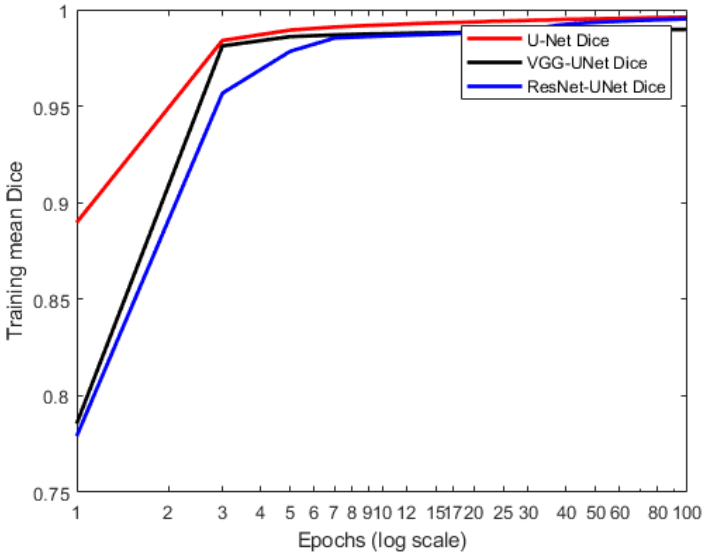

Figure 11: Training mean Dice score

Epoch	**U-Net**		**VGG-UNet**		**ResNet-UNet**	
	Loss	**Dice**	**Loss**	**Dice**	**Loss**	**Dice**
5	0.1102	0.8898	0.2144	0.7856	0.2209	0.7791
10	0.0082	0.9918	0.0126	0.9874	0.0140	0.9860
20	0.0065	0.9935	0.0118	0.9882	0.0121	0.9879
30	0.0057	0.9943	0.0114	0.9886	0.0102	0.9898
40	0.0051	0.9949	0.0111	0.9889	0.0078	0.9922
50	0.0048	0.9952	0.0109	0.9891	0.0067	0.9933
60	0.0046	0.9954	0.0108	0.9892	0.0062	0.9938
70	0.0043	0.9957	0.0107	0.9893	0.0056	0.9944
80	0.0041	0.9959	0.0106	0.9894	0.0053	0.9947
90	0.0040	0.9960	0.0103	0.9897	0.0051	0.9949
100	0.0039	0.9961	0.0102	0.9898	0.0049	0.9951

Table 2: Loss and Dice scores in training

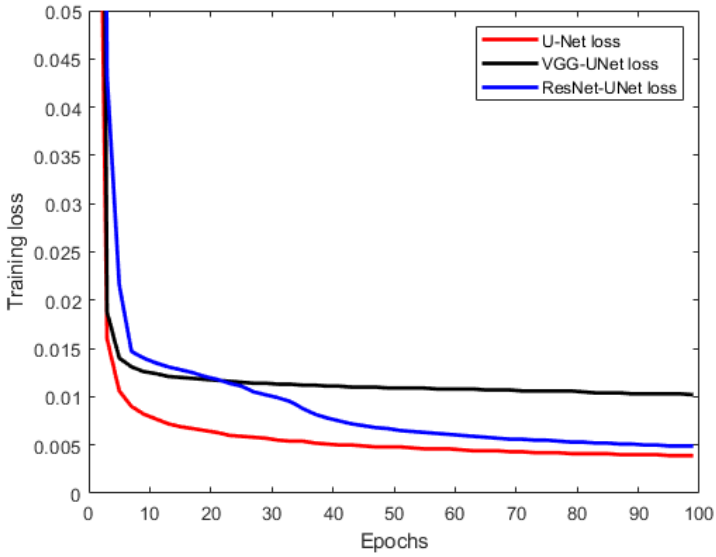

Figure 12: Training loss

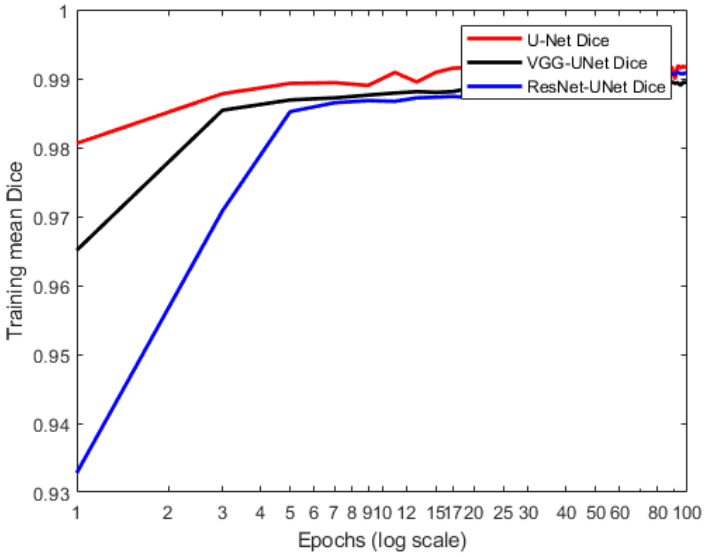

Figure 13: Validation mean Dice score

Form the standpoint of an autonomous systems the generalization capability is essential. A CNN is capable of generalization i.e. recognizes non-seen images with the same precision as in training if the validation score on the unseen validation set is similar to those obtained on the training set. Figures 13 and 14 and Table 3 present the results on the validation set.

The mean Dice score is very similar for all 3 networks. A very small change in the mean Dice score has a great impact on class-wise Dice scores. If the mean Dice score is not over 0.9915, then the segmentation of different classes is not high enough.

The real segmentation accuracy of the trained CNNs is determined by the performance scores of the different classes.

Tables 4 and 5 show the class-wise performance measure of the Dice score on the training and test sets. The optimization of the CNN models were done not on the class-wise Dice scores, but on the weighted mean Dice score. Small changes in the weighted mean Dice score may lead to noticeable class-wise Dice score change.

These tables show a superior performance for the simple U-Net and ResNet-UNet. The background and healthy tissues are detected with a Dice score of 0.9984-0.9985. Class1+3 represent necrosis and the non-enhanced tumor,

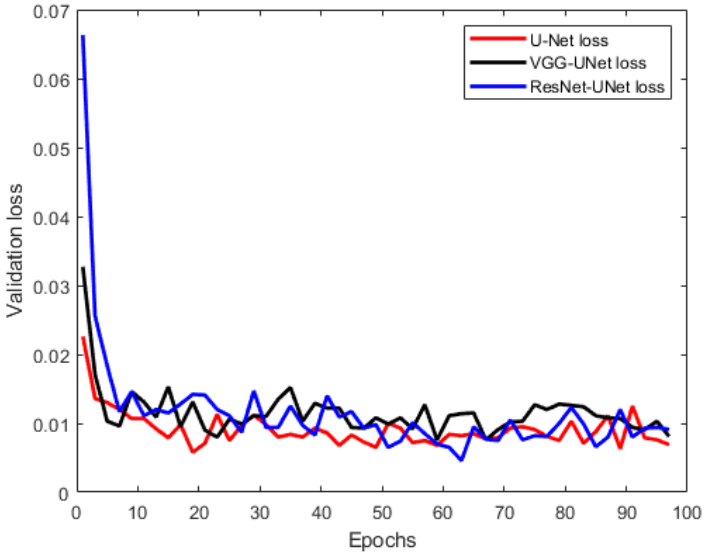

Figure 14: Validation loss

Epoch	**U-Net**		**VGG-UNet**		**ResNet-UNet**	
	Loss	**Dice**	**Loss**	**Dice**	**Loss**	**Dice**
5	0.0226	0.9806	0.0327	0.9651	0.0663	0.9328
10	0.0107	0.9890	0.0146	0.9876	0.0146	0.9868
20	0.0058	0.9916	0.0131	0.9885	0.0142	0.9873
30	0.0112	0.9904	0.0111	0.9885	0.0147	0.9885
40	0.0093	0.9914	0.0129	0.989	0.0083	0.9906
50	0.0065	0.9918	0.0108	0.9887	0.0098	0.9905
60	0.0075	0.9917	0.0127	0.9888	0.0085	0.9905
70	0.0079	0.9918	0.0091	0.9895	0.0075	0.9908
80	0.0075	0.9916	0.0128	0.989	0.0100	0.9907
90	0.0063	0.9916	0.0107	0.9895	0.012	0.9906
100	0.0074	0.9915	0.0102	0.9894	0.0108	0.9909

Table 3: Loss and Dice scores for the validation set

Training	Dice-Cl0	Dice-Cl1+3	Dice-Cl2	Dice-Cl4	Dice-WT	Dice-TC
U-Net	0.9991	0.7153	0.8557	0.8113	0.9200	0.8793
VGG-UNet	0.9981	0.4785	0.7237	0.7088	0.8219	0.7704
ResNet-UNet	0.9991	0.6989	0.8495	0.7860	0.9186	0.8722

Table 4: Class-wise Dice scores in training

Test	Dice-Cl0	Dice-Cl1+3	Dice-Cl2	Dice-Cl4	Dice-WT	Dice-TC
U-Net	0.9984	0.474	0.7272	0.7338	**0.8359**	**0.7773**
VGG-UNet	0.9984	0.4156	0.7117	0.7334	**0.8217**	**0.7618**
ResNet-UNet	0.9985	0.5005	0.7372	0.7488	**0.8434**	**0.7865**

Table 5: Class-wise Dice scores for the test set

respectively. This class can be easily mistaken for the dark background because of its very dark intensity on the MRI image. The Dice score results for this class are the lowest (47%-50%). Compared to the difficult class, the other two classes Class2 and Class4 are detected with a higher Dice score of (73%-74%).

In the literature, it is not the class-wise Dice coefficients that are compared; nevertheless, from the perspective of a physician, the Whole Tumor (WT), the Tumor Core (TC) and the Enhanced Tumor (ET) are much more important. The WT is the joint region of all the tumor types (Class1+3 $\cup$ Class2 $\cup$ Class4). The TC is the union of Class1+3 $\cup$ Class4, without the edema region. The third type ET is Class4.

If we consider these tumoral regions, the results become much better. Tables 6 and 7 show the results for WT and TC, and the results for ET are the same as those specified for Cl4 (Tables 4 and 5).

All the three U-Net models were improved via post-processing steps. The two main corrections steps applied were fillholes and connected components. In the 3D image if a region inside a tumor was detected background it was set to be Class1, i.e. necrosis. From the detection results only the greatest connected components were kept for which the cumulative sum of the total pixels is above 90% of the total detected tumor pixels. The rest (small regions compared to the volume of greatest) was considered false positive and was

Training	**Dice-WT**	**Sens-WT**	**Spec-WT**	**Dice-TC**	**Sens-TC**	**Spec-TC**
U-Net	0.9200	0.9278	0.999	0.8793	0.8820	0.9987
VGG-UNet	0.8219	0.9081	0.9972	0.7704	0.7395	0.9983
ResNet-UNet	0.9186	0.9432	0.9988	0.8722	0.8563	0.9989

Table 6: Dice score of tumor regions in training

Test	**Dice-WT**	**Sens-WT**	**Spec-WT**	**Dice-TC**	**Sens-TC**	**Spec-TC**
U-Net	0.8359	0.8335	0.9986	0.7773	0.8259	0.9977
VGG-UNet	0.8217	0.8524	0.9982	0.7618	0.7843	0.9980
ResNet-UNet	0.8434	0.8586	0.9984	0.7865	0.8122	0.9981

Table 7: Dice score of tumor regions for the test set

erased from the segmentation. These post-processing steps brought a 2-3% improvement compared to the original results (Tables 5 and 9).

The best results here are obtained by ResNet-UNet WT=0.8688 and TC=0.8286. We also considered the ensemble model, which is the joint response of the probability maps for the 3 individual networks and the ensemble. The joint response obtains a 1-2% improvement compared to the best out of the three models presented (Table 8).

Figure 15 shows the segmentation results for the three U-Net variants studied. Visual comparison of the results becomes exceedingly difficult. The results are very similar; however, U-Net and ResNet-UNet achieve the best results, especially on Class1+3. On Figure 15 different colors denote different tissues: background (Class0) is black, Class2 is the edema denoted by light gray, Class4

Test	**Dice-WT**	**Sens-WT**	**Spec-WT**	**Dice-TC**	**Sens-TC**	**Spec-TC**
Ensemble model	0.8765	0.8727	0.9988	0.8169	0.8461	0.9981

Table 8: Dice score of ensemble model

Test	Dice-WT	Sens-WT	Spec-WT	Dice-TC	Sens-TC	Spec-TC
U-Net	0.8623	0.8542	0.9986	0.7992	0.8496	0.9976
VGG-UNet	0.8534	0.8660	0.9983	0.7892	0.8276	0.9978
ResNet-UNet	0.8688	0.8836	0.9984	0.8076	0.8286	0.9981

Table 9: Dice score of tumor regions with post-processing

BraTS 2020	Dice-WT	Dice-ET	Dice-TC
McHugh [19]	0.859	0.766	0.788
Savadikar [23]	0.818	0.688	0.716
Ali [1]	0.871	0.748	0.748
Bommineni [7]	0.883	0.718	0.787
Isensee [15]	0.889	0.820	0.850
Our ResNet-UNet	0.8688	0.7507	0.8076
Our Ensemble	0.8765	0.7588	0.8169

Table 10: Comparison to BraTS2020

enhanced tumor is the white part, and the innermost tumor region is the non-enhanced+necrotic part (Class1+3) labelled with light gray.

Table 10 shows the most up-to-date results published for the BraTS2020 competition in 2021. The models featured all are different version of the U-Net network. Our WT, ET and TC results are similar to the results described in the literature.

4 Conclusions

In this paper we present an automated system used for brain tumor segmentation. We compare three well-known CNN networks used for object detection and adapt them for the purpose of brain tumor segmentation. The three net-

(a) Ground truth (b) U-Net (c) VGG-UNet (d) ResNet-UNet (e) Ensemble

Figure 15: Segmented images – black: background; light gray: edema; white: enhanced tumor; dark gray: non-enhanced tumor+necrosis

works converted to encoder-decoder networks were U-Net, VGG16-UNet and ResNet50-UNet. The main contributions of this paper are: the intensity uniformization of the BraTS2020 dataset, the adaptation of CNN networks for brain tumor segmentation, training and evaluation of the segmentation system obtained. In the preprocessing phase all of the different image intensity ranges were transformed into the standard grayscale domain of [0,255] while maintaining the histogram form of the original image. Using this preprocessed dataset we have adapted and trained the mentioned three models for brain tumor segmentation. Moreover, these models were combined into an ensemble that achieved an overall performance boost of 2%.

To obtain even better results, we further suggest to implement and apply other types of CNN networks that use the attention module and multi-pathway models with different scales and resolutions with the role of correcting the segmentation on the tissue borders. We also propound to implement the 3D U-Net for brain tumor segmentation and compare the results presented to those of a 3D-CNN. The 3D models require more GPU capacity to fit into the memory and are usually implemented in HPC environments. In addition, a cascade of multiply applied binary classifications of the different tumor regions would improve segmentation. In our future work, we suggest to first segment the whole tumor, followed by the edema, tumor core and finally the enhanced tumor and necrosis. The role of this type of classification is an even better delimitation of different tissue types. Moreover, we set to improve our results even more by concentrating especially on the tissue borders that are the least accurately detected. All these suggestions would additionally improve the results presented in this paper.

Acknowledgements

The work was supported by the University of Medicine, Pharmacy, Science and Technology "George Emil Palade" of Târgu Mureș, Research Grant Number 292/4/14.01.2020.

References

[1] M. J. Ali, M. T. Akram, H. Saleem, B. Raza, A. R. Shahid, Glioma segmentation using ensemble of 2D/3D U-nets and survival prediction using multiple features fusion, *Brainlesion: Glioma, Multiple Sclerosis, Stroke and Traumatic Brain Injuries*, *Lecture Notes in Comput. Sci.*, **12659** (2021), 189–199. ⇒70

[2] U. Baid, S. Ghodasara, M. Bilello et al. The RSNA-ASNR-MICCAI BraTS 2021 benchmark on brain tumor segmentation and radiogenomic classification, *CoRR*, abs/2107.02314, 2021. ⇒51

[3] V. Badrinarayanan, A. Kendall, R. Cipolla, Segnet: A deep convolutional encoder-decoder architecture for image segmentation. *CoRR*, abs/1511.00561, 2015. ⇒56

[4] S. Bakas, M. Reyes, A. Jakab et al. Identifying the best machine learning algorithms for brain tumor segmentation, progression assessment, and overall survival prediction in the BRATS challenge, *CoRR*, abs/1811.02629, 2018. ⇒51

[5] S. Bakas, H. Akbari, A. Sotiras, M. Bilello, M. Rozycki, J. Kirby, J. Freymann, K. Farahani, C. Davatzikos, Segmentation labels for the pre-operative scans of the TCGA-GBM collection, 2017. ⇒52

[6] S. Bakas, H. Akbari, A. Sotiras, M. Bilello, M. Rozycki, J. Kirby, J. Freymann, K. Farahani, C. Davatzikos, Segmentation labels for the pre-operative scans of the TCGA-LGG collection, 2017. ⇒52

[7] V. L. Bommineni, Piecenet: A redundant Unet ensemble,*Brainlesion: Glioma, Multiple Sclerosis, Stroke and Traumatic Brain Injuries*, *Lecture Notes in Comput. Sci*, **12659** (2021), pp. 331–341. ⇒70

[8] A. Bäuerle, C. van Onzenoodt, T. Ropinski, Net2vis – a visual grammar for automatically generating publication-tailored CNN architecture visualizations, *IEEE Transactions on Visualization and Computer Graphics*, **27**, 6,(2021) 2980–2991. ⇒59

[9] S. Chen, C. Ding, M. Liu, Dual-force convolutional neural networks for accurate brain tumor segmentation, *Pattern Recognition*, **88** (2019), 90–100. ⇒51

[10] C.-B. S. Sang-Geun Choi, Detection of HGG and LGG brain tumors using U-Net,*Medico Legal Update*, **19**, 1, (2019) 560–565. ⇒50

[11] Y. Ding, C. Li, Q. Yang, Z. Qin, Z. Qin, How to improve the deep residual network to segment multi-modal brain tumor images, *IEEE Access*, **7**, (2019) 152 821–152 831. ⇒51

[12] N. Gordillo, E. Montseny, P. Sobrevilla, State of the art survey on MRI brain tumor segmentation, *Magnetic Resonance Imaging Journal*, **31**, 8, (2013) 1426–1438. ⇒51

[13] A. Győrfi, L. Szilágyi, L. Kovács, A fully automatic procedure for brain tumor segmentation from multi-spectral MRI records using ensemble learning and atlas-based data enhancement, *Applied Sciences*, **11**, 2 (2021). ⇒54

[14] K. He, X. Zhang, S. Ren, J. Sun, Deep residual learning for image recognition, *CoRR* abs/1512.03385, 2015. ⇒59

[15] F. Isensee, P. F. Jäger, P. M. Full, P. Vollmuth, K. H. Maier-Hein, nnU-net for brain tumor segmentation, *Brainlesion: Glioma, Multiple Sclerosis, Stroke and Traumatic Brain Injuries.Lecture Notes in Comput. Sci.*, **12659** (2021), 118–132. ⇒51, 70

[16] K. Kamnitsas, C. Ledig, V. F. Newcombe, J. P. Simpson, A. D. Kane, D. K. Menon, D. Rueckert, B. Glocker, Efficient multi-scale 3D CNN with fully connected CRF for accurate brain lesion segmentation, *Medical Image Analysis*, **36**, (2017) 61–78. ⇒51

[17] Kőble, A., Győrfi, Á., Csaholczi, S., Surányi, B., Dénes-Fazakas, L., Kovács, L., Szilágyi, L. Identifying the most suitable histogram normalization technique for machine learning based segmentation of multispectral brain MRI data. *2021 IEEE AFRICON, Arusha, Tanzania*, 2021, pp. 71-76. ⇒54

[18] L. Lefkovits, S. Lefkovits, L. Szilágyi, Brain tumor segmentation with optimized random forest, *International Workshop on Brainlesion: Glioma, Multiple Sclerosis, Stroke and Traumatic Brain Injuries.Lecture Notes in Comput. Sci.* **10154** (2016), 88–99. ⇒51

[19] H. McHugh, G. M. Talou, A. Wang, 2D dense-unet: A clinically valid approach to automated glioma segmentation, *Brainlesion: Glioma, Multiple Sclerosis, Stroke and Traumatic Brain Injuries*, *Lecture Notes in Comput. Sci.* **12659** (2021), 69–80. ⇒70

[20] B. H. Menze, A. Jakab, S. Bauer, J. Kalpathy-Cramer et al. The multimodal brain tumor image segmentation benchmark (brats), *IEEE Transactions on Medical Imaging*, **34**, 10 (2015) 1993–2024. ⇒51

[21] S. Pereira, A. Pinto, V. Alves, C. A. Silva, Brain tumor segmentation using convolutional neural networks in MRI images, *IEEE Transactions on Medical Imaging*, **35**, 5 (2016) 1240–1251. ⇒51

[22] O. Ronneberger, P. Fischer, T. Brox, U-Net: Convolutional networks for biomedical image segmentation,*CoRR*, abs/1505.04597, 2015. ⇒56, 57, 62

[23] C. Savadikar, R. Kulhalli, B. Garware, Brain tumour segmentation using probabilistic U-Net,*Brainlesion: Glioma, Multiple Sclerosis, Stroke and Traumatic Brain Injuries*, *Lecture Notes in Comput. Sci.* **12659** (2021), pp. 255–264. ⇒70

[24] E. Shelhamer, J. Long, T. Darrell, Fully convolutional networks for semantic segmentation, *IEEE Transactions on Pattern Analysis and Machine Intelligence*, **39**, 4, (2017) 640–651. ⇒56

[25] K. Simonyan, A. Zisserman, Very deep convolutional networks for large-scale image recognition, *CoRR* abs/1409.1556, 2015. ⇒58

[26] D. Wu, Y. Ding, M. Zhang, Q. Yang, Z. Qin, Multi-features refinement and aggregation for medical brain segmentation, *IEEE Access*, **8** (2020), 57 483–57 496. ⇒51

[27] Y. Xue, T. Xu, H. Zhang, L. R. Long, X. Huang, SegAN: Adversarial network with multi-scale L1 loss for medical image segmentation, *Neuroinformatics*, **16**, 3-4, (2018), 383–392. ⇒51

[28] X. Zhao, Y. Wu, G. Song, Z. Li, Y. Zhang, Y. Fan, A deep learning model integrating FCNNs and CRFs for brain tumor segmentation, *Medical Image Analysis*, **43**, (2018) 98–111. ⇒51

[29] ∗∗∗ Brain Tumor Segmentation (BraTS) challenge, `https://www.med.upenn.edu/cbica/brats2021/`, 2021, online; accessed, April 2022. ⇒51

[30] ∗∗∗ ImageNet,`https://image-net.org`, 2022, online; accessed, April 2022. ⇒58

[31] ∗∗∗ Medical Segmentation Decathlon Challenge, `http://medicaldecathlon.com/`, 2021, online; accessed, April 2022. ⇒52

Received: April 20, 2022 • Revised: May 9, 2022

Acta Univ. Sapientiae Informatica **14,1** (2022) 75–83

DOI: 10.2478/ausi-2022-0005

On graphs associated to ring of Guassian integers and ring of integers modulo n

S. PIRZADA
Department of Mathematics, University of Kashmir, Srinagar, Kashmir, India
email: pirzadasd@kashmiruniversity.ac.in

M. Imran BHAT
Department of Mathematics, University of Kashmir, Srinagar, Kashmir, India
email: imran.uok.maths@gmail.com

Abstract. For a commutative ring R with identity 1, the zero-divisor graph of R, denoted by $\Gamma(R)$, is a simple graph whose vertex set is the set of non-zero zero divisors $Z^*(R)$ and the two vertices x and $y \in Z^*(R)$ are adjacent if and only if $xy = 0$. In this paper, we compute the values of some graph parameters of the zero-divisor graph associated to the ring of Gaussian integers modulo n, $\mathbb{Z}_n[i]$ and the ring of integers modulo n, $\mathbb{Z}_n$.

1 Introduction

Throughout this paper, all rings are assumed to be commutative with unity unless explicitly stated otherwise. Given a commutative ring with identity R, the zero-divisor graph of R, denoted by $\Gamma(R)$, is the graph where the vertices are the nonzero zero-divisors ($Z^*(R)$) of R, and there is an undirected edge between two distinct vertices x and y if and only if $xy = 0$. An annihilator of an element x of a ring R, denoted by $ann(x)$, is the set$ann(x) = \{r \in R : rx = 0\}$. The zero-divisor graph that Anderson and Livingston [1] introduced allows us to

Computing Classification System 1998: G.2.2
Mathematics Subject Classification 2010: 13A99, 05C78, 05C12
Key words and phrases: ring, zero-divisor graph, ring of Gaussian integers, ring of integers modulo n

visually represent algebraic properties of a commutative, unital ring through graph theoretic properties. This ability to use graph-theoretic properties to visualize underlying algebraic properties is applicable to many different types of rings.

The set of Gaussian integers $\mathbb{Z}[i]$ is a subset of $\mathbb{C}$ defined as $\mathbb{Z}[i] = \{a + ib \mid a, b \in \mathbb{Z} \text{ and } i = \sqrt{-1}\}$. Let $\mathbb{Z}_n = \{0, 1, 2, \ldots, n-1\}$ be the ring of integers modulo n. Then, the quotient ring $\mathbb{Z}[i]/\langle n\rangle$ is isomorphic to $\mathbb{Z}_n[i] = \{a + ib \mid a, b \in \mathbb{Z}_n\}$, where $\langle n\rangle$ is a principal ideal generated by n for some positive integer larger than 1 in $\mathbb{Z}[i]$. Several results on zero-divisor graphs of the ring of integers modulo n and the ring of Gaussian integers modulo n can be found in [5, 6, 7, 8, 11].

All graphs G in this article will be simple. The vertex set of G will be denoted by $V(G)$. In G, the distance between two vertices x and y, denoted $d(x, y)$, is the length of the shortest path. A maximal connected subgraph of a graph G is called a *component* of G, and the number of components of a graph G is denoted by $k(G)$. A vertex v of G is called a cut vertex of G if $k(G - v) > k(G)$. The *vertex-connectivity* of G, denoted by $\kappa_v(G)$, is the smallest number of vertices whose removal from the graph G results in either a disconnected graph or a single vertex graph. The eccentricity of x, denoted by $e(x)$, is the maximum of the distances from x to the other vertices of G. The minimum eccentricity value is the radius of G. Note that any graph G with radius 1 necessarily has at least one vertex adjacent to all other vertices of G. We denote the *minimum* and *maximum* degree of a graph G by $d_\delta(G)$ and $d_\Delta(G)$ respectively. For $n \geq 1$, K_n will denote a *complete graph* on n vertices containing all $\binom{n}{2}$ possible edges. In a graph G, if no two vertices of a subset $\mathcal{A}$ of the vertex set V are adjacent, then $\mathcal{A}$ is said to be an *independent* set. A maximal complete subgraph of G is a *clique* of G and the order of a clique of G is the *clique number*, denoted by $clq(G)$. More on graph theory definitions, the reader is referred to [9].

In Section 2, we obtain the values of some parameters, like clique number $\omega(G)$, chromatic number $\chi G)$ and radius $rad(G)$ of the zero-divisor graph associated to the ring of integers modulo n, denoted by $\mathbb{Z}_n$, and the ring Gaussian integers modulo n, denoted by $\mathbb{Z}_n[i]$.

2 Zero-divisor graph of $\mathbb{Z}_{q^m}[i]$, $q \cong 3 \pmod 4$ and $\mathbb{Z}_n$

Theorem 1 *Let* $\Gamma(\mathbb{Z}_{q^m}[i])$ *be the zero-divisor graph of* $\mathbb{Z}_{q^m}[i]$, *where* $q \cong 3 \pmod 4$. *Then the clique number of* $\Gamma(\mathbb{Z}_{q^m}[i])$ *is given by* $\begin{cases} q^{2\lceil \frac{m}{2} \rceil} - 1 & \text{if } m \text{ is even} \\ q^{2\lceil \frac{m}{2} \rceil} & \text{if } m \text{ is odd} \end{cases}$

Proof. If α and β are two nonzero zero-divisors in $\mathbb{Z}_{q^m}[i]$ such that $q^{\lceil \frac{m}{2} \rceil} \mid \alpha$ and $q^{\lceil \frac{m}{2} \rceil} \mid \beta$, $\alpha \neq \beta$, then α and β are adjacent in $\Gamma(\mathbb{Z}_{q^m}[i])$. Thus, all such zero-divisors form a clique in $\Gamma(\mathbb{Z}_{q^m}[i])$ and there are $\dfrac{q^{2m}}{q^{2\lceil \frac{m}{2} \rceil}} - 1 = q^{2\lfloor \frac{m}{2} \rfloor} - 1$ such zero-divisors. Also notice that the vertices of $\Gamma(\mathbb{Z}_{q^m}[i])$ that are not in the clique form an independent set of vertices. Moreover, if m is odd then each vertex of the subring generated by $< q^{\lceil \frac{m}{2} \rceil} >$ is adjacent to α, where $q^{\lceil \frac{m}{2} \rceil} \mid \alpha$. Therefore, the clique number is given by $\begin{cases} q^{2\lceil \frac{m}{2} \rceil} - 1 & \text{if } m \text{ is even} \\ q^{2\lceil \frac{m}{2} \rceil} & \text{if } m \text{ is odd} \end{cases}$ □

Notice that for a Gaussian prime q and $m > 1$, $\mathbb{Z}_{q^m}[i] \cong \mathbb{Z}[i]/\langle q^m \rangle$ is a local ring with unique maximal ideal $\langle q \rangle$. Also, $|U(\mathbb{Z}_{q^m}[i])| = q^{2m} - q^{2m-2}$ [4], so that $|Z^*(\mathbb{Z}_{q^m}[i])| = q^{2m} - (q^{2m} - q^{2m-2}) - 1 = q^{2m-2} - 1$.

Theorem 2 *If* m *is a positive integer and* q *is a Gaussian prime, then*
(i) $d_\delta(\Gamma(\mathbb{Z}_{q^m}[i])) = q^2 - 1$, $d_\Delta(\Gamma(\mathbb{Z}_{q^m}[i])) = q^{2m-2} - 2$, $\kappa_v(\Gamma(\mathbb{Z}_{q^m}[i])) = q^2 - 1$, *where* κ_v *denotes the vertex connectivity.*

Proof. To find the minimum and maximum degree of $\Gamma(\mathbb{Z}_{q^m}[i])$, let $\lambda \in V(\mathbb{Z}_{q^m}[i])$. Then λq is the vertex with least degree because no vertex λq is adjacent to any other vertex except the vertices obtained as multiples of q^{m-1}. Thus, $d_\delta(\Gamma(\mathbb{Z}_{q^m}[i])) = q^2 - 1$.

Also, every vertex of the clique induced by vertices from the subring $< q^{m-1} >$ is adjacent to every vertex of $\Gamma(\mathbb{Z}_{q^m}[i])$. Therefore, $d_\Delta(\Gamma(\mathbb{Z}_{q^m}[i])) = q^{2m-2} - 2 = |Z^*(\mathbb{Z}_{q^m}[i])| - 1$. This implies that $rad(\Gamma(\mathbb{Z}_{q^m}[i])) = 1$ and the vertex connectivity of $\Gamma(\mathbb{Z}_{q^m}[i])$ can be obtained by removing the vertices associated to the subring generated by $< q^{m-1} >$, since their removal leaves each vertex of the form λq as isolated, where $\lambda \in V(\mathbb{Z}_{q^m}[i])$. Thus, the vertex connectivity is $q^2 - 1$. □

The following lemma gives a formula for calculating the clique number of zero-divisor graph $\Gamma(\mathbb{Z}_n)$ of $\mathbb{Z}_n$, for $n \geq 1$.

Lemma 3 [2] *If* $n = p_1^{\alpha_1} p_2^{\alpha_2} \dots p_r^{\alpha_r}$ *is the canonical representation of* n, *then* $\mathbb{Z}/n\mathbb{Z} \cong \mathbb{Z}/p_1^{\alpha_1}\mathbb{Z} \times \cdots \times \mathbb{Z}/p_k^{\alpha_k}\mathbb{Z}$ *as rings. If each* α_i $(1 \le i \le r)$ *is even, then* $\omega(\Gamma(\mathbb{Z}_n) = p_1^{\frac{\alpha_1}{2}} p_2^{\frac{\alpha_2}{2}} \dots p_r^{\frac{\alpha_r}{2}} - 1$ *and if*

$$n = p_1^{\alpha_1} p_2^{\alpha_2} \dots p_r^{\alpha_r} q_1^{\beta_1} q_2^{\beta_2} \dots p_s^{\beta_s}$$

such that ${\alpha_i}^s$ *are even and* ${\beta_i}^s$ *are odd, then*

$$\omega(\Gamma(\mathbb{Z}_n) = p_1^{\frac{\alpha_1}{2}} p_2^{\frac{\alpha_2}{2}} \dots p_r^{\frac{\alpha_r}{2}} q^{\frac{\beta_1-1}{2}} q^{\frac{\beta_2-1}{2}} \dots q^{\frac{\beta_s-1}{2}} + s - 1,$$

where s *is the number of odd primes.*

From Lemma 3, the following observation is immediate.

Theorem 4 *If* p *is a prime number and* $n \in \mathbb{N}$, *then the clique number of* $\Gamma(\mathbb{Z}_{p^n})$ *is given by*

$$\omega(\Gamma(\mathbb{Z}_{p^n})) = \begin{cases} p^{\frac{n}{2}-1} & \text{if } n \text{ is even} \\ p^{\frac{n-1}{2}} & \text{if } n \text{ is odd} \end{cases}$$

Theorem 5 *If* $\Gamma(\mathbb{Z}_{2^m}[i])$ *be a zero-divisor graph of the ring* $\mathbb{Z}_{2^m}[i]$, *where* $m \ge 1$ *is an integer, then* $d_\Delta(\Gamma(\mathbb{Z}_{2^m}[i])) = 2^{2m-1} - 2$, $\omega(\Gamma(\mathbb{Z}_{2^m}[i])) = 2^m - 1$, $d_\delta(\Gamma(\mathbb{Z}_{2^m}[i])) = 1$, $k_v(\Gamma(\mathbb{Z}_{2^m}[i])) = 1$ *and* $\mathrm{rad}(\Gamma(\mathbb{Z}_{2^m}[i])) = 1$, *where* $m \ge 2$.

Proof. For $m = 1$, the case is trivial. For $m > 1$, one can see that $\mathbb{Z}_{2^m}[i] \cong \mathbb{Z}[i]/\langle 2^m \rangle = \mathbb{Z}[i]/\langle (1+i)^{2m} \rangle$. Clearly, $Z^*(\mathbb{Z}_{2^m}[i]) = \langle 1+i \rangle - \{0\}$ is an annihilator ideal, that is, there exists a vertex, say $\alpha \in Z^*(\mathbb{Z}_{2^m}[i])$, adjacent to every other vertex. Also, by Proposition 2.4 in [3], $\Gamma(\mathbb{Z}_{2^m}[i]) \cong \Gamma(\mathbb{Z}_{2^{2m}})$. With this property, we have $d_\Delta(\Gamma(\mathbb{Z}_{2^m}[i])) = 2^{2m-1} - 2$, $\omega(\Gamma(\mathbb{Z}_{2^m}[i])) = 2^m - 1$, $d_\delta(\Gamma(\mathbb{Z}_{2^m}[i])) = 1$, $k_v(\Gamma(\mathbb{Z}_{2^m}[i])) = 1$, where $m \ge 2$. Also, the degree of the vertices are given as $\deg(v_i) = 2^i - 1$, if $1 \le i < m$ and $\deg(v_i) = 2^i - 2$, for $m \le i \le 2m - 1$.

Now, we claim that there exists a pendent vertex $1+i$ in $\Gamma(\mathbb{Z}_{2^m}[i])$. Assume that $(1+i)(a+ib) = 0$, which implies that $(a-b) + i(a+b) = 0$, that is, $a = b$ or $a + b = 0$, that is $a + b = 2^m$. Thus, $(1+i) \sim (\frac{2^m}{2} + i\frac{2^m}{2})$. Hence, $1+i$ is a pendent vertex. □

By Theorem 3 in [10], if we partition the vertex set of $\Gamma(\mathbb{Z}_{p^m})$ into the sets $S_1, S_2, \dots, S_{m-1}$, where $S_i = \{k_i p^i : p \nmid k_i\}$, $1 \le i \le m-1$, then it is easy to see that $|V_i| = (p-1)p^{m-i-1}$, $1 \le i \le m-1$ and therefore $|\Gamma(\mathbb{Z}_{p^m})| = \sum_{i=1}^{m-1} (p-1)p^{m-i-1} = p^{m-1} - 1$. Also, for a positive integer k, $1 \le k \le m-1$, the degrees of the vertices in $\Gamma(\mathbb{Z}_{p^m})$ are given by

$\deg(V_k) = \begin{cases} p^k - 1 & \text{if } 1 \le k < \lceil \frac{m}{2} \rceil \\ p^k - 2 & \text{if } \lceil \frac{m}{2} \rceil \le k \le m-1 \end{cases}$ where $\lceil x \rceil$ denotes the smallest integer function.

A nontrivial connected graph G is Eulerian if and only if every vertex of G has even degree.

Theorem 6 *For each $m \ge 1$, the graph $\Gamma(\mathbb{Z}_{p^m})$, where p is a prime, is not Eulerian.*

Proof. We divide the vertex set of $\Gamma(\mathbb{Z}_{p^m})$ into the sets $S_1, S_2, \ldots, S_{m-1}$, where $S_i = \{k_i p^i : p \nmid k_i\}$, $1 \le i \le m-1$. Clearly, a vertex of S_i is adjacent to a vertex of S_j if and only if $i + j \ge m$. This implies that a vertex $v \in S_1$ is adjacent to a vertex $u \in V(\Gamma(\mathbb{Z}_{p^m}))$ if and only if $u \in S_{m-1}$. Now, for each $v_1 \in S_1$ and $v_{m-1} \in S_{m-1}$, we have $\deg(v_1) = p-1$ and $\deg(v_{m-1}) = p^{m-1}-2$. So, for each prime p and a positive integer m, it follows that either $\deg(v_1)$ or $\deg(v_{m-1})$ is odd, where $v_1 \in S_1$, $v_{m-1} \in S_{m-1}$. □

Now, we obtain the values of some graph parameters of the zero-divisor graph associated to the ring $\mathbb{Z}_{pq^2}$, where p and q are distinct prime integers.

Theorem 7 *Let $\Gamma(\mathbb{Z}_{pq^2})$ be the zero-divisor graph of the ring $\mathbb{Z}_{pq^2}$, where p and q are distinct prime integers. If*
(i) p is odd prime and $q = 2$, then $\mathrm{diam}(\Gamma(\mathbb{Z}_{pq^2})) = 3$, $d_\delta(\Gamma(\mathbb{Z}_{pq^2})) = q-1$, $d_\Delta(\Gamma(\mathbb{Z}_{pq^2})) = pq - q$, $\mathrm{rad}(\Gamma(\mathbb{Z}_{pq^2})) = 1$, $\kappa_v(\Gamma(\mathbb{Z}_{pq^2})) = 1$ and $\omega(\Gamma(\mathbb{Z}_{pq^2}) = q-1$.
(ii) $p = 2$ and q is odd, then $\mathrm{diam}(\Gamma(\mathbb{Z}_{pq^2})) = 3$, $\mathrm{rad}(\Gamma(\mathbb{Z}_{pq^2}) = 1$, $d_\Delta(\Gamma(\mathbb{Z}_{pq^2}) = q^2 - 1$, $d_\delta(\Gamma(\mathbb{Z}_{pq^2})) = q-1$ and $\omega(\Gamma(\mathbb{Z}_{pq^2}) = q-1$.
(iii) $\mathrm{diam}(\Gamma(\mathbb{Z}_{pq^2})) = 3$, $\mathrm{rad}(\Gamma(\mathbb{Z}_{pq^2}) = 1$, $d_\Delta(\Gamma(\mathbb{Z}_{pq^2}) = q^2+p-1$, $d_\delta(\Gamma(\mathbb{Z}_{pq^2})) = q-1$ and $\omega(\Gamma(\mathbb{Z}_{pq^2}) = q-1$.

Proof. The number of zero-divisors in $\mathbb{Z}_m$ is given by $m - \phi(m) - 1 = pq^2 - \phi(pq^2) - 1 = pq^2 - (p-1)(q^2-q) - 1 = q(p+q-1) - 1$.
(i). When p is odd prime and $q = 2$. In this case, we partition the vertex set as $V_1 = \{q^2 k : 1 \le k < p, (k,p) = 1\}$, $V_2 = \{kp : 1 \le k < q^2\}$ and $V_3 = \{2k : 1 \le k < pq, k \ne p, (2,k) = 1\}$. Now, in $\Gamma(\mathbb{Z}_{pq^2})$, we take pq as a center vertex. Clearly, no two vertices of V_1 are adjacent. However, for each $u \in V_1$ and $v \in V_2$, $uv = 0$. Thus, V_1 and V_2 form a complete bipartite graph. Furthermore, the vertices of V_3 are adjacent to the vertex pq, which form an independent set (tail vertices). In this way, we get $p-1$ number of

pendent vertices. So, clearly $d_\delta(\Gamma(\mathbb{Z}_{pq^2})) = q-1$. Also, $diam(\Gamma(\mathbb{Z}_{pq^2})) = 3$, $d_\Delta(\Gamma(\mathbb{Z}_{pq^2})) = 2$, $\kappa_v(\Gamma(\mathbb{Z}_{pq^2})) = 1$, $rad(\Gamma(\mathbb{Z}_{pq^2})) = 1$ and $\omega(\Gamma(\mathbb{Z}_{pq^2})) = q-1$. For illustration, consider $\mathbb{Z}_{28}$ in Figure 1(a).

(ii). When $p = 2$ and q is odd prime, we partition the vertex set into the subsets: $V_1 = \{k(2q) : 1 \le k < q, (2k, q) = 1\}$, $V_2 = \{kq : 1 \le k \le q, (k, q) = 1\}$ and $V_3 = \{2k : 1 \le k \le q^2 - q, (2, q) = 1\}$. Clearly, no two vertices of V_1 and V_2 are adjacent. However, for each $u \in V_1$ and $v \in V_2$, $uv = 0$. Also, there exists a vertex $q^2 \in V_2$ such that each vertex $v_i \in V_3$ is adjacent to q^2. So, we observe that $diam(\Gamma(\mathbb{Z}_{pq^2})) = 3$, $rad(\Gamma(\mathbb{Z}_{pq^2})) = 1$, $d_\Delta(\Gamma(\mathbb{Z}_{pq^2})) = q^2 - 1$, $d_\delta(\Gamma(\mathbb{Z}_{pq^2})) = q - 1$, the set of vertices $\{2q, 2.2q, 3.2q, \dots q - 1.2q\}$ form a clique, that is, $\omega(\Gamma(\mathbb{Z}_{pq^2})) = q - 1$. For example, consider $\mathbb{Z}_{2.5^2}$, see Figure 1(b).

(iii). When both p and q are odd primes. In this case, we partition the vertex set as: $V_1 = \{kq : 1 \le k < q^2, (k, p) = 1\}$, $V_2 = \{kp : 1 \le k < q^2 - q, (k, q) = 1\}$, $V_3 = \{kq^2 : 1 \le k < p, (k, p) = 1\}$ and $V_4 = \{kpq : 1 \le k < pq - p, (k, p) = 1, (k, q) = 1\}$. It is clear that $diam(\Gamma(\mathbb{Z}_{pq^2})) = 3$, $rad = 1$, $d_\Delta(\Gamma(\mathbb{Z}_{pq^2})) = q^2 + p - 1$, $d_\delta(\Gamma(\mathbb{Z}_{pq^2})) = q - 1$ and $\omega(\Gamma(\mathbb{Z}_{pq^2})) = q - 1$. For example, consider $\mathbb{Z}_{3^2.5}$, see Figure 2. □

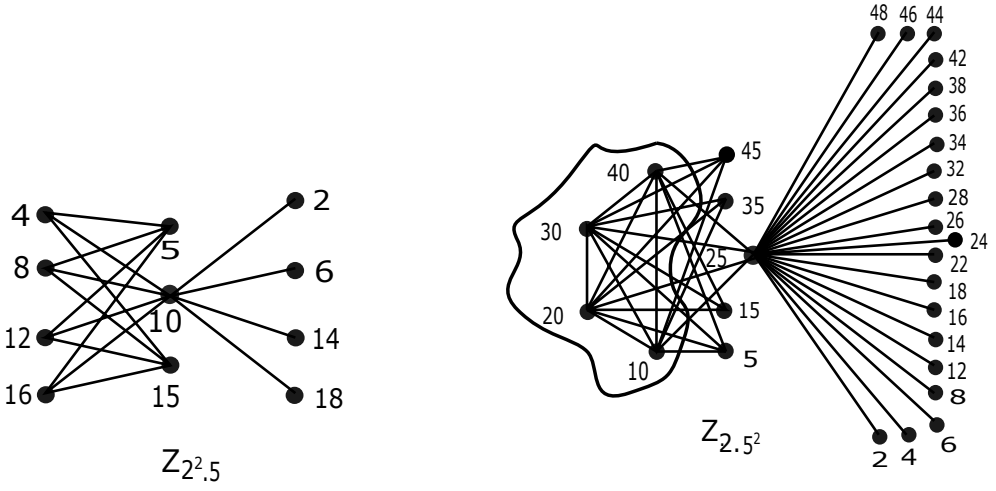

Figure 1: Example $\Gamma(\mathbb{Z}_{p^2q})$, p and q are odd

A ring R is said to be decomposable if it can be written as a direct product $R_1 \times R_2$, where R_1 and R_2 are nonzero rings, otherwise R is said to be indecomposable. In the next two results, we find the values of graph parameters of

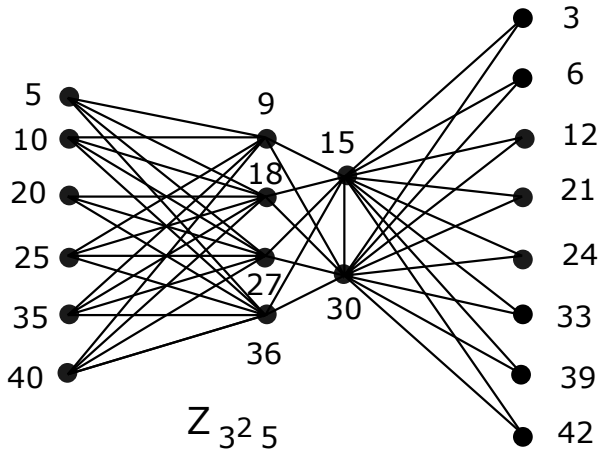

Figure 2: Example $\Gamma(\mathbb{Z}_{p^2q})$, p, q are odd primes

the zero divisor graph associated to the finite commutative ring which is the direct product of finite local rings.

Theorem 8 *Let* $R \cong R_1 \times R_2$ *be a commutative ring and* $ann(x)$ *be minimal non-trivial ideal.*
(i) If $R_1 = \mathbb{Z}_2$, *then* $k_v(\Gamma(R)) = 1$, $d_\Delta(\Gamma(R)) = |R_2| - 1$, $d_\delta(\Gamma(R)) = 1$.
(ii) If $R_2 = \mathbb{Z}_2$, *then* $k_v(\Gamma(R)) = 1$, $d_\Delta(\Gamma(R)) = |R_1| - 1$, $d_\delta(\Gamma(R)) = 1$.
(iii) $\kappa_v(\Gamma(R)) = d_\delta(\Gamma(R)) = min(|R_1|, |R_2|)$, $d_\Delta(\Gamma(R)) = max(|R_1|, |R_2|)$, *if* $R_1 = \mathcal{F}$, *where* $\mathcal{F}$ *is a field and* $R_1 \ncong \mathbb{Z}_2$.
(iv) $\kappa_v(\Gamma(R)) = |ann(x, 1)|$.

Proof. (i). As $\mathbb{Z}_2$ is a field, we partition the vertex set of $\mathbb{Z}_2 \times R_2$ as $V_1 = \{(0,1), (0,x_1), \ldots, (0,x_m)\}$ and $V_2 = \{(1,0)\}$. Now, there exists a vertex $(1,0)$ joined to every vertex of V_1. When the cut-vertex $(1,0)$ is removed from $\Gamma(R)$, the resulting graph is no longer connected leaving $(0,1)$ as an isolated vertex. Hence, $\kappa_v(\Gamma(R)) = 1$. Also, if $ann(x)$ is a minimal non-trivial annihilator ideal in R_2, where $x \in Z^*(R_2)$, then $ann(0, x_i) = \{(0, x_j)$ and $(1, x_j) \mid x_j \in ann(x_i)\}$. Thus, the graph $\Gamma(R)$ is incomplete. Clearly, $|ann(0, x_i)| < deg(1,0)$ implies that $d_\Delta(\Gamma(R)) = |R_2| - 1$ and $d_\delta(\Gamma(R)) = 1$.
(ii). This follows by using the argument similar to above.
(iii). Since $R \cong \mathcal{F} \times R_2$ is a commutative ring, where $\mathcal{F}$ is a field and $R_2 \ncong \mathbb{Z}_2$, so $S_1 = \{(u, 0) \mid u \in \mathcal{F}^*\}$ is a cut-set of $\Gamma(R)$ if $|\mathcal{F}| < |R_2|$ and $S_2 = \{(0, a) \mid a \in R_2\}$ if $|\mathcal{F}| > |R_2|$. Thus, $\kappa_v(\Gamma(R)) = min(|R_1|, |R_2|)$, $d_\Delta = max(|R_1|, |R_2|)$. In case $R_2 \cong \mathbb{Z}_2$, then $(0,1)$ is the cut-vertex of $\Gamma(R)$.

(iv). Let $x \in Z^*(R_1)$. If $ann(x) = \{y \in Z^*(R_1) : xy = 0\}$ and $ann(x)$ is the minimal non-trivial annihilator ideal, then $ann(x, 1) = \{(y, 0)\}$. Clearly, when $S = \{(y, 0) : y \in ann(x)\}$ is removed, $\Gamma(R)$ becomes disconnected. Thus, S is the minimal cut-set. Hence, $\kappa_v(\Gamma(R)) = |S|$. □

Theorem 9 *Let* $R = R_1 \times R_2 \times \cdots \times R_n$, $n \geq 2$, $R \ncong \mathbb{Z}_2 \times \mathbb{Z}_2$ *and each* R_i *is a finite local ring, then*
(i) $\kappa_v(\Gamma(R)) = 1$, *if* $R_1 \cong \mathbb{Z}_2$
(ii) $\kappa_v(\Gamma(R)) = 1$, *if* $R_1 \cong \mathbb{Z}_4$ *or* $\frac{\mathbb{Z}_2[x]}{x^2}$.

Proof. (i). Let $R = R_1 \times R_2 \times \cdots \times R_n$, $n \geq 2$, $R \ncong \mathbb{Z}_2 \times \mathbb{Z}_2$ and each R_i be a finite local ring. When $R_1 \cong \mathbb{Z}_2$, then $R \cong \mathbb{Z}_2 \times R_2 \times \cdots \times R_n$. Clearly, $ann((1, 0, \ldots, 0))$ consists of at least one pendent vertex $(0, 1, \ldots, 1)$. Deletion of the vertex $(1, 0, \ldots, 0)$ isolates $(0, 1, \ldots, 1)$ and hence disconnects the graph with $\kappa_v(\Gamma(R)) = 1$.
(ii). When $R_1 \cong \mathbb{Z}_4$, let $ann(2)$ be the minimal annihilator ideal of $\mathbb{Z}_4$. Then $ann((2, 0, \ldots, 0)) = \{(2, 1, \ldots, 1), \ldots : 2 \in ann(2)\}$. Clearly, the vertex $(2, 1, \ldots, 1)$ is only adjacent to $(2, 0, \ldots, 0)$. Hence, $\kappa_v(\Gamma(R)) = 1$, in this case also.

When $R_1 \cong \frac{\mathbb{Z}_2[x]}{x^2}$, there exists only one path from $(x, 0, \ldots, 0)$ to $(x, 1, \ldots, 1)$. Then the graph becomes disconnected on removing $(x, 0, \ldots, 0)$. □

Using Lemma 3, we can find the clique number of a zero-divisor graph $\Gamma(\mathbb{Z}_n)$ for any large n. To calculate this, we factorize the integers in different forms. For example, $\omega(\Gamma(\mathbb{Z}_{2000})) = 2^2 \cdot 5 + 1 - 1 = 20$. For distinct prime integers p, q, we have (i) $\omega(\Gamma(\mathbb{Z}_{pq})) = p^0q^0 + 2 - 1 = 2$. (ii) If $n = p^2q$, then $\omega = pq^0 + 1 - 1 = p$. (iii) $\omega(\Gamma(\mathbb{Z}_{p^3q}) = pq^0 + 2 - 1 = p + 1$ (iv) $\omega(\Gamma(\mathbb{Z}_{p^2q^2}))$ $= pq - 1$. (v) $\omega(\Gamma(\mathbb{Z}_{p^3}) = p$. (vi) $\omega(\Gamma(\mathbb{Z}_{p^4}) = p^2 - 1$.

References

[1] D. F. Anderson, P. S. Livingston. The zero-divisor graph of a commutative ring, *J. Algebra* **217** (1999) 434–447. ⇒75

[2] M. I, Bhat, S. Pirzada, A. M. Alghamdi. On planarity of compressed zero-divisor graphs associated to commutative rings, *Creative Math. Infor.* **29**, 2 (2020) 131–136. ⇒78

[3] H. J. Chiang-Hsieh, H-J. Wang, Commutative rings with toroidal zero-divisor graphs, *Houst. J. Math.* **36**, 1 (2010) 1–31. ⇒78

[4] J. Cross, The Euler ϕ-function in the Gaussian integers, *Amer. Math. Monthly* **90,** 8 (1983) 518–528. ⇒77

[5] A. Duane, Proper colorings and $\mathfrak{p}$-partite structures of the zero-divisor graph, *Rose-Hulman Undergraduate Mathematics Journal* **7,** 2 (2006) Art. 16. ⇒76

[6] D. Endean, K. Henry, E. Manlove, Zero-divisor graphs of $\mathbb{Z}_\mathfrak{n}$ and polynomial quotient rings over $\mathbb{Z}_\mathfrak{n}$, *Rose-Hulman Undergraduate Mathematics Journal* **8,** 2 (2007) Art. 15. ⇒76

[7] K. Nazzal, M. Ghanem, Some properties of the zero-divisor graph of a commutative ring, *Discussiones Math. General Algebra and Appl.* **34** (2014) 167–181. ⇒76

[8] E. A. Osba, S. A-Addasi and N. A. Jaradeh, Zero divisor graph for the ring of Gaussian integers modulo $\mathfrak{n}$, *Comm. Algebra* **36,** 10 (2008) 3865–3877. ⇒76

[9] S. Pirzada, *An Introduction to Graph Theory*, Universities Press, Hyderabad, India, 2012. ⇒76

[10] S. Pirzada, M. Aijaz, M. Imran Bhat, On zero-divisor graphs of the rings $\mathbb{Z}_\mathfrak{n}$, *Afrika Matematika* **31** (2020) 727–737. ⇒78

[11] S. Pirzada, A. Altaf, S. Khan, Structure of the zero-divisor graphs associated to the ring of integers modulo $\mathfrak{n}$, J. Algebraic Systems, to appear. ⇒76

Received: April 24, 2022 • Revised: May 13, 2022

Acta Univ. Sapientiae Informatica **14,** 1 (2022) 84–103

DOI: 10.2478/ausi-2022-0006

Transmission-reciprocal transmission index and coindex of graphs

Harishchandra S. RAMANE
Department of Mathematics
Karnatak University
Dharwad-580003, India
email: hsramane@yahoo.com

Deepa V. KITTURMATH
Department of Mathematics
Karnatak University
Dharwad-580003, India
email: deepakitturmath@gmail.com

Kavita BHAJANTRI
Department of Mathematics
JSS Banashankari Arts, Commerce and
Shantikumar Gubbi Science College,
Vidyagiri, Dharwad-580004, India
email: kavitabhajantri5@gmail.com

Abstract. The transmission of a vertex u in a connected graph G is defined as $\sigma(u) = \sum_{v \in V(G)} d(u,v)$ and reciprocal transmission of a vertex u is defined as $rs(u) = \sum_{v \in V(G)} \frac{1}{d(u,v)}$, where $d(u,v)$ is the distance between vertex u and v in G. In this paper we define new distance based topological index of a connected graph G called transmission-reciprocal transmission index $TRT(G) = \sum_{uv \in E(G)} \left(\frac{\sigma(u)}{rs(u)} + \frac{\sigma(v)}{rs(v)} \right)$ and its coindex $\overline{TRT}(G) = \sum_{uv \notin E(G)} \left(\frac{\sigma(u)}{rs(u)} + \frac{\sigma(v)}{rs(v)} \right)$, where $E(G)$ is the edge set of a graph G and establish the relation between $TRT(G)$ and $\overline{TRT}(G)$. Further compute this index for some standard class of graphs and obtain bounds for it.

Computing Classification System 1998: G.2.2
Mathematics Subject Classification 2010: 05C12, 05C09
Key words and phrases: Distance, transmission of a vertex, reciprocal transmission of a vertex, transmission-reciprocal transmission index.

1 Introduction

Throughout this paper, we consider a finite connected graph G that has no loops and multiple edges. We respectively denote by n and m the cardinality of its vertex set $V(G)$ and its edge set $E(G)$. As customary, we denote by $d(u)$ the degree of u and by $d(u,v)$ the distance between u and v.

In recent years a large number of topological indices have been reported and utilized for chemical documentation, isomer discrimination, study of molecular complexity, similarity/dissimilarity, drug design, and database selection, least optimization, rational combinatorial library design and for deriving multilinear regression models.

The use of topological and information theoretical indices in QSAR (Quantative structure-activity relationship) has become of growing importance seems to play an important role in situations where biological activity is determined predominantly by topological architecture of molecular structure, where simple connectivity among neighbouring atoms without considering the chemical nature of atom or nature of chemical bonding, may be the major determinant of biological activity of a molecule.

The status [11, 16] (or transmission [1]) of a vertex u in G is defined as the sum of the distances between u and all other vertices of G and is denoted by $\sigma(u)$. That is,

$$\sigma(u) = \sum_{v \in V(G)} d(u,v).$$

The reciprocal status of a vertex [15] $u \in V(G)$ is defined as the sum of reciprocal of its distance from every other vertex in $V(G)$ and is denoted by $rs(u)$. That is,

$$rs(u) = \sum_{uv \in E(G),\, u \neq v} \frac{1}{d(u,v)}.$$

The Wiener index of graph G is defined as [18]

$$W(G) = \sum_{\{u,v\} \subseteq V(G)} d(u,v) = \frac{1}{2} \sum_{u \in V(G)} \sigma(u).$$

More results about Wiener index can be found in [5, 6, 10, 12, 13, 14, 17].

The first and second Zagreb indices of a graph G are defined as [9]

$$Z_1(G) = \sum_{uv \in E(G)} [d(u) + d(v)] \quad \text{and} \quad Z_2(G) = \sum_{uv \in E(G)} d(u)d(v).$$

Results on the Zagreb indices can be found in [4] and the references cited therein.

The Zagreb coindices of a graph G are defined as [7]

$$\overline{Z_1}(G) = \sum_{uv \notin E(G)} [d(u) + d(v)] \quad \text{and} \quad \overline{Z_2}(G) = \sum_{uv \notin E(G)} d(u)d(v).$$

More results on Zagreb coindices can be found in [2, 3].

We introduce here new distance based index called as transmission-reciprocal transmission (T-RT) index of a graph and is defined as

$$TRT(G) = \sum_{uv \in E(G)} \left(\frac{\sigma(u)}{rs(u)} + \frac{\sigma(v)}{rs(v)} \right). \tag{1}$$

The transmission-reciprocal transmission coindex of a graph is defined as

$$\overline{TRT}(G) = \sum_{uv \notin E(G)} \left(\frac{\sigma(u)}{rs(u)} + \frac{\sigma(v)}{rs(v)} \right). \tag{2}$$

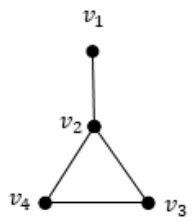

Figure 1: Graph G.

Example 1 *In a graph* G *of Fig. 1,* $V(G) = \{v_1, v_2, v_3, v_4\}$. *Status of vertices are* $\sigma(v_1) = 5$, $\sigma(v_2) = 3$, $\sigma(v_3) = 4$, $\sigma(v_4) = 4$ *and reciprocal status of vertices are* $rs(v_1) = 2$, $rs(v_2) = 3$, $rs(v_3) = \frac{5}{2}$, $rs(v_4) = \frac{5}{2}$. *By definition,* $TRT(G) = 11.9$ *and* $\overline{TRT}(G) = 8.2$.

2 Computation of transmission-reciprocal transmission index of graphs

Let $diam(G)$ denotes the diameter of a graph G.

Theorem 2 *Let* G *be a connected graph with* n *vertices and* m *edges and let* $\mathrm{diam}(G) \leq 2$. *Then*

$$TRT(G) = \sum_{uv \in E(G)} \frac{2[4n^2 - 8n + (n-1)(d(u)+d(v)) - 2d(u)d(v) + 4]}{n^2 - 2n + (n-1)(d(u)+d(v)) + d(u)d(v) + 1}.$$

Proof. If $\mathrm{diam}(G) \leq 2$ then $d(u)$ be the number of vertices at distance 1 from the vertex u and the remaining $(n-1-d(u))$ vertices are at distance 2. Therefore for each vertex u in G, $\sigma(u) = d(u)+2(n-1-d(u)) = 2n-2-d(u)$.

If $\mathrm{diam}(G) \leq 2$, then $d(u)$ number of vertices are at distance 1 from the vertex u and the remaining $n-1-d(u)$ vertices are at distance 2. Therefore for each vertex u in G, $rs(u) = \frac{1}{2}(n-1+d(u))$. Now by the Eq. (1) we have

$$\begin{aligned}
&TRT(G)\\
&= \sum_{uv \in E(G)} \left(\frac{\sigma(u)}{rs(u)} + \frac{\sigma(v)}{rs(v)} \right)\\
&= \sum_{uv \in E(G)} \left(\frac{2n-2-d(u)}{\frac{1}{2}(n-1+d(u))} + \frac{2n-2-d(v)}{\frac{1}{2}(n-1+d(v))} \right)\\
&= \sum_{uv \in E(G)} \left(\frac{2(2n-2-d(u))}{(n-1+d(u))} + \frac{2(2n-2-d(v))}{(n-1+d(v))} \right)\\
&= \sum_{uv \in E(G)} \frac{\left[\begin{array}{l} 2(n-1+d(v))(2n-2-d(u)) + \\ 2(n-1+d(u))(2n-2-d(v)) \end{array} \right]}{(n-1+d(u))(n-1+d(v))}\\
&= \sum_{uv \in E(G)} \frac{2[4n^2 - 8n + (d(u)+d(v))(-n+1+2n-2) - 2d(u)d(v) + 4]}{n^2 - 2n + (n-1)(d(u)+d(v)) + d(u)d(v) + 1}\\
&= \sum_{uv \in E(G)} \frac{2[4n^2 - 8n + (n-1)(d(u)+d(v)) - 2d(u)d(v) + 4]}{n^2 - 2n + (n-1)(d(u)+d(v)) + d(u)d(v) + 1}.
\end{aligned}$$

□

Corollary 3 *Let* G *be a connected regular graph of degree* r *on* n *vertices and* m *edges and let* $\mathrm{diam}(G) \leq 2$. *Then*

$$TRT(G) = \frac{2m[4n^2 - 8n + 4 + 2r(n-1) - 2r^2]}{n^2 - 2n + 2r(n-1) + r^2 + 1}.$$

Proof. By Theorem 2 we have

$$TRT(G) = \sum_{uv \in E(G)} \frac{2[4n^2 - 8n + (n-1)(d(u) + d(v)) - 2d(u)d(v) + 4]}{n^2 - 2n + (n-1)(d(u) + d(v)) + d(u)d(v) + 1}.$$

Since G is a regular graph, $d(u) = r$, for all $u \in V(G)$. Therefore

$$\begin{aligned} TRT(G) &= \sum_{uv \in E(G)} \frac{2[4n^2 - 8n + 2r(n-1) - 2r^2 + 4]}{n^2 - 2n + 2r(n-1) + r^2 + 1} \\ &= \frac{2m[4n^2 - 8n + 2r(n-1) - 2r^2 + 4]}{n^2 - 2n + 2r(n-1) + r^2 + 1}. \end{aligned}$$

□

Corollary 4 *For a complete graph K_n on n vertices,*

$$TRT(K_n) = n(n-1).$$

Proof. As K_n is a complete graph, $d(u) = n - 1$ for all $u \in V(K_n)$. Therefore

$$\begin{aligned} TRT(K_n) &= \sum_{uv \in E(K_n)} \frac{2[4n^2 - 8n + (n-1)(d(u) + d(v)) - 2(u)d(v) + 4]}{n^2 - 2n + (n-1)(d(u) + d(v)) + d(u)d(v) + 1} \\ &= \sum_{uv \in E(K_n)} \frac{2[4n^2 - 8n + 2(n-1) - 2(n-1)^2 + 4]}{n^2 - 2n + 2(n-1)^2 + (n-1)^2 + 1} \\ &= \sum_{uv \in E(K_n)} 2 \\ &= 2\frac{n(n-1)}{2} = n(n-1). \end{aligned}$$

□

Proposition 5 *For a complete bipartite graph $K_{p,q}$,*

$$TRT(K_{p,q}) = \frac{2pq[(p+q)(5p+5q-9) - 2pq + 4]}{(p+q)(2p+2q-3) + pq + 1}.$$

Proof. The graph $K_{p,q}$ has $n = p + q$ vertices and $m = pq$ edges. Also $diam(K_{p,q}) \leq 2$. The vertex set $V(K_{p,q})$ can be partitioned into two sets V_1 and V_2 such that for every edge uv of $K_{p,q}$ the vertex $u \in V_1$ and $v \in V_2$, where

$|V_1| = p$ and $|V_2| = q$. Therefore $d(u) = q$ and $d(v) = p$. By Theorem 2, we have

$$\begin{aligned}
&TRT(K_{p,q}) \\
&= \sum_{uv\in E(K_{p,q})} \frac{2[4(p+q)^2 - 8(p+q) + (p+q-1)(p+q) - 2pq + 4]}{(p+q)^2 - 2(p+q) + (p+q-1)(p+q) + pq + 1} \\
&= \sum_{uv\in E(K_{p,q})} \frac{2[(p+q)(4p+4q+p+q-9) - 2pq + 4]}{(p+q)(p+q+p+q-3) + pq + 1} \\
&= \sum_{uv\in E(K_{p,q})} \frac{2[(p+q)(5p+5q-9) - 2pq + 4]}{(p+q)(2p+2q-3) + pq + 1} \\
&= \frac{2pq[(p+q)(5p+5q-9) - 2pq + 4]}{(p+q)(2p+2q-3) + pq + 1}.
\end{aligned}$$

□

Proposition 6 *For a path* P_n *on* n *vertices,*

$$TRT(P_n) = \left(\frac{n(n-1)}{\sum_{j=1}^{n-1} \frac{1}{j}} \right) + \sum_{i=2}^{n-1} \left(\frac{n^2 + n + 2i(i-n-1)}{\sum_{j=1}^{i-1} \frac{1}{j} + \sum_{j=1}^{n-i} \frac{1}{j}} \right).$$

Proof. Let $v_1, v_2, \ldots, v_n$ be the vertices of P_n, where v_i is adjacent to v_{i+1}, $i = 1, 2, \ldots, n-1$. Therefore,

$$\begin{aligned}
\sigma(v_i) &= (i-1) + (i-2) + \cdots + 1 + 1 + 2 + \cdots + (n-i) \\
&= \frac{(i-1)i}{2} + \frac{(n-i)(n-i+1)}{2} \\
&= \frac{n^2+n}{2} + i(i-n-1), \quad \text{for } i = 1, 2, 3, \ldots, n-1,
\end{aligned}$$

$$rs(v_i) = \sum_{j=1}^{i-1} \frac{1}{j} + \sum_{j=1}^{n-i} \frac{1}{j}, \qquad \text{for } i = 2, 3, \ldots, n-1$$

and

$$rs(v_1) = rs(v_n) = \sum_{j=1}^{n-1} \frac{1}{j}.$$

Therefore

$$\begin{aligned}
TRT(P_n) &= \sum_{i=1}^{n-1}\left(\frac{\sigma(v_i)}{rs(v_i)}+\frac{\sigma(v_{i+1})}{rs(v_{i+1})}\right)\\
&= \frac{\sigma(v_1)}{rs(v_1)}+2\sum_{i=2}^{n-1}\left(\frac{\sigma(v_i)}{rs(v_i)}\right)+\frac{\sigma(v_n)}{rs(v_n)}\\
&= \left(\frac{\frac{n(n-1)}{2}}{\sum_{j=1}^{n-1}\frac{1}{j}}\right)+2\sum_{i=2}^{n-1}\left(\frac{\frac{n^2+n}{2}+i(i-n-1)}{\sum_{j=1}^{i-1}\frac{1}{j}+\sum_{j=1}^{n-i}\frac{1}{j}}\right)+\left(\frac{\frac{n(n-1)}{2}}{\sum_{j=1}^{n-1}\frac{1}{j}}\right)\\
&= \left(\frac{n(n-1)}{\sum_{j=1}^{n-1}\frac{1}{j}}\right)+\sum_{i=2}^{n-1}\left(\frac{n^2+n+2i(i-n-1)}{\sum_{j=1}^{i-1}\frac{1}{j}+\sum_{j=1}^{n-i}\frac{1}{j}}\right).
\end{aligned}$$

□

Proposition 7 *For a cycle* C_n *on* $n \geq 3$ *vertices,*

$$TRT(C_n) = \begin{cases} \dfrac{n^4}{4\left(1+n\sum\limits_{i=1}^{\frac{n-2}{2}}\frac{1}{i}\right)}, & \text{if } n \text{ is even} \\ \dfrac{n(n^2-1)}{4\sum\limits_{i=1}^{\frac{n-1}{2}}\frac{1}{i}}, & \text{if } n \text{ is odd.} \end{cases}$$

Proof. If n is even, then for every vertex u of C_n

$$\sigma(u) = 2\left[1+2+3+\cdots+\frac{n-1}{2}\right]+\frac{n}{2} = \frac{n^2}{4}$$

and

$$rs(u) = \frac{2}{n}+2\sum_{i=1}^{\frac{n-2}{2}}\frac{1}{i}.$$

Therefore

$$\begin{aligned}
TRT(C_n) &= \sum_{uv\in E(C_n)} \left(\frac{\sigma(u)}{rs(u)} + \frac{\sigma(v)}{rs(v)}\right) \\
&= \sum_{uv\in E(C_n)} \left(\frac{\frac{n^2}{4}}{\frac{2}{n} + 2\sum\limits_{i=1}^{\frac{n-2}{2}} \frac{1}{i}} + \frac{\frac{n^2}{4}}{\frac{2}{n} + 2\sum\limits_{i=1}^{\frac{n-2}{2}} \frac{1}{i}}\right) \\
&= \sum_{uv\in E(C_n)} \frac{n^2}{2\left(\frac{2}{n} + 2\sum\limits_{i=1}^{\frac{n-2}{2}} \frac{1}{i}\right)} \\
&= \frac{n^4}{4\left(1 + n\sum\limits_{i=1}^{\frac{n-2}{2}} \frac{1}{i}\right)}.
\end{aligned}$$

If n is odd, then for every vertex u of C_n

$$\sigma(u) = 2\left[1 + 2 + \cdots + \frac{n-1}{2}\right] = \frac{n^2-1}{4} \quad \text{and} \quad rs(u) = 2\sum_{i=1}^{\frac{n-1}{2}} \frac{1}{i}.$$

Therefore

$$\begin{aligned}
TRT(C_n) &= \sum_{uv\in E(C_n)} \left(\frac{\sigma(u)}{rs(u)} + \frac{\sigma(v)}{rs(v)}\right) \\
&= \sum_{uv\in E(C_n)} \left(\frac{\frac{n^2-1}{4}}{2\sum\limits_{i=1}^{\frac{n-1}{2}} \frac{1}{i}} + \frac{\frac{n^2-1}{4}}{2\sum\limits_{i=1}^{\frac{n-1}{2}} \frac{1}{i}}\right) \\
&= \sum_{uv\in E(C_n)} \frac{n^2-1}{4\left(\sum\limits_{i=1}^{\frac{n-1}{2}} \frac{1}{i}\right)}
\end{aligned}$$

$$= \frac{n(n^2-1)}{4\left(\sum_{i=1}^{\frac{n-1}{2}} \frac{1}{i}\right)}.$$

□

Definition 8 *A wheel W_{n+1}, is a graph obtained from the cycle C_n, $n \geq 3$, by adding a new vertex and making it adjacent to all the vertices of C_n (see Fig. 2).*

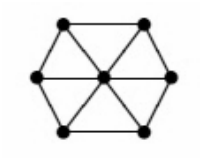

Figure 2: Wheel W_7.

Definition 9 *A friendship graph (or Dutch windmill graph) F_n, $n \geq 2$, is a graph that can be constructed by coalescence n copies of the cycle C_3 of length 3 with a common vertex (see Fig. 3). It has $2n+1$ vertices and $3n$ edges.*

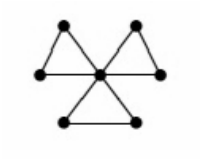

Figure 3: Friendship graph F_3.

Proposition 10 *For a wheel W_{n+1}, $n \geq 3$,*

$$TRT(W_{n+1}) = \frac{n}{n+3}(13n-15).$$

Proof. The wheel W_{n+1} has $n+1$ vertices, $2n$ edges and $\mathrm{diam}(w_{n+1}) = 2$. The edge set $E(W_{n+1})$ can be partitioned into two sets E_1 and E_2, such that $E_1(W_{n+1}) = \{uv \mid d(u) = n, d(v) = 3\}$ and $E_2(W_{n+1}) = \{uv \mid d(u) = 3, d(v) = 3\}$. It is easy to check that $|E_1(W_{n+1})| = n$ and $|E_2(W_{n+1})| = n$. By the Theorem 2 we have

$$\begin{aligned}
&TRT(W_{n+1}) \\
&= \sum_{uv\in E(W_{n+1})} \frac{2[4n^2-8n+(n-1)(d(u)+d(v))-2d(u)d(v)+4]}{n^2-2n+(n-1)(d(u)+d(v))+d(u)d(v)+1} \\
&= \sum_{uv\in E_1(W_{n+1})} \frac{2[4(n+1)^2-8(n+1)+n(n+3)-6n+4]}{(n+1)^2-2(n+1)+n(n+3)+3n+1} \\
&\quad + \sum_{uv\in E_2(W_{n+1})} \frac{2[4(n+1)^2-8(n+1)+n(6)-18+4]}{(n+1)^2-2(n+1)+n(6)+9+1} \\
&= \sum_{uv\in E_1(W_{n+1})} \frac{2[4n^2+4+8n-8n-8+n^2+3n-6n+4]}{n^2+1+2n-2n-2+n^2+3n+3n+1} \\
&\quad + \sum_{uv\in E_2(W_{n+1})} \frac{2[4n^2+4+8n-8n-8+6n-18+4]}{n^2+1+2n-2n-2+6n+9+1} \\
&= \frac{2n(5n^2-3n)}{2n^2+6n} + \frac{2n(4n^2+6n-18)}{n^2+6n+9} \\
&= \frac{n}{n+3}(13n-15).
\end{aligned}$$

□

Proposition 11 *For a friendship graph* F_n, $n \geq 2$,

$$TRT(F_n) = \frac{6n}{n+1}(3n-1).$$

Proof. The edge set $E(F_n)$ can be partitioned into two sets E_1 and E_2 such that $E_1(F_n) = \{uv \mid d(u) = 2n, d(v) = 2\}$ and $E_2(F_n) = \{uv \mid d(u) = 2, d(v) = 2\}$. It is easy to check that $|E_1(F_n)| = 2n$ and $|E_2(F_n)| = n$. By the Theorem 2 we have

$$TRT(F_n) = \sum_{uv\in E(F_n)} \frac{2[4n^2-8n+(n-1)(d(u)+d(v))-2d(u)d(v)+4]}{n^2-2n+(n-1)(d(u)+d(v))+d(u)d(v)+1}$$

$$
\begin{aligned}
&= \sum_{uv\in E_1(F_n)} \frac{2[4(2n+1)^2-8(2n+1)+2n(2n+2)-8n+4]}{(2n+1)^2-2(2n+1)+2n(2n+2)+4n+1} \\
&\quad + \sum_{uv\in E_2(F_n)} \frac{2[4(2n+1)^2-8(2n+1)+8n-8+4]}{(2n+1)^2-2(2n+1)+8n+4+1} \\
&= \sum_{uv\in E_1(F_n)} \frac{2[4(4n^2+1+4n)-16n-8+4n^2+4n-8n+4]}{4n^2+1+4n-4n-2+4n^2+4n+4n+1} \\
&\quad + \sum_{uv\in E_2(F_n)} \frac{2[4(4n^2+1+4n)-16n-8+8n-8+4]}{4n^2+1+4n-4n-2+8n+4+1} \\
&= \frac{2n(5n-1)}{n+1} + \frac{4n(2n-1)}{n+1} \\
&= \frac{6n}{n+1}(3n-1).
\end{aligned}
$$

□

3 Transmission-reciprocal transmission index of cluster graphs

The graphs with large number of edges are referred as cluster graphs. Some of the cluster graphs obtained from complete graph are defined below.

Definition 12 [8] *Let* e_i, $i = 1, 2, \ldots, k$, $1 \le k \le n-2$, *be the distinct edges of a complete graph* K_n, $n \ge 3$, *all being incident to a single vertex. The graph* $Ka_n(k)$ *is obtained by deleting* e_i, $i = 1, 2, \ldots, k$ *from* K_n. *In addition* $Ka_n(0) \cong K_n$.

Definition 13 [8] *Let* f_i, $i = 1, 2, \ldots, k$, $1 \le k \le \lfloor \frac{n}{2} \rfloor$ *be independent edges of the complete graph* K_n, $n \ge 3$. *The graph* $Kb_n(k)$ *is obtained by deleting* f_i, $i = 1, 2, \ldots, k$ *from* K_n. *In addition* $Kb_n(0) \cong K_n$.

Definition 14 [8] *Let* V_k *be a* k*-element subset of the vertex set of the complete graph* K_n, $2 \le k \le n-1$, $n \ge 3$. *The graph* $Kc_n(k)$ *is obtained by deleting from* K_n *all the edges connecting pairs of vertices from* V_k. *In addition* $Kc_n(0) \cong Kc_n(1) \cong K_n$.

Definition 15 [8] *Let* $3 \leq k \leq n$, $n \geq 3$. *The graph* $Kd_n(k)$ *is obtained by deleting from the complete graph* K_n, *the edges belonging to a* k*-membered cycle.*

Proposition 16 *For* $n \geq 3$ *and* $1 \leq k \leq n-2$,

$$\begin{aligned} TRT(Ka_n(k)) &= \frac{(n-k-1)(4n^2-8n+k(n-1)+4)}{2n^2-4n+k(1-n)+2} \\ &+\frac{2k(k-1)(2n^2-3n)}{4n^2-12n+9} \\ &+\frac{k(n-k-1)(4n^2-7n+3)}{(2n^2-5n+3)}+(n-k-1)(n-k-2). \end{aligned}$$

Proof. The graph $Ka_n(k)$ has n vertices, $\frac{n(n-1)}{2}-k$ edges and $diam(Ka_n(k)) = 2$. The edge set $E(Ka_n(k))$ can be partitioned into four sets $E_1 = \{uv \mid d(u) = n-1-k,\ d(v) = n-1\}$, $E_2 = \{uv \mid d(u) = n-2 = d(v)\}$, $E_3 = \{uv \mid d(u) = n-2,\ d(v) = n-1\}$ and $E_4 = \{uv \mid d(u) = n-1 = d(v)\}$. It is easy to check that $|E_1| = n-k-1$, $|E_2| = \frac{k(k-1)}{2}$, $|E_3| = k(n-k-1)$ $|E_4| = \frac{(n-k-1)(n-k-2)}{2}$. Now we have

$$\begin{aligned} &TRT(Ka_n(k)) \\ &= \sum_{uv\in E(Ka_n(k))} \frac{2[4n^2-8n+(n-1)(d(u)+d(v))-2d(u)d(v)+4]}{n^2-2n+(n-1)(d(u)+d(v))+d(u)d(v)+1} \\ &= \sum_{uv\in E_1} \frac{2[4n^2-8n+(n-1)(n-1-k+n-1)-2(n-1-k)(n-1)+4]}{n^2-2n+(n-1)(n-1-k+n-1)+(n-1-k)(n-1)+1} \\ &\quad+\sum_{uv\in E_2} \frac{2[4n^2-8n+(n-1)(n-2+n-2)-2(n-2)^2+4]}{n^2-2n+(n-1)(n-2+n-2)+(n-2)^2+1} \\ &\quad+\sum_{uv\in E_3} \frac{2[4n^2-8n+(n-1)(n-2+n-1)-2(n-1)(n-2)+4]}{n^2-2n+(n-1)(n-2+n-1)+(n-2)(n-1)+1} \\ &\quad+\sum_{uv\in E_4} \frac{2[4n^2-8n+(n-1)(n-1+n-1)-2(n-1)^2+4]}{n^2-2n+(n-1)(n-1+n-1)+(n-1)^2+1} \end{aligned}$$

$$
\begin{aligned}
&= \sum_{uv\in E_1(Ka_n(k))} \frac{2(4n^2-8n+nk-k+4)}{4n^2-8n-2nk+2k+4} + \sum_{uv\in E_2(Ka_n(k))} \frac{4(2n^2-3n)}{4n^2-12n+9} \\
&\quad + \sum_{uv\in E_3(Ka_n(k))} \frac{2(4n^2-7n+3)}{4n^2-10n+6} + \sum_{uv\in E_4(Ka_n(k))} \frac{2(4n^2-8n+4)}{4n^2-8n+4} \\
&= \frac{(n-k-1)(4n^2-8n+k(n-1)+4)}{2n^2-4n+k(1-n)+2} + \frac{2k(k-1)(2n^2-3n)}{4n^2-12n+9} \\
&\quad + \frac{k(n-k-1)(4n^2-7n+3)}{(2n^2-5n+3)} + (n-k-1)(n-k-2).
\end{aligned}
$$

□

Proposition 17 *For* $n \geq 3$ *and* $1 \leq k \leq \lfloor n/2 \rfloor$,

$$
\begin{aligned}
TRT(Kb_n(k)) &= \frac{4k(n-2k)(4n^2-7n+3)}{4n^2-9n+6} + (n-2k)(n-2k-1) \\
&\quad + \left(\left(\frac{2k(2k-1)}{2}\right) - k\right)\left(\frac{4(2n^2-3n)}{4n^2-12n+9}\right)
\end{aligned}
$$

Proof. The graph $Kb_n(k)$ has n vertices, $\frac{n(n-1)}{2}-k$ edges and $diam(Kb_n(k)) = 2$. The edge set $E(Kb_n(k))$ can be partitioned into three sets $E_1 = \{uv \mid d(u) = n-2,\ d(v) = n-1\}$, $E_2 = \{uv \mid d(u) = n-1 = d(v)\}$ and $E_3 = \{uv \mid d(u) = n-2 = d(v)\}$. It is easy to check that $|E_1| = 2k(n-2k)$, $|E_2| = \frac{(n-2k)(n-2k-1)}{2}$, $|E_3| = \left(\frac{2k(2k-1)}{2}\right) - k$. Therefore we have

$$
\begin{aligned}
&TRT(Kb_n(k)) \\
&= \sum_{uv\in E(Kb_n(k))} \frac{2[4n^2-8n+(n-1)(d(u)+d(v))-2d(u)d(v)+4]}{n^2-2n+(n-1)(d(u)+d(v))+d(u)d(v)+1} \\
&= \sum_{uv\in E_1(Kb_n(k))} \frac{2[4n^2-8n+(n-1)(n-2+n-1)-2(n-2)(n-1)+4]}{n^2-2n+(n-1)(n-2+n-1)+(n-2)(n-1)+1} \\
&\quad + \sum_{uv\in E_2(Kb_n(k))} \frac{2[4n^2-8n+(n-1)(n-1+n-1)-2(n-1)^2+4]}{n^2-2n+(n-1)(n-1+n-1)+(n-1)^2+1} \\
&\quad + \sum_{uv\in E_3(Kb_n(k))} \frac{2[4n^2-8n+(n-1)(n-2+n-2)-2(n-2)^2+4]}{n^2-2n+(n-1)(n-2+n-2)+(n-2)^2+1}
\end{aligned}
$$

$$
\begin{aligned}
&= \sum_{uv\in E_1(Kb_n(k))} \frac{2(4n^2-7n+3)}{4n^2-9n+6} + \sum_{uv\in E_2(Kb_n(k))} \frac{2(4n^2-8n+4)}{4n^2-8n+4} \\
&\quad + \sum_{uv\in E_3(Kb_n(k))} \frac{4(2n^2-3n)}{4n^2-12n+9} \\
&= \frac{4k(n-2k)(4n^2-7n+3)}{4n^2-9n+6} + (n-2k)(n-2k-1) \\
&\quad + \left(\left(\frac{2k(2k-1)}{2}\right) - k\right)\left(\frac{4(2n^2-3n)}{4n^2-12n+9}\right).
\end{aligned}
$$

□

Proposition 18 *For* $n \geq 3$ *and* $2 \leq k \leq n-1$,

$$TRT(Kc_n(k)) = \frac{2k(n-k)(4n^2-9n+k(n+3)+5)}{4n^2-6n-2k(n-1)+2} + (n-k)(n-k-1).$$

Proof. The graph $Kc_n(k)$ has n vertices and $\frac{1}{2}(n-k)(n+k-1)$ edges. Also $diam(Kc_n(k)) = 2$. The edge set $E(Kc_n(k))$ can be partitioned into two sets $E_1 = \{uv \mid d(u) = n-k,\ d(v) = n-1\}$ and $E_2 = \{uv \mid d(u) = n-1 = d(v)\}$. It is easy to check that $|E_1| = k(n-k)$, $|E_2| = \frac{(n-k)(n-k-1)}{2}$. Therefore we have

$$
\begin{aligned}
&TRT(Kc_n(k)) \\
&= \sum_{uv\in E(Kc_n(k))} \frac{2[4n^2-8n+(n-1)(d(u)+d(v))-2d(u)d(v)+4]}{n^2-2n+(n-1)(d(u)+d(v))+d(u)d(v)+1} \\
&= \sum_{uv\in E_1(Kc_n(k))} \frac{2[4n^2-8n+(n-1)(n-k+n-1)-2(n-k)(n-1)+4]}{n^2-2n+(n-1)(n-k+n-1)+(n-k)(n-1)+1} \\
&\quad + \sum_{uv\in E_2(Kc_n(k))} \frac{2[4n^2-8n+(n-1)(n-1+n-1)-2(n-1)^2+4]}{n^2-2n+(n-1)(n-1+n-1)+(n-1)^2+1} \\
&= \sum_{uv\in E_1(Kc_n(k))} \frac{(4n^2-9n+nk-k+5)}{2n^2-3n-nk+k+1} + \sum_{uv\in E_2(Kc_n(k))} \frac{2(4n^2-8n+4)}{4n^2-8n+4} \\
&= \frac{k(n-k)(4n^2-9n+nk-k+5)}{2n^2-3n-nk+k+1} + (n-k)(n-k-1).
\end{aligned}
$$

□

Proposition 19 *For* $3 \leq k \leq n$ *and* $n \geq 5$,

$$TRT(Kd_n(k)) = \frac{k(n-k)(2n^2-3n+1)}{n^2-3n+2} + (n-k)(n-k-1) + \left(\left(\frac{k(k-1)}{2}\right)-k\right)\left(\frac{2(n^2-n-2)}{n^2-4n+4}\right).$$

Proof. The graph $Kd_n(k)$ has n vertices and $\frac{n(n-1)}{2}-k$ edges.
Also $diam(Kd_n(k)) = 2$. The edge set $E(Kd_n(k))$ can be partitioned into three sets $E_1 = \{uv \mid d(u) = n-3 = d(v)\}$, $E_2 = \{uv \mid d(u) = n-3,\ d(v) = n-1\}$ and $E_3 = \{uv \mid d(u) = n-1 = d(v)\}$. It is easy to check that $|E_1| = \frac{k(k-1)}{2} - k$, $|E_2| = (n-k)k$, $|E_3| = \frac{(n-k-1)(n-k)}{2}$. Therefore we have

$$\begin{aligned}
&TRT(Kd_n(k))\\
&= \sum_{uv\in E(Kd_n(k))} \frac{2[4n^2-8n+(n-1)(d(u)+d(v))-2d(u)d(v)+4]}{n^2-2n+(n-1)(d(u)+d(v))+d(u)d(v)+1}\\
&= \sum_{uv\in E_1(Kd_n(k))} \frac{2[4n^2-8n+(n-1)(n-3+n-3)-2(n-3)^2+4]}{n^2-2n+(n-1)(n-3+n-3)+(n-3)^2+1} +\\
&\quad \sum_{uv\in E_2(Kd_n(k))} \frac{2[4n^2-8n+(n-1)(n-3+n-1)-2(n-3)(n-1)+4]}{n^2-2n+(n-1)(n-3+n-1)+(n-3)(n-1)+1}\\
&\quad + \sum_{uv\in E_3(Kd_n(k))} \frac{2[4n^2-8n+(n-1)(n-1+n-1)-2(n-1)^2+4]}{n^2-2n+(n-1)(n-1+n-1)+(n-1)^2+1}\\
&= \sum_{uv\in E_1(Kd_n(k))} \frac{2(n^2-n-2)}{n^2-4n+4} + \sum_{uv\in E_2(Kd_n(k))} \frac{2n^2-3n+1}{n^2-3n+2}\\
&\quad + \sum_{uv\in E_3(Kd_n(k))} \frac{2(4n^2-8n+4)}{4n^2-8n+4}\\
&= \left(\left(\frac{k(k-1)}{2}\right)-k\right)\left(\frac{2(n^2-n-2)}{n^2-4n+4}\right) + \frac{k(n-k)(2n^2-3n+1)}{n^2-3n+2}\\
&\quad +(n-k)(n-k-1).
\end{aligned}$$

□

4 Bounds for transmission-reciprocal transmission index of graphs

Theorem 20 *Let* G *be a connected graph with* n *vertices,* m *edges and let* $diam(G) = D$. *Then*

$$\sum_{uv\in E(G)} \frac{8(n-1)^2 + 2(n-1)(d(u)+d(v)) - 4d(u)d(v)}{(n-1)^2 + (n-1)(d(u)+d(v)) + d(u)d(v)} \leq TRT(G) \leq$$
$$\sum_{uv\in E(G)} \frac{2D^2(n-1)^2 + D(D-1)^2(n-1)(d(u)+d(v)) - 2D(D-1)^2 d(u)d(v)}{(n-1)^2 + (n-1)(D-1)(d(u)+d(v)) + (D-1)^2 d(u)d(v)}.$$

Proof. Lower bound: For any vertex u of G, there are $d(u)$ vertices which are at distance 1 from u and remaining $n-1-d(u)$ vertices are at distance at least 2. Therefore

$$\sigma(u) \geq d(u) + 2(n-1-d(u)) = 2n-2-d(u)$$

and

$$rs(u) \leq d(u) + \frac{1}{2}(n-1-d(u)) \leq \frac{1}{2}(n-1+d(u)).$$

This implies

$$\frac{1}{rs(u)} \geq \frac{2}{(n-1+d(u))}.$$

Therefore

$$\begin{aligned}
&TRT(G)\\
&= \sum_{uv\in E(G)} \left(\frac{\sigma(u)}{rs(u)} + \frac{\sigma(v)}{rs(v)}\right)\\
&\geq \sum_{uv\in E(G)} \left(\frac{2(2n-2-d(u))}{n-1+d(u)} + \frac{2(2n-2-d(v))}{n-1+d(v)}\right)\\
&= \sum_{uv\in E(G)} \frac{(4n-4-2d(u))(n-1+d(v)) + (4n-4-2d(v))(n-1+d(u))}{(n-1+d(u))(n-1+d(v))}\\
&= \sum_{uv\in E(G)} \frac{8(n-1)^2 + 2(n-1)(d(u)+d(v)) - 4d(u)d(v)}{(n-1)^2 + (n-1)(d(u)+d(v)) + d(u)d(v)}.
\end{aligned}$$

Upper Bound: For any vertex u of G, there are $d(u)$ vertices which are at distance 1 from u and the remaining $(n-1-d(u))$ vertices are at distance at most D. Therefore

$$\sigma(u) \leq d(u) + D(n-1-d(u)) = D(n-1) - (D-1)d(u)$$

and

$$rs(u) \geq d(u) + \frac{1}{D}(n-1-d(u)) = \frac{1}{D}(n-1) + \left(1 - \frac{1}{D}\right) d(u).$$

This implies

$$\frac{1}{rs(u)} \leq \frac{D}{(n-1)+(D-1)d(u)}.$$

Therefore

$$\begin{aligned} & TRT(G) \\ = & \sum_{uv \in E(G)} \left(\frac{\sigma(u)}{rs(u)} + \frac{\sigma(v)}{rs(v)} \right) \\ \leq & \sum_{uv \in E(G)} \left[\frac{(D(n-1)-(D-1)d(u))D}{((n-1)+(D-1)d(u))} + \frac{(D(n-1)-(D-1)d(v))D}{((n-1)+(D-1)d(v))} \right] \\ = & \sum_{uv \in E(G)} \frac{\begin{bmatrix} 2D^2(n-1)^2 + D(D-1)^2(n-1)(d(u)+d(v)) \\ -2D(D-1)^2 d(u)d(v) \end{bmatrix}}{(n-1)^2 + (n-1)(D-1)(d(u)+d(v)) + (D-1)^2 d(u)d(v)}. \end{aligned}$$

□

5 Transmission-reciprocal transmission coindex of graphs

Proposition 21 *Let G be a connected graph on n vertices. Then*

$$\overline{TRT}(G) = (n-1) \sum_{u \in V(G)} \frac{\sigma(u)}{rs(u)} - TRT(G).$$

Proof.

$$\begin{aligned}\overline{TRT}(G) &= \sum_{uv\notin E(G)}\left(\frac{\sigma(u)}{rs(u)}+\frac{\sigma(v)}{rs(v)}\right)\\ &= \sum_{\{u,v\}\subseteq V(G)}\left(\frac{\sigma(u)}{rs(u)}+\frac{\sigma(v)}{rs(v)}\right)-\sum_{uv\in E(G)}\left(\frac{\sigma(u)}{rs(u)}+\frac{\sigma(v)}{rs(v)}\right)\\ &= (n-1)\sum_{u\in V(G)}\frac{\sigma(u)}{rs(u)}-TRT(G).\end{aligned}$$

□

Corollary 22 *Let* G *be a connected graph on* n *vertices and* $diam(G)\leq 2$. *Then*

$$\begin{aligned}\overline{TRT}(G) &= (n-1)\sum_{u\in V(G)}\frac{4n-4-2d(u)}{n-1+d(u)}\\ &\quad-\sum_{uv\in E(G)}\frac{2[4n^2-8n+(n-1)(d(u)+d(v))-2d(u)d(v)+4]}{n^2-2n+(n-1)(d(u)+d(v))+d(u)d(v)+1}.\end{aligned}$$

Proof. For a graph with $diam(G)\leq 2$, we know that $\sigma(u)=2n-2-d(u)$ and $rs(u)=\frac{1}{2}(n-1+d(u))$. By Proposition 21 result follows. □

Proposition 23 *For any connected graph with* n *vertices and* $diam(G)\leq 2$,

$$\overline{TRT}(G)=\sum_{uv\notin E(G)}\frac{8(n-1)^2+2(n-1)(d(u)+d(v))-4d(u)d(v)}{(n-1)^2+(n-1)(d(u)+d(v))+d(u)d(v)}.$$

Proof. For any graph with $diam(G)\leq 2$, $\sigma(u)=2n-2-d(u)$ and $rs(u)=\frac{1}{2}(n-1+d(u))$. Therefore

$$\begin{aligned}&\overline{TRT}(G)\\ &= \sum_{uv\notin E(G)}\left(\frac{2(2n-2-d(u))}{n-1+d(u)}+\frac{2(2n-2-d(v))}{n-1+d(v)}\right)\\ &= \sum_{uv\notin E(G)}\frac{(4n-4-2d(u))(n-1+d(v))+(4n-4-2d(v))(n-1+d(u))}{(n-1+d(u))(n-1+d(v))}\\ &= \sum_{uv\notin E(G)}\frac{8(n-1)^2+2(n-1)(d(u)+d(v))-4d(u)d(v)}{(n-1)^2+(n-1)(d(u)+d(v))+d(u)d(v)}.\end{aligned}$$

□

Proposition 24 *Let* G *be a graph with* n *vertices. Let* $\overline{G}$ *be the complement of* G *and it is connected. Then*

$$TRT(\overline{G}) \geq \sum_{uv \in E(\overline{G})} \frac{8(n-1)^2 - 6(n-1)(d(u)+d(v)) + 4d(u)d(v)}{4(n-1)^2 - 2(n-1)(d(u)+d(v)) + d(u)d(v)}.$$

Proof. For any vertex u in $\overline{G}$, there are $n-1-d_G(u)$ vertices which are at distance 1 and the remaining $d_G(u)$ vertices are at distance at least 2. Therefore

$$\sigma_{\overline{G}}(u) \geq [n-1-d_G(u)] + 2d_G(u) = n-1-d_G(u)$$

and

$$rs_{\overline{G}}(u) \leq (n-1-d_G(u)) + \frac{1}{2}d_G(u) = n-1-\frac{1}{2}d_G(u).$$

Therefore

$$\begin{aligned}
&TRT(\overline{G}) \\
&= \sum_{uv \in E(\overline{G})} \left(\frac{\sigma(u)}{rs(u)} + \frac{\sigma(v)}{rs(v)} \right) \\
&\geq \sum_{uv \in E(\overline{G})} \left(\frac{2n-2-2d(u)}{2n-2-d(u)} + \frac{2n-2-2d(v)}{2n-2-d(v)} \right) \\
&= \sum_{uv \in E(\overline{G})} \frac{8n^2 - 16n + 8 - (6n-6)(d(u)+d(v)) + 4d(u)d(v)}{4n^2 - 8n + 4 - (2n-2)(d(u)+d(v)) + d(u)d(v)} \\
&= \sum_{uv \in E(\overline{G})} \frac{8(n-1)^2 - 6(n-1)(d(u)+d(v)) + 4d(u)d(v)}{4(n-1)^2 - 2(n-1)(d(u)+d(v)) + d(u)d(v)}.
\end{aligned}$$

□

Acknowledgements

The author D. V. Kitturmath is thankful to Karnatak University, Dharwad for University Research Studentship (URS) No. KUD/Scholarship/URS/2021/615. The author K. Bhajantri is thankful to Karnataka Science and Technology Promotion Society, Bengaluru for fellowship No. DST/KStePS/Ph.D. Fellowship/OTH-02: 2019-20.

References

[1] M. Aouchiche, P. Hansen, Distance spectra of graphs: A survey, *Linear Algebra Appl.* **458** (2014) 301–386. ⇒85

[2] A. Ashrafi, T. Došlić, A. Hamzeh, The Zagreb coindices of graph operations, *Discrete Appl. Math.*, **158** (2010) 1571–1578. ⇒86

[3] A. Ashrafi, T. Došlić, A. Hamzeh, Extremal graphs with respect to the Zagreb coindices, *MATCH Commun. Math. Comput. Chem.*, **65** (2011) 85–92. ⇒86

[4] B. Borovićanin, K. C. Das, B. Furtula, I. Gutman, Bounds for Zagreb indices, *MATCH Commun. Math. Comput. Chem.*, **78** (2017) 17–100. ⇒86

[5] K. C. Das, I. Gutman, Estimating the Wiener index by means of number of vertices, number of edges and diameter, *MATCH Commun. Math. Comput. Chem.*, **64** (2010) 647–660. ⇒85

[6] A. A. Dobrynin, R. Entringer, I. Gutman, Wiener index of trees: theory and applications, *Acta Appl. Math.*, **66** (2001) 211–249. ⇒85

[7] I. Gutman, B. Furtula, Ž. Vukićević, G. Popivoda, On Zagreb indices and coindices, *Math. Comput. Chem.*, **74** (2015) 5–16. ⇒86

[8] I. Gutman, L. Pavlovic, The energy of some graphs with large number of edges, *Bull. Acad. Serbe Sci. Arts (Cl. Math. Natur.)*, **118** (1999) 35–50. ⇒94, 95

[9] I. Gutman, N. Trinajstić, Graph theory and molecular orbitals. Total π-electron energy of alternant hydrocarbons, *Chem. Phys. Lett.*, **17** (1972) 535–538. ⇒85

[10] I. Gutman, Y. Yeh, S. Lee, Y. Luo, Some recent results in the theory of the Wiener number, *Indian J. Chem.*, **32A** (1993) 651–661. ⇒85

[11] F. Harary, Status and contrastatus, *Sociometry*, **22** (1959) 23–43. ⇒85

[12] S. Nikolic, N. Trinajstić, Z. Mihalic, The Wiener index: development and applications, *Croat. Chem. Acta*, **68** (1995) 105–129. ⇒85

[13] H. S. Ramane, V. V. Manjalapur, Note on the bounds on Wiener number of a graph, *MATCH Commun. Math. Comput. Chem.*, **76** (2016) 19–22. ⇒85

[14] H. S. Ramane, D. S. Revankar, A. B. Ganagi, On the Wiener index of a graph, *J. Indones. Math. Soc.*, **18** (2012) 57–66. ⇒85

[15] H. S. Ramane, S. Y. Talwar, Reciprocal status connectivity indices of graphs, *J. Adv. Math. Stud.*, **12** (2019) 289–298. ⇒85

[16] H. S. Ramane, A. S. Yalnaik, Status connectivity indices of graphs and its applications to the boiling point of benzenoid hydrocarbons, *J. Appl. Math. Comput.*, **55** (2017) 609–627. ⇒85

[17] H. B. Walikar, V. S. Shigehalli, H. S. Ramane, Bounds on the Wiener number of a graph, *MATCH Commun. Math. Comput. Chem.*, **50** (2004) 117–132. ⇒85

[18] H. Wiener, Structural determination of paraffin boiling points, *J. Am. Chem. Soc.*, **69** (1947) 17–20. ⇒85

Received: April 27, 2022 • Revised: May 18 , 2022

Acta Univ. Sapientiae Informatica **14,** 1 (2022) 104–118

DOI: 10.2478/ausi-2022-0007

On Seidel Laplacian matrix and energy of graphs

N. Feyza YALÇIN
Harran University
63290 Şanlıurfa, Turkey
email: fyalcin@harran.edu.tr

Abstract. In this work, the Seidel Laplacian spectrum of graphs are determined. Then new bounds are presented for the Seidel Laplacian energy of regular graphs and graphs by using their Seidel Laplacian spectrum and other techniques. Further, the Seidel Laplacian energy of specific graphs are computed.

1 Introduction

Let G be a simple graph with vertex set and edge set of cardinality n and e, respectively. The adjacent vertices are denoted by $v_i \sim v_j$, otherwise $v_i \nsim v_j$. Degree of a vertex v_i is denoted by d_i. The adjacency matrix $A(G)$ is defined with (i,j)-entries as 1 and 0, if $v_i \sim v_j$ and otherwise, respectively. The energy of a graph is introduced in [8] as $En(G) = \sum_{i=1}^{n} |\lambda_i|$, where λ_i are the eigenvalues of $A(G)$, namely $En(G) = En(A(G))$. Graph energy and its types have long been an interesting topic for chemists and mathematicians (see [3],[11],[15],[18]).

Let $D(G) = diag(d_1, d_2, ..., d_n)$ be the diagonal matrix of vertex degrees of G. The Laplacian matrix $L(G)$ is defined as $L(G) = D(G) - A(G)$ with eigenvalues $n \geq \vartheta_1 \geq \vartheta_2 \geq ... \geq \vartheta_n = 0$ which are called as Laplacian eigenvalues of G. The Laplacian energy of G is introduced in [6] as $En(L(G)) = \sum_{i=1}^{n} \left|\vartheta_i - \frac{2e}{n}\right|$.

Computing Classification System 1998: G.2.2
Mathematics Subject Classification 2010: 05C50, 15A18
Key words and phrases: Graph energy, Seidel Laplacian matrix, Seidel Laplacian energy

The Seidel matrix of G is defined by $S(G) = A(G^c) - A(G)$, where G^c is the complement of the graph G. The Seidel energy $En(S(G))$ of G is proposed in [9] as $En(S(G)) = \sum_{i=1}^{n} |\xi_i|$, where ξ_i are the Seidel eigenvalues of G. In [15], the relations between the Seidel energy and energy of graphs are given.

The Seidel Laplacian matrix $S_{\mathcal{L}}(G)$ of G is introduced in [17] as

$$S_{\mathcal{L}}(G) = D_s(G) - S(G), \tag{1}$$

where $D_s(G)$ be the diagonal matrix with main diagonal entries $n - 1 - 2d_i$. Also, $D_s(G) = D(G^c) - D(G)$ and $S_{\mathcal{L}}(G) = L(G^c) - L(G)$. The eigenvalues $\xi_1^L, \xi_2^L, ..., \xi_n^L$ of $S_{\mathcal{L}}(G)$ are called as the Seidel Laplacian eigenvalues of G. Further, the Seidel Laplacian energy of G is proposed in [17] as

$$En(S_{\mathcal{L}}(G)) = \sum_{i=1}^{n} \left| \xi_i^L - \frac{n(n-1) - 4e}{n} \right|$$

and some bounds for the Seidel Laplacian energy are presented by using mathematical inequalities. The eigenvalues ξ_i^L with multiplicities form the Seidel Laplacian spectrum of G and ξ_1^L denotes the spectral radius of $S_{\mathcal{L}}(G)$. Further studies on Seidel Laplacian energy see [1],[5]. Throughout this work, the order of all matrices is n.

Let $t_i := \xi_i^L - X$, where $X = \frac{n(n-1)-4e}{n}$. Hence,

$$En(S_{\mathcal{L}}(G)) = \sum_{i=1}^{n} |t_i|. \tag{2}$$

In this work, we initially determine the Seidel Laplacian spectrum of graphs. Then we propose new bounds for the Seidel Laplacian energy of graphs and regular graphs. Besides, we calculate the Seidel Laplacian energy of specific graphs.

In [17], it is shown that

$$\sum_{i=1}^{n} t_i = 0, \tag{3}$$

$$\sum_{i=1}^{n} t_i^2 = n(n-1) + 4Zg - \frac{16e^2}{n}, \tag{4}$$

where $Zg = Zg(G) = \sum_{u \sim v} d_u + d_v$ is the first Zagreb index of G. The inequality (5) is given in [1].

$$|t_1| \geq |X| \tag{5}$$

Lemma 1 ([17]) *If ξ_i^L are the Seidel Laplacian eigenvalues of G, then $-\xi_i^L$ are the Seidel Laplacian eigenvalues of G^c, for $i = 1, 2, ..., n$.*

Lemma 2 ([17]) *If $\xi_1, \xi_2, ..., \xi_n$ are the Seidel eigenvalues of a r-regular graph G, then $n - 1 - 2r - \xi_i$ $(i = 1, 2, ..., n)$ are the Seidel Laplacian eigenvalues of G.*

2 Seidel Laplacian eigenvalues

Let $\vartheta_1 \geq \vartheta_2 \geq ... \geq \vartheta_n$ be the Laplacian eigenvalues of G and associated Laplacian eigenvectors be $\overrightarrow{c_1}, \overrightarrow{c_2}, ..., \overrightarrow{c_n}$ are column-vectors of dimension n. Let I be the unit matrix and J be the all-ones matrix.

Lemma 3 ([7]) *The vector $\overrightarrow{j}$ with all components are 1 is a Laplacian eigenvector of any order n graph corresponding to the eigenvalue of $\vartheta_n = 0$.*

According to the previous lemma $\overrightarrow{c_n} = \overrightarrow{j}$ can be choosen. Assume that for $i = 1, 2, ..., n-1$ the Laplacian eigenvectors $\overrightarrow{c_i}$ are orthogonal to $\overrightarrow{c_n}$. For any vector $\overrightarrow{c}$, the scalar product is $\overrightarrow{j}^t \cdot \overrightarrow{c} = \rho\left(\overrightarrow{c}\right)$.

Lemma 4 ([7]) *If G is a graph, then $\rho\left(\overrightarrow{c_i}\right) = 0$ for any $1 \leq i \leq n-1$.*

Now we give the relationship between the Seidel Laplacian and Laplacian eigenvalues as follows.

Theorem 5 *If $\overrightarrow{c_i}$ is a Laplacian eigenvector of the graph G, then $\overrightarrow{c_i}$ is a Seidel Laplacian eigenvector of the graph G and $\xi_i^L = n - 2\vartheta_i$, for $1 \leq i \leq n-1$. If $i = n$, then $\xi_i^L = \vartheta_i = 0$.*

Proof. Clearly $S_{\mathcal{L}}(G) = L(G^c) - L(G) = nI - J - 2L(G)$. Thus from Lemma 4, we have

$$\begin{aligned} S_{\mathcal{L}}(G)\overrightarrow{c_i} &= [nI - J - 2L(G)]\,\overrightarrow{c_i} \\ &= nI\overrightarrow{c_i} - J\overrightarrow{c_i} - 2L(G)\overrightarrow{c_i} \\ &= n\overrightarrow{c_i} - \rho\left(\overrightarrow{c_i}\right)\overrightarrow{j} - 2\vartheta_i\overrightarrow{c_i} \\ &= (n - 2\vartheta_i)\,\overrightarrow{c_i}. \end{aligned} \tag{6}$$

From (6) obviously we have $\xi_i^L = n - 2\vartheta_i$ for $1 \leq i \leq n-1$. If $i = n$, then $\xi_i^L = \vartheta_i = 0$ see [1]. □

Corollary 6 *The following assertions hold for the Seidel Laplacian eigenvalues of* G *and* G^c :

(i) $\overline{\xi_i^L} = -n + 2\vartheta_{n-i}$, *for* $1 \leq i \leq n-1$ *and* $\overline{\xi_i^L} = \overline{\vartheta_i} = \vartheta_i = 0$ *for* $i = n$, *where* $\overline{\xi_i^L}$ *and* $\overline{\vartheta_i}$ *are the Seidel Laplacian and Laplacian eigenvalues of* G^c, *respectively.*

(ii) The Seidel Laplacian eigenvalues of G *and* G^c *can be given respectively as*

$$n - 2\vartheta_1, n - 2\vartheta_2, ..., n - 2\vartheta_{n-1}, 0 \tag{7}$$

$$-n + 2\vartheta_{n-1}, -n + 2\vartheta_{n-2}, ..., -n + 2\vartheta_1, 0. \tag{8}$$

Proof.

(i) Obviously for $i = n$, $\overline{\vartheta_i} = \vartheta_i = 0$ and for $1 \leq i \leq n-1$, $\overline{\vartheta_i} = n - \vartheta_{n-i}$. From Theorem 5, $\xi_i^L = n - 2\vartheta_i$ for $1 \leq i \leq n-1$, we also have $\overline{\xi_i^L} = n - 2\overline{\vartheta_i} = n - 2(n - \vartheta_{n-i}) = -n + 2\vartheta_{n-i}$. For $i = n$, $\overline{\xi_i^L} = \overline{\vartheta_i} = \vartheta_i = 0$.

(ii) The proof of (7) and (8) can be seen as a result of Theorem 5 and (i), respectively.

□

Remark 7 ([2]) *Let* $\lambda_1 \geq \lambda_2 \geq ... \geq \lambda_n$ *be the eigenvalues of a* r*-regular graph, then* $\lambda_1 = r$ *and its Laplacian eigenvalues are*

$$0, r - \lambda_2, ..., r - \lambda_n,$$

and the Seidel eigenvalues are

$$n - 1 - 2r, -1 - 2\lambda_2, ..., -1 - 2\lambda_n. \tag{9}$$

Corollary 8 *If* G *is a* r*-regular graph, then the Seidel Laplacian eigenvalues of* G *are*

$$0, n - 2r + 2\lambda_2, ..., n - 2r + 2\lambda_n. \tag{10}$$

Proof. From Lemma 2, $n - 1 - 2r - \xi_i$ are the Seidel Laplacian eigenvalues of G and using (9) yields the result. □

We will determine the Seidel Laplacian spectrum of certain graphs by using Theorem 5 and their Laplacian spectrum.

Proposition 9 *If S_n is a star, then the Seidel Laplacian spectrum of S_n is* $\left\{-n, 0, \underbrace{n-2, ..., n-2}_{n-2}\right\}$.

Proof. Laplacian spectrum of S_n is $\left\{n, 0, \underbrace{1, ..., 1}_{n-2}\right\}$. Then by using $\xi_i^L = n - 2\vartheta_i$, for $1 \leq i \leq n-1$ and $\xi_n^L = \vartheta_n = 0$, the proof can be seen. □

Proposition 10 *If C_n is a cycle graph, then the Seidel Laplacian spectrum of C_n is $n - 4\left(1 - \cos\frac{2\pi i}{n}\right)$, $i = 0, 1, ..., n-1$.*

Proof. Laplacian spectrum of C_n is $2\left(1 - \cos\frac{2\pi i}{n}\right)$ for $i = 0, 1, ..., n-1$ (see [19]). Using Theorem 5 completes the proof. □

Proposition 11 *If P_n is a path graph, then the Seidel Laplacian spectrum of P_n is $n - 4\left(1 - \cos\frac{\pi i}{n}\right)$, $i = 0, 1, ..., n-1$.*

Proof. Laplacian spectrum of P_n is $2\left(1 - \cos\frac{\pi i}{n}\right)$ for $i = 0, 1, ..., n-1$ (see [19]), using Theorem 5 yields the result. □

Proposition 12 *If $K_{m,n}$ be a complete bipartite graph, then Seidel Laplacian eigenvalues of $K_{m,n}$ are $-(m+n), 0$; $n-m$ of multiplicity $n-1$; $m-n$ of multiplicity $m-1$.*

Proof. Laplacian eigenvalues of $K_{m,n}$ are $m+n, 0$; m of multiplicity $n-1$; n of multiplicity $m-1$. As $K_{m,n}$ has $m+n$ vertices, then from Theorem 5 $\xi_i^L = m + n - 2\vartheta_i$ for $1 \leq i \leq m+n-1$ and $\xi_{m+n}^L = \vartheta_{m+n} = 0$. □

The friendship graph is formed by s triangles with a common vertex, which has $2s+1$ vertices and $3s$ edges.

Proposition 13 *If F_s $(s \geq 1)$ is a friendship graph, then the Seidel Laplacian spectrum of F_s is $-(2s+1), 0$; $2s-5$ of multiplicity s; $2s-1$ of multiplicity $s-1$.*

Proof. The friendship graph has Laplacian eigenvalues $2s+1, 0$; 3 of multiplicity s; 1 of multiplicity $s-1$ (see [19]). The proof is clear from Theorem 5. □

Lemma 14 ([10]) *If* B *is an irreducible non-negative matrix with spectral radius* $\theta(B)$ *and* $s_i(B)$ *be the* i^{th} *row sum of* B, *then*

$$\theta(B) \leq \max_{1\leq i\leq n} s_i(B).$$

Now we present an upper bound for ξ_1^L.

Theorem 15 *Let* G *be an order* n *connected graph with maximum degree* Δ. *Then*

$$\xi_1^L \leq 2\Delta.$$

Proof. Using the previous lemma we get

$$\begin{aligned}\xi_1^L \leq & \theta(|S_{\mathcal{L}}|)\\ \leq & \max_{1\leq i\leq n} s_i(|S_{\mathcal{L}}|)\\ = & \max_{1\leq i\leq n} \{|n-1-2d_i|+n-1\}\end{aligned}$$

If $n-1 \geq 2d_i$, then $s_i(|S_{\mathcal{L}}|) = 2(n-1-d_i)$ and if $n-1 < 2d_i$, then $s_i(|S_{\mathcal{L}}|) = 2d_i$. Therefore we have

$$\begin{aligned}\xi_1^L \leq & 2\max_{1\leq i\leq n} \{d_i, n-1-d_i\}\\ \leq & 2\max_{1\leq i\leq n} \{\Delta, n-1-\delta\} = 2\Delta,\end{aligned}$$

where δ is the minimum degree. □

3 Bounds for Seidel Laplacian energy

Several bounds will be obtained for the Seidel Laplacian energy of graphs via their Seidel Laplacian spectrum, mathematical inequalities and Ky Fan theorem in this section. Now, we can begin with the following theorem which states that the Seidel Laplacian energy and Seidel energy coincides for regular graphs.

Theorem 16 *If* G *is a* r*-regular graph of order* n, *then*

$$En(S_{\mathcal{L}}(G)) = En(S(G)).$$

Proof. We have $X = n-1-2r$ and by Lemma 2, $\xi_i^L = n-1-2r-\xi_i$ which yields

$$\begin{aligned} En(S_{\mathcal{L}}(G)) =& \sum_{i=1}^{n} |n-1-2r-\xi_i-(n-1-2r)| \\ =& En(S(G)). \end{aligned}$$

□

Theorem 17 ([12]) *If* G *is a graph of order* n *with* e *edges, then*

$$En(G) \leq \sqrt{2en}. \tag{11}$$

Here, we can give two bounds for the Seidel Laplacian energy of regular graphs.

Theorem 18 *If* G *is a* r*-regular graph of order* n*, then*

$$En(S_{\mathcal{L}}(G)) \quad \leq \quad |n-1-2r| + n-1-2r+2En(G). \tag{12}$$

Proof. From (10) and as $X = n-1-2r$, we get

$$\begin{aligned} En(S_{\mathcal{L}}(G)) =& \sum_{i=1}^{n} \left|\xi_i^L-(n-1-2r)\right| \\ =& |n-1-2r| + \sum_{i=2}^{n} |n-2r+2\lambda_i-(n-1-2r)| \\ \leq& |n-1-2r| + \sum_{i=2}^{n} (2|\lambda_i|+1) \\ =& |n-1-2r| + n-1+2(En(G)-|\lambda_1|). \end{aligned}$$

The proof is clear by using $\lambda_1 = r$. □

Corollary 19 *If* G *is a* r*-regular graph of order* n*, then*

$$En(S_{\mathcal{L}}(G)) \leq |n-1-2r| + n-1-2r+2n\sqrt{r}.$$

Proof. From (11), $En(G) \leq n\sqrt{r}$. By using this fact in (12) yields the result. □

Theorem 20 *Let* G *be a graph of order* n *with* e *edges. Then*

$$En(S_{\mathcal{L}}(G)) \geq \sqrt{n(n-1)+4Zg-\frac{16e^2}{n}}.$$

Proof. If we apply the Radon inequality [16], then

$$\sum_{i=1}^{n} |t_i| = \sum_{i=1}^{n} \frac{|t_i|^2}{|t_i|} \geq \frac{\sum_{i=1}^{n} |t_i|^2}{\sum_{i=1}^{n} |t_i|}.$$

Hence, from (2) and (4) the proof is clear. □

Theorem 21 *Let* G *be a graph. Then*

$$En(S_{\mathcal{L}}(G)) \geq 2|X|.$$

Proof. Clearly

$$\begin{aligned} En(S_{\mathcal{L}}(G)) &= |t_1| + \sum_{i=2}^{n} |t_i| \\ &\geq |t_1| + \left| \sum_{i=2}^{n} t_i \right|. \end{aligned}$$

From (3), $|t_1| = \left| -\sum_{i=2}^{n} t_i \right|$. Thus by (5)

$$En(S_{\mathcal{L}}(G)) \geq 2|t_1| \geq 2\left| n - 1 - \frac{4e}{n} \right|,$$

completes the proof. □

Theorem 22 *If* G *is a graph with* n *vertices and* e *edges, then*

$$En(S_{\mathcal{L}}(G)) \geq \frac{2\left(n(n-1) + 4Zg - \frac{16e^2}{n}\right)}{\xi_1^L}.$$

Proof. Let $(a_i), (b_i)$, $i = 1, 2, ..., n$ be real numbers with $\sum_{i=1}^{n} |a_i| = 1$ and $\sum_{i=1}^{n} a_i = 0$. Then

$$\left| \sum_{i=1}^{n} a_i b_i \right| \leq \frac{1}{2} \left(\max_{1 \leq i \leq n} b_i - \min_{1 \leq i \leq n} b_i \right) \tag{13}$$

holds ([13],p.346).

Setting $b_i := \xi_i^L - X$ and $a_i = \frac{\xi_i^L - X}{\sum_{i=1}^{n} |\xi_i^L - X|}$ satisfies the conditions for inequality (13). Thus

$$\left| \frac{\sum_{i=1}^{n} \left(\xi_i^L - X\right)^2}{\sum_{i=1}^{n} \left|\xi_i^L - X\right|} \right| \leq \frac{1}{2} \left(\max_{1 \leq i \leq n} \left(\xi_i^L - X\right) - \min_{1 \leq i \leq n} \left(\xi_i^L - X\right) \right),$$

then, by (4)

$$\frac{n(n-1) + 4Zg - \frac{16e^2}{n}}{En(S_{\mathcal{L}}(G))} \leq \frac{1}{2} \left(\xi_1^L - X - (0 - X) \right),$$

yields

$$En(S_{\mathcal{L}}(G)) \geq \frac{2\left(n(n-1) + 4Zg - \frac{16e^2}{n}\right)}{\xi_1^L}.$$

□

Combining Theorem 15 with Theorem 22 results as follows.

Corollary 23 *Let* G *be a connected graph. Then*

$$En(S_{\mathcal{L}}(G)) \geq \frac{n(n-1) + 4Zg - \frac{16e^2}{n}}{\Delta}.$$

Let H be a symmetric matrix, $y_i(H)$ be its eigenvalues and $\sigma_i(H)$ be its singular values, $i = 1, 2, ..., n$. Then $\sigma_i(H) = |y_i(H)|$ for $i = 1, 2, ..., n$. In [14], the energy of a graph G is reconsidered as sum of the singular values of its adjacency matrix $A(G)$. This point of view has brought a new approach to the graph energy theory and made the following theorem proved by Fan [4] to be included in the graph energy theory.

Theorem 24 ([4]) *If* A, B *and* C *are square matrices of order* n*, then*

$$\sum_{i=1}^{n} \sigma_i(A) \leq \sum_{i=1}^{n} \sigma_i(B) + \sum_{i=1}^{n} \sigma_i(C),$$

where $A = B + C$.

Theorem 25 *Let* G *be a graph, then*

$$En\left(S_{\mathcal{L}}(G)\right) \leq En\left(S(G)\right) + 2\sum_{i=1}^{n}\left|\overline{d} - d_i\right|, \tag{14}$$

where $\overline{d}$ *is the average degree of* G.

Proof. From (1), we can write

$$\left(S_{\mathcal{L}}(G) - \frac{n(n-1)-4e}{n}I\right) = (-S(G)) + \left(D_s(G) - \frac{n(n-1)-4e}{n}I\right).$$

Also, $\left(D_s(G) - \frac{n(n-1)-4e}{n}I\right)$ is a diagonal matrix with eigenvalues $\frac{4e}{n} - 2d_i$ that is, $2\left(\overline{d} - d_i\right)$ for $i = 1, 2, ..., n$ where $\overline{d}=\frac{2e}{n}$. Then by (2) and applying Theorem 24 satisfies the result. □

Corollary 26 *If* G *is a graph of order* n*, then*

$$En\left(S_{\mathcal{L}}(G)\right) \leq \sqrt{n\left(n^2-n\right)} + 2\sum_{i=1}^{n}\left|\overline{d} - d_i\right|.$$

Proof. In [11], it is shown that $En\left(S(G)\right) \leq \sqrt{n\left(n^2-n\right)}$. If we use this bound in (14), then we get the result. □

Different bounds for $En\left(S_{\mathcal{L}}(G)\right)$ can also be derived by using the bounds for Seidel energy.

4 Seidel Laplacian energy of specific graphs

The Seidel Laplacian energy of certain graphs will be calculated here by using their Seidel Laplacian spectrum.

Proposition 27 *If* S_n *is a star with* $n\,(\geq 4)$ *vertices, then* $En\left(S_{\mathcal{L}}(S_n)\right) = 6n + \frac{16}{n} - 20$.

Proof. *Star graph has* $n-1$ *edges, thus* $X = \frac{n^2-5n+4}{n}$. *From Proposition 9*

$$\begin{aligned} En\left(S_{\mathcal{L}}(S_n)\right) &= \left|-n - \frac{n^2-5n+4}{n}\right| + \left|\frac{n^2-5n+4}{n}\right| \\ &\quad + (n-2)\left|n-2-\frac{n^2-5n+4}{n}\right| \\ &= \left|5 - \left(2n + \frac{4}{n}\right)\right| + \left|n + \frac{4}{n} - 5\right| + (n-2)\left|3 - \frac{4}{n}\right|. \end{aligned}$$

Since $5-\left(2n+\frac{4}{n}\right)<0$, $3-\frac{4}{n}>0$ *and* $n+\frac{4}{n}-5\geq 0$ *for* $n\geq 4$, *we obtain*

$$\begin{aligned}En\left(S_{\mathcal{L}}\left(S_n\right)\right)=&-5+2n+\frac{4}{n}+n+\frac{4}{n}-5+(n-2)\left(3-\frac{4}{n}\right)\\=&6n+\frac{16}{n}-20.\end{aligned}$$

□

Proposition 28 *If* C_n *is the cycle graph with* n *vertices, then*

$$En\left(S_{\mathcal{L}}\left(C_n\right)\right)=\sum_{i=0}^{n-1}\left|1+4\cos\frac{2\pi i}{n}\right|.$$

Proof. From Proposition 10 and $X=n-5$, we have

$$En\left(S_{\mathcal{L}}\left(C_n\right)\right)=\sum_{i=0}^{n-1}\left|n-4\left(1-\cos\frac{2\pi i}{n}\right)-(n-5)\right|=\sum_{i=0}^{n-1}\left|1+4\cos\frac{2\pi i}{n}\right|.$$

□

Proposition 29 *If* P_n *is the path graph with* n *vertices, then*

$$En\left(S_{\mathcal{L}}\left(P_n\right)\right)=\sum_{i=0}^{n-1}\left|1+4\left(\cos\frac{\pi i}{n}\right)-\frac{4}{n}\right|.$$

Proof. From Proposition 11 and as $X=\frac{n^2-5n+4}{n}$, we obtain

$$\begin{aligned}En\left(S_{\mathcal{L}}\left(P_n\right)\right)=&\sum_{i=0}^{n-1}\left|n-4\left(1-\cos\frac{\pi i}{n}\right)-\frac{n^2-5n+4}{n}\right|\\=&\sum_{i=0}^{n-1}\left|1+4\left(\cos\frac{\pi i}{n}\right)-\frac{4}{n}\right|.\end{aligned}$$

□

Proposition 30 *If* $K_{m,n}$ $(1<n<m)$ *is a complete bipartite graph, then*

$$En\left(S_{\mathcal{L}}\left(K_{m,n}\right)\right)=\begin{cases}\frac{4\left(m^2n-n^2m+n^2\right)+2\left(m^2-m-n-mn\right)}{m+n}, & \text{if } X>0\\ \frac{4\left(m^2n-n^2m\right)+2\left(n^2+mn\right)}{m+n}, & \text{if } X<0\end{cases},$$

where $X = \frac{(m-n)^2-(m+n)}{m+n}$.

Proof. $K_{m,n}$ has $m+n$ vertices, mn edges, then $X = \frac{(m-n)^2-(m+n)}{m+n}$. Thus from Proposition 12

$$\begin{aligned} En\left(S_{\mathcal{L}}\left(K_{m,n}\right)\right) = &\left|-(m+n) - \frac{(m-n)^2-(m+n)}{m+n}\right| \\ &+ (n-1)\left|n-m - \frac{(m-n)^2-(m+n)}{m+n}\right| \\ &+ (m-1)\left|m-n - \frac{(m-n)^2-(m+n)}{m+n}\right| \\ &+ \left|\frac{(m-n)^2-(m+n)}{m+n}\right|. \end{aligned} \tag{15}$$

Denote the terms in RHS of (15) as A_1, A_2, A_3, A_4, respectively. Then

$$A_1 = (m+n) + \frac{(m-n)^2-(m+n)}{m+n} = \frac{2m^2+2n^2-m-n}{m+n},$$

as $-(m+n) - \frac{(m-n)^2-(m+n)}{m+n} = \frac{(m+n)-\left[(m-n)^2+(m+n)^2\right]}{m+n} < 0.$

$$\begin{aligned} A_2 &= (n-1)\left[\frac{-(m+n)+\left(m^2-n^2\right)+(m-n)^2}{m+n}\right] \\ &= (n-1)\left(\frac{2m^2-2mn-m-n}{m+n}\right) \\ &= \frac{2m^2n-2n^2m-2m^2-n^2+mn+m+n}{m+n}, \end{aligned}$$

as $n-m-\frac{(m-n)^2-(m+n)}{m+n} = \frac{m+n-\left[\left(m^2-n^2\right)+(m-n)^2\right]}{m+n} < 0.$

$$\begin{aligned} A_3 &= (m-1)\left(m-n-\frac{(m-n)^2-(m+n)}{m+n}\right) \\ &= (m-1)\left(\frac{-2n^2+2mn+m+n}{m+n}\right) \\ &= \frac{-2n^2m+2m^2n+m^2+2n^2-mn-m-n}{m+n}, \end{aligned}$$

as $m-n-\frac{(m-n)^2-(m+n)}{m+n}=\frac{m^2-n^2-(m-n)^2+m+n}{m+n}=\frac{2n(m-n)+m+n}{m+n}>0$. Now consider $A_4=\left|\frac{(m-n)^2-(m+n)}{m+n}\right|=|X|$. Obviously if $X>0$, then $A_4=\frac{m^2-2mn+n^2-m-n}{m+n}$ and if $X<0$, then $A_4=-\frac{m^2-2mn+n^2-m-n}{m+n}$. If we sum A_1,A_2,A_3,A_4 in case $X>0$, then

$$En\left(S_{\mathcal{L}}\left(K_{m,n}\right)\right)=\frac{4m^2n-4n^2m+2m^2+4n^2-2m-2n-2mn}{m+n}.$$

Repeating above operations in case $X<0$, we have

$$En\left(S_{\mathcal{L}}\left(K_{m,n}\right)\right)=\frac{4m^2n-4n^2m+2n^2+2mn}{m+n}.$$

□

Example 31 *Let $K_{4,3}$ be a complete bipartite graph. Then the Seidel Laplacian eigenvalues of $K_{4,3}$ are $-7,0$; -1 of multiplicity 2; 1 of multiplicity 3. Since $X=\frac{1^2-7}{7}=-\frac{6}{7}<0$, from Proposition 30 we have $En\left(S_{\mathcal{L}}\left(K_{m,n}\right)\right)=\frac{4\left(m^2n-n^2m\right)+2\left(n^2+mn\right)}{m+n}$, thus $En\left(S_{\mathcal{L}}\left(K_{4,3}\right)\right)=\frac{90}{7}$. Consider $K_{5,2}$, then the Seidel Laplacian eigenvalues of $K_{5,2}$ are $-7,0$; -3 of multiplicity 1; 3 of multiplicity 4. Since $X=\frac{3^2-7}{7}=\frac{2}{7}>0$, from Proposition 30 we have $En\left(S_{\mathcal{L}}\left(K_{m,n}\right)\right)=\frac{4\left(m^2n-n^2m+n^2\right)+2\left(m^2-m-n-mn\right)}{m+n}$, then $En\left(S_{\mathcal{L}}\left(K_{5,2}\right)\right)=\frac{152}{7}$.*

Proposition 32 *If F_s $(s\geq 3)$ is the friendship graph, then $En\left(S_{\mathcal{L}}\left(F_s\right)\right)=\frac{24s^2-32s+21}{2s+1}$.*

Proof. By Proposition 13 and as $X=\frac{(2s+1)2s-12s}{2s+1}=\frac{4s^2-10s}{2s+1}$, we have

$$\begin{aligned}
En\left(S_{\mathcal{L}}\left(F_s\right)\right)&=\sum_{i=0}^{2s+1}\left|\xi_i^L-X\right|\\
&=\left|-(2s+1)-\frac{4s^2-10s}{2s+1}\right|+s\left|2s-5-\frac{4s^2-10s}{2s+1}\right|\\
&\quad+(s-1)\left|2s-1-\frac{4s^2-10s}{2s+1}\right|+\left|\frac{4s^2-10s}{2s+1}\right|\\
&=\frac{1}{2s+1}\left(\left|8s^2-6s+1\right|+s\left|2s-5\right|+(s-1)\left|10r-1\right|+\left|4s^2-10s\right|\right).
\end{aligned}\tag{16}$$

In RHS of (16), all of the expressions in absolute value are positive for $s \geq 3$, thus

$$En\left(S_{\mathcal{L}}\left(F_s\right)\right) = \frac{1}{2s+1}\left(24s^2 - 32s + 2\right).$$

□

Corollary 33 *If* G *is the friendship graph with* n *vertices, then*

$$En\left(S_{\mathcal{L}}\left(G\right)\right) = \frac{6n^2 - 28n + 24}{n}.$$

Proof. Setting $s = \frac{n-1}{2}$ in Proposition 32 yields the result. □

References

[1] J. Askari, A Note on the Seidel and Seidel Laplacian matrices, *Bol. Soc. Paran. Mat.*, (2020) 1–6. ⇒105, 106

[2] D. Cvetković, P. Rowlinson, S. Simić, *An Introduction to the Theory of Graph Spectra*, Cambridge University Press, 2010. ⇒107

[3] K. C. Das, S. Elumalai, On energy of graphs, *MATCH Commun. Math. Comput. Chem.*, 77 (2017) 3–8. ⇒104

[4] K. Fan, Maximum properties and inequalities for the eigenvalues of completely continuous operators, *Proc. Natl. Acad. Sci.,* **37,** 11 (1951) 760–766. ⇒112

[5] G. K. Gök, Some bounds on the Seidel energy of graphs, *TWMS J. Appl. Eng. Math.,* **9,** 4 (2019) 949–956. ⇒105

[6] I. Gutman, B. Zhou, Laplacian energy of a graph, *Linear Algebra Appl.,* **414,** 1 (2006) 29–37. ⇒104

[7] I. Gutman, The star is the tree with greatest Laplacian eigenvalue, *Kragujevac J. Math.,* **24** (2002) 61-65. ⇒106

[8] I. Gutman, The energy of a graph, 10. Steiermärkisches Mathematisches Symposium, *Ber. Math.-Statist. Sekt. Forsch.* Graz **103** 1978, pp.1–22. ⇒104

[9] W. H. Haemers, Seidel switching and graph energy, *MATCH Commun. Math. Comput. Chem.,* 68 (2012) 653–659. ⇒105

[10] R. A. Horn, C.R. Johnson, *Matrix analysis*, Cambridge University Press, New York, 1985. ⇒109

[11] M. R. R. Kanna, R. P. Kumar, M.R. Farahani, Milovanović Bounds for Seidel Energy of a Graph, *Advances in Theoretical and Applied Mathematics,* 10, 1 (2016) 37—44. ⇒104, 113

[12] B. J. McClelland, Properties of the latent roots of a matrix: The estimation of π-electron energies, *J. Chem. Phys.,* 54, 2 (1971) 640–643. ⇒110

[13] D. S. Mitrinović and P. M. Vasić, *Analytic inequalities*, Springer Verlag, Berlin-Heidelberg-New York, 1970. ⇒111

[14] V. Nikiforov, The energy of graphs and matrices, *J. Math. Anal. Appl.,* **326** (2007) 1472–1475. ⇒112
[15] M. R. Oboudi, Energy and Seidel energy of graphs, *MATCH Commun. Math. Comput. Chem.,* 75 (2016) 291–303. ⇒104, 105
[16] J. Radon, Theorie und Anwendungen der absolut additiven Mengenfunktionen, *Sitzungsber. Acad. Wissen. Wien,* 122 (1913) 1295–1438. ⇒111
[17] H. S. Ramane, R.B. Jummannaver, I. Gutman, Seidel Laplacian energy of graphs, *Int. J. Appl. Graph Theory*, 1 (2017) 74–82. ⇒105, 106
[18] H. S. Ramane, I. Gutman, J.B. Patil, R.B. Jummannaver, Seidel signless Laplacian energy of graphs, *Math. Interdisc. Res.,* 2 (2017) 181–191. ⇒104
[19] P. B. Sarasija, P. Nageswari, Laplacian energy of certain graphs, *International J. Math. Combin.,* 1 (2012) 78–82. ⇒108

Received: June 6, 2022 • Revised: June 18, 2022

Acta Univ. Sapientiae Informatica **14,** 1 (2022) 119–136

DOI: 10.2478/ausi-2022-0008

Annihilator graphs of a commutative semigroup whose Zero-divisor graphs are a complete graph with an end vertex

Seyed Mohammad SAKHDARI
Department of Basic Sciences,
Sabzevar Branch, Islamic Azad University,
Sabzevar, Iran
email: sakhdari85@yahoo.com

Mojgan AFKHAMI
Department of Mathematics,
University of Neyshabur,
P.O.Box 91136-899,
Neyshabur, Iran
email: mojgan.afkhami@yahoo.com

Abstract. Suppose that the zero-divisor graph of a commutative semigroup S, be a complete graph with an end vertex. In this paper, we determine the structure of the annihilator graph S and we show that if $Z(S) = S$, then the annihilator graph S is a disconnected graph.

1 Introduction

In this paper S is a commutative semigroup with zero whose operation is written multiplicatively and $Z(S)$ is the set of all zero-divisors of S also $Z(S)^* = Z(S) \setminus \{0\}$.

The zero-divisor graph of a commutative semigroup S with zero, is denoted by $\Gamma(S)$, is an undirected graph with vertex set $Z(S)^*$ and two distinct vertices x and y are adjacent if and only if $xy = 0$. $\Gamma(S)$ is a connected graph and the

Computing Classification System 1998: G.2.2
Mathematics Subject Classification 2010: 68R15
Key words and phrases: zero-divisor graph, annihilator graph, isolated vertex, connected graph, complete graph

diameter of $\Gamma(S)$ is less than or equal to three. For other results on zero divisor graphs one can see [5, 6, 7, 8, 9, 10].

In [1], we introduced and studied the annihilator graph for a commutative semigroup S, and showed it with $AG(S)$. The graph $AG(S)$ is an undirected graph with vertex set $Z(S)^*$ and two distinct vertices x and y are adjacent if and only if $\text{ann}_S(xy) \neq \text{ann}_S(x) \cup \text{ann}_S(y)$, where $\text{ann}_S(x) = \{s \in S \mid xs = 0\}$. We proved that if $Z(S) \neq S$, then $\Gamma(S)$ is a subgraph of $AG(S)$, and so $AG(S)$ is connected. Also if $Z(S) = S$, then $AG(S)$ may be connected or disconnected and if there exists $x \in S^* = S \setminus \{0\}$ such that x is adjacent to all vertices in $\Gamma(S)$, then x is an isolated vertex in $AG(S)$.

In [1, section 4] and in [2], we characterized all annihilator graphs with three and four vertices. Also in [3], we studied the structure of the annihilator graph of a commutative semigroup S whose $\Gamma(S)$ is a refinement of a star graph.

A complete graph and a complete graph with an end vertex are one of the graphs can be zero-divisor graph of a commutative semigroup.

In this paper, we study the annihilator graph associated with a commutative semigroup with zero using the zero-divisor graph $\Gamma(S)$, where $\Gamma(S)$ is a complete graph K_n with an end vertex $u \notin V(K_n)$ and u is only adjacent to $z \in V(K_n)$. Let m be the number of edges between u and $V(K_n)$ in $AG(S)$. We show that the following four statements hold.

(i) Let $u^2 = 0$. If $Z(S) \neq S$, then $m \in \{1, 2, 3, ..., n\}$ and if $Z(S) = S$, then $m \in \{0, 1, 2, 3, ..., n-1\}$.

(ii) Let $u^2 = z$. If $Z(S) \neq S$, then $m = n$ and so u is adjacent to all vertices of $V(K_n)$ in $AG(S)$ and if $Z(S) = S$, then $m = n-1$ and u is not adjacent to z in $AG(S)$.

(iii) Let $u^2 = u$. If $Z(S) \neq S$, then $m \in \{1, 2, 3, ..., n-1\}$ and if $Z(S) = S$, then $m \in \{0, 1, 2, 3, ..., n-2\}$ and so there is at least one vertex of $V(K_n)$ that u is not adjacent to it in $AG(S)$.

(iv) Let $u^2 = b \notin \{0, z, u\}$. If $Z(S) \neq S$, then $m \in \{n-1, n\}$ and so there is at most one vertex ($u^2 = b$) of $V(K_n)$ that u is not adjacent to it in $AG(S)$. Also if $Z(S) = S$, then $m \in \{n-1, n-2\}$ and u is not adjacent to z in $AG(S)$.

2 Preliminaries

In this section, we recall some definitions and notations of graphs and we use the standard terminology of graphs is contained in [4]. Here, G is a graph with vertex set $V(G)$ and edge set $E(G)$. If a is adjacent to b in G, then the edge between a and b will denote by $\{ab\}$ and we write $a \sim b$.

The *distance* between two distinct vertices x and y is the length of the shortest path connecting x and y and will denote by $d(x, y)$, if such a path exists; otherwise, we use $d(x, y) := \infty$. Also $diam(G) = \sup\{d(x, y) : x$ and y are distinct vertices of $G\}$ is the *diameter* of the graph G.

The *girth* of G, denoted by $gr(G)$, is the length of the shortest cycle in G. If there exists a path between any two distinct vertices of G, we say that graph G is a *connected* graph, and if for each two vertices x and y of $V(G)$ we have x is adjacent to y, we say that G is a complete graph and K_n is the complete graph with n vertices. If no two vertices of G are adjacent, we say that G is a *totally disconnected* graph and nK_1 is the totally disconnected graph with n vertices.

We say that u is an end vertex in G, If u is adjacent to only one vertex of G and if for each vertex $x \in V(G)$ we have u is not adjacent to x, then we say that u is an *isolated* vertex in G.

Suppose that H and G are two graphs. We use the notation $G \leq H$ to denote that G is a subgraph of H and if H is isomorphic to G, we write $H \cong G$. Let G be a graph. $G \setminus \{\{x_1y_1\}, \{x_2y_2\}, \{x_3y_3\}, ..., \{x_ny_n\}\}$ is a graph such that edges $\{x_1y_1\}, \{x_2y_2\}, \{x_3y_3\}, ..., \{x_ny_n\}$ are deleted.
P_n is the path of length n and C_n is the cycle of length n.
mK_n is a graph with m components such that each component is isomorphic to K_n. $G \cup H$, the union of the graphs G and H, is a graph with vertex set $V(G) \cup V(H)$ and edge set $E(H) \cup E(G)$.

Now, we recall some results which we are used in the next section.

Theorem 1 [1] *If $Z(S) \neq S$, then we have $\Gamma(S) \leq AG(S)$.*

Theorem 2 [1] *Let $Z(S) = S$ and there exists $x \in S^*$ such that, for each non zero element $y \neq x$ of S, we have $xy = 0$. Then x is an isolated vertex in $AG(S)$.*

Lemma 3 [2] *If $Z(S) \neq S$ and $\Gamma(S) \cong P_3$, then $AG(S) \cong C_4$.*

Lemma 4 [2] *Let $Z(S) \neq S$. Then $AG(S) \cong C_4$ if and only if we either have $\Gamma(S) \cong P_3$ or $\Gamma(S) \cong C_4$.*

Lemma 5 [2] *Let* $Z(S) = S$. *Then* $AG(S) \cong P_3$ *with* $x \sim w \sim z \sim y$ *if and only if* $\Gamma(S) \cong P_3$ *with* $w \sim x \sim y \sim z$.

Lemma 6 [2] *Let* S *be a commutative semigroup with* $Z(S) \neq S$, *and let* $\Gamma(S) \cong K_3 + \{wx\}$ *with* $wx = xy = yz = zx = 0$. *Then* $AG(S) \cong K_4 \setminus \{wy\}$ *if and only if the relations between the zero-divisors of* S *satisfies in one of the following four conditions.*

(i) $wy = y$, $wz = x$, $w^2 = y^2 = y$, $x^2 = 0$, *and* $z^2 \in \{0, x\}$.

(ii) $wy = wz = x$, $w^2 = y^2 = x^2 = 0$, *and* $z^2 = x$.

(iii) $wy = y = wz$, $w^2 = w$, $z^2 = x$, *and* $y^2 = x^2 = 0$.

Lemma 7 [2] *Let* S *be a commutative semigroup with* $Z(S) \neq S$, *and let* $\Gamma(S) \cong K_3 + \{wx\}$ *with* $wx = xy = yz = zx = 0$. *Then* $AG(S) \cong K_4$ *if and only if the relations between the zero-divisors of* S *satisfies in one of the following eleven conditions.*

(i) $wx = xy = yz = zx = 0$, $wy = x$, $wz = y$, $y^2 = x^2 = 0$, $w^2 = z$ *and* $z^2 = x$.

(ii) $wx = xy = yz = zx = 0$, $wy = z$, $wz = x$, $w^2 = y$, $y^2 = x$ *and* $z^2 = x^2 = 0$.

(iii) $wx = xy = yz = zx = 0$, $wy = wz = x$, $x^2 = 0$ *and one of the following nine cases holds.*

(1) $w^2 = 0$, $y^2 = x$ *and* $z^2 = x$.
(2) $w^2 = y$, $y^2 = 0$ *and* $z^2 \in \{0, x\}$.
(3) $w^2 = z$, $z^2 = 0$ *and* $y^2 \in \{0, x\}$.
(4) $w^2 = x$, $y^2 = 0$ *and* $z^2 \in \{0, x\}$.
(5) $w^2 = x$, $y^2 = x$ *and* $z^2 \in \{0, x\}$.

Lemma 8 [2] *Let* S *be a commutative semigroup with* $Z(S) \neq S$, *and let* $\Gamma(S) \cong K_3 + \{wx\}$ *with* $wx = xy = yz = zx = 0$. *Then* $AG(S) \cong K_3 + \{wx\}$ *with* $w \sim x \sim y \sim z \sim x$ *if and only if the relations between the zero-divisors of* S *satisfies in one of the following nineteen conditions.*

(i) $wx = xy = yz = zx = 0$, $wy = y = wz$, $z^2 = y^2 = 0$, $w^2 = w$ *and* $x^2 \in \{0, x\}$.

(ii) $wx = xy = yz = zx = 0$, $wz = wy = x$ *and* $w^2 = y^2 = z^2 = x^2 = 0$.

(iii) $wx = xy = yz = zx = 0$, $wz = z = wy$, $w^2 = w$, $y^2 = z^2 = 0$ *and* $x^2 \in \{0, x\}$.

(iv) $wx = xy = yz = zx = 0$, $wz = y$, $wy = z$, $w^2 = w$, $y^2 = z^2 = 0$ *and* $x^2 \in \{0, x\}$.

(v) $wx = xy = yz = zx = 0$, $wy = y$, $wz = z$, $w^2 = w$ *and we have the following twelve situations.*

(1) $y^2 = 0$, $z^2 = 0$ *and* $x^2 \in \{0, x\}$.
(2) $y^2 = 0$, $z^2 = z$ *and* $x^2 \in \{0, x\}$.
(3) $y^2 = 0$, $z^2 = y$ *and* $x^2 \in \{0, x\}$.
(4) $y^2 = y$, $z^2 = 0$ *and* $x^2 \in \{0, x\}$.
(5) $y^2 = y$, $z^2 = z$ *and* $x^2 \in \{0, x\}$.
(6) $y^2 = z$, $z^2 = 0$ *and* $x^2 \in \{0, x\}$.

Lemma 9 [2] *Let* S *be a commutative semigroup with* $Z(S) = S$, *and let* $\Gamma(S) \cong K_3 + \{wx\}$ *with* $wx = xy = yz = zx = 0$. *Then* $AG(S) \cong 2K_1 \cup K_2$, *where* x *and* w *are isolated vertices and* z *is adjacent to* y, *if and only if the semigroup* S *satisfies in one of the nineteen conditions of Lemma* (8).

Lemma 10 [2] *Let* S *be a commutative semigroup with* $Z(S) = S$. *Then* $AG(S) \cong K_{1,2} \cup K_1$, *where* x *is an isolated vertex and the vertices* y, z, w *form a star graph with center* z, *if and only if* $\Gamma(S) \cong K_3 + \{wx\}$ *with* $wx = xy = yz = zx = 0$, *and the semigroup* S *satisfies in one of the four conditions of Lemma* (6).

Lemma 11 [2] *Let* S *be a commutative semigroup with* $Z(S) = S$, *and let* $\Gamma(S) \cong K_3 + \{wx\}$ *with* $wx = xy = yz = zx = 0$. *Then* $AG(S) \cong K_3 \cup K_1$, *where* x *is an isolated vertex and the vertices* w, z, y *form a triangle if and only if the semigroup* S *satisfies in one of the eleven conditions of Lemma* (7).

Suppose that G is a complete graph K_n with an end vertex u that u is adjacent to $z \in V(K_n)$ and $n = 1$. Then $\Gamma(S) \cong K_2$. Now if $Z(S) = S$, then clearly $AG(S) \cong 2K_1$, and if $Z(S) \neq S$, then $AG(S) \cong \Gamma(S) \cong K_2$.

Let $n = 2$. We have $\Gamma(S) \cong K_{1,2} = P_2$ with $u \sim z \sim x$. In [1], we show that, if $Z(S) = S$, then $AG(S) \cong 3K_1$ or $AG(S) \cong K_1 \cup K_2$, and if $Z(S) \neq S$, then $AG(S) \cong K_{1,2}$ or $AG(S) \cong K_3$.

Morover assume that complete graph K_2 has two end vertices u_1 and u_2 adjacent to z_1 and z_2. Then $\Gamma(S) \cong P_3$ with $u_1 \sim z_1 \sim z_2 \sim u_2$. Now by lemma 5, if $Z(S) = S$, then $AG(S) \cong P_3$ with $z_1 \sim u_1 \sim u_2 \sim z_2$ such that z_1 and z_2 are two end vertices in $AG(S)$, and by lemma 3, if $Z(S) \neq S$, then $AG(S) \cong C_4$.

3 Properties of $AG(S)$

In this section, we assume that $|Z(S)^*| \geq 4$ and K_n is a complete graph with at least three vertices and $z \in V(K_n)$ and $u \notin V(K_n)$. we add to K_n an end vertex u, which is adjacent to a unique vertex z of $V(K_n)$ and denote it by $\Gamma(S) \cong K_n + \{uz\}$ and so $\Gamma(S) \cong K_n + \{uz\}$ is the graph of a commutative semigroup such that $Z(S) = V(K_n) \cup \{0\} \cup \{u\}$. Thus for each two distinct vertices x and y in$V(K_n)$, we have $xy = zu = 0$ and $xu \neq 0$ and Since z is a cut vertex in $\Gamma(S)$, thus $\{0, z\}$ is an ideal of S and so $z^2 = 0$ or $z^2 = z$.

In following, we distinguish the structure of the annihilator graph a commutative semigroup whose $\Gamma(S) \cong K_n + \{uz\}$, for cases $u^2 = 0$ or $u^2 = z$ or $u^2 = u$ or $u^2 \neq 0, z, u$.

The following lemma show that if $\Gamma(S)$ is a complete graph K_n with an end vertex u, then for all $x, y \in V(K_n) \setminus \{z\}$ always, x is adjacent to y in $AG(S)$.

Lemma 12 *Suppose that $\Gamma(S)$ is a complete graph K_n with an end vertex u. Then for all $x, y \in V(K_n) \setminus \{z\}$, we have x is adjacent to y in $AG(S)$.*

Proof. Since $\Gamma(S) \cong K_n + \{uz\}$ and $x, y \in V(K_n) \setminus \{z\}$, we have $xy = 0$ and so $ann_S(xy) = S$. since u is an end vertex adjacent to only z in $\Gamma(S)$ thus $ux \neq 0$ and $uy \neq 0$ so $u \notin ann_S(x) \cup ann_S(y)$ which follows that $ann_S(x) \cup ann_S(y) \neq ann_S(xy)$. Therefore x is adjacent to y in $AG(S)$. □

Lemma 13 *Suppose that $\Gamma(S)$ is a complete graph K_n with an end vertex u. Then the following statements hold.*

(i) If $Z(S) \neq S$, then $AG(S)$ is a connected graph and u is adjacent to z in $AG(S)$.

(ii) If $Z(S) = S$, then $AG(S)$ is a disconnected graph and z is an isolated vertex in $AG(S)$.

Proof. (i) Since $Z(S) \neq S$ by theorem 1, we have $\Gamma(S) \leq AG(S)$. Since $\Gamma(S)$ is a connected graph and z is adjacent to u in $\Gamma(S)$, we have $AG(S)$ is a connected graph and u is adjacent to z in $AG(S)$.

(ii) Since z is adjacent to all vertices in $\Gamma(S)$ and $Z(S) = S$ by theorem 2, z is an isolated vertex in $AG(S)$ and so $AG(S)$ is a disconnected graph. □

Let $\Gamma(S) \cong K_n + \{uz\}$. By lemma 12 and lemma 13, to study the graph $AG(S)$, it is sufficient to examine the edges between u and x, for all $x \in V(K_n) \setminus \{z\}$.

Proposition 14 *Suppose that* $\Gamma(S)$ *is a complete graph* K_n *with an end vertex* u. *Also assume that* $u^2 = 0$ *and* $x, y \in V(K_n) \setminus \{z\}$. *Then* $ux = z$, $z^2 = 0$ *and* $x^2 = 0$ *or* $x^2 = z$.

Proof. Since u is not adjacent to x in $\Gamma(S)$, we have $ux \neq 0$. If $ux = u$, then $uy = (ux)y = u(xy) = 0$, which is impossible and so $ux \neq u$. Now let $ux = y$. We have $uy = u(ux) = u^2x = 0$ which is again impossible. Since $Z(S) = V(K_n) \cup \{0\} \cup \{u\}$, we have $ux = z$ and so $z^2 = (ux)z = u(xz) = 0$. Finally, since $ux = z$, we have $ux^2 = (ux)x = zx = 0$ and so $x^2 \in \text{ann}_S(u) = \{0, u, z\}$. If $x^2 = u$, then $uy = x^2y = x(xy) = 0$, which is impossible. Therefore $x^2 = 0$ or $x^2 = z$. □

Let $u^2 = 0$. The following lemma states which vertices of $V(K_n) \setminus \{z\}$ are connected to the end vertex u in $AG(S)$

Lemma 15 *Suppose that* $\Gamma(S)$ *is a complete graph* K_n *with an end vertex* u. *Also assume that* $u^2 = 0$ *and* $x, y \in V(K_n) \setminus \{z\}$. *Then the following statements hold.*

(i) u *is adjacent to* x *in* $AG(S)$ *if and only if* $x^2 = z$.

(ii) u *is not adjacent to* x *in* $AG(S)$ *if and only if* $x^2 = 0$.

Proof. (i) By proposition 14, we have $u^2 = z^2 = uz = 0$, $ux = z$ and $x^2 = 0$ or $x^2 = z$.

First suppose that $x^2 = z$. Then $x \notin \text{ann}_S(x)$. Since $ux = z$ so $x \notin \text{ann}_S(u)$ and since $zx = 0$, we have $x \in \text{ann}_S(z) = \text{ann}_S(ux)$. Thus $\text{ann}_S(x) \cup \text{ann}_S(u) \neq \text{ann}_S(ux)$. Therefore x is adjacent to u in $AG(S)$.

Conversely, assume that u is adjacent to x in $AG(S)$ and $x^2 = 0$. Then $\text{ann}_S(x) = V(K_n)$. Also $\text{ann}_S(u) = \{0, u, z\}$ hence $\text{ann}_S(x) \cup \text{ann}_S(u) = Z(S) = \text{ann}_S(z) = \text{ann}_S(ux)$. Thus u is not adjacent to x in $AG(S)$ which is impossible. Therefore $x^2 \neq 0$ and by proposition 14, $x^2 = z$.

(ii) It is clear. □

By the above lemma, we have the following theorem.

Theorem 16 *Suppose that* $\Gamma(S)$ *is a complete graph* K_n *with an end vertex* u *and* $u^2 = 0$. *Also assume that* $Z(S) \neq S$ *and* $V(K_n) = \{x_1, x_2, x_3, ., ., ., x_{n-1}, z\}$.

Then $AG(S) \cong K_{n+1} \setminus \{\{ux_1\},\{ux_2\},\{ux_3\},.,.,.,\{ux_m\}\}$ *if and only if for all* $0 \leq i \leq m$ *and* $m+1 \leq j \leq n-1$*, we have* ${x_i}^2 = 0$ *and* ${x_j}^2 = z$*.*

Proof. First suppose that $AG(S) \cong K_{n+1} \setminus \{\{ux_1\},\{ux_2\},\{ux_3\},.,.,.,\{ux_m\}\}$. Then for all $0 \leq i \leq m$, we have u is not adjacent to x_i in $AG(S)$ and for all $m+1 \leq j \leq n-1$, we have u is adjacent to x_j in $AG(S)$. By lemma 15, for all $0 \leq i \leq m$ and $m+1 \leq j \leq n-1$, we have ${x_i}^2 = 0$ and ${x_j}^2 = z$.

Conversely, Since $Z(S) \neq S$ by theorem 1, we have $\Gamma(S) \leq AG(S)$ and by lemma 15, for all $0 \leq i \leq m$ and $m+1 \leq j \leq n-1$, we have u is not adjacent to x_i in $AG(S)$ and u is adjacent to x_j in $AG(S)$. Therefore $AG(S) \cong K_{n+1} \setminus \{\{ux_1\},\{ux_2\},\{ux_3\},.,.,.,\{ux_m\}\}$. □

If $m = 0$ or $m = 1$ or $m = n-1$, we have the following corollary.

Corollary 17 *Suppose that* $\Gamma(S)$ *is a complete graph* K_n *with an end vertex* u *and* $u^2 = 0$*. Also assume that* $Z(S) \neq S$ *and* $V(K_n) = \{x_1, x_2, x_3, ., ., ., x_{n-1}, z\}$*. Then the following statements hold.*

(i) $AG(S) \cong K_{n+1}$ *if and only if for all* $1 \leq i \leq n-1$*, we have* ${x_i}^2 = z$*.*

(ii) $AG(S) \cong K_{n+1} \setminus \{\{ux_1\}\}$ *if and only if* ${x_1}^2 = 0$ *and for all* $2 \leq i \leq n-1$*, we have* ${x_i}^2 = z$*.*

(iii) $AG(S) \cong K_n + \{uz\}$ *if and only if for all* $1 \leq i \leq n-1$*, we have* ${x_i}^2 = 0$*.*

The next corollary follows from theorem 16.

Corollary 18 *Suppose that* $\Gamma(S)$ *is a complete graph* K_n *with an end vertex* u *and* $u^2 = 0$*. Also assume that* $V(K_n) = \{x_1, x_2, x_3, ., ., ., x_{n-1}, z\}$*. Then the following statements hold.*

(i) If $Z(S) \neq S$*, then* $AG(S)$ *can be one of the graphs:* K_{n+1} *or* $K_{n+1} \setminus \{\{ux_1\}\}$ *or* $K_{n+1} \setminus \{\{ux_1\},\{ux_2\}\}$ *or* $K_{n+1} \setminus \{\{ux_1\},\{ux_2\},\{ux_3\}\}$ *or ..... or* $K_{n+1} \setminus \{\{ux_1\},\{ux_2\},\{ux_3\},.,.,.,\{ux_{n-1}\}\} = K_n + \{uz\}$

(ii) If $Z(S) = S$*, then* $AG(S)$ *can be one of the graphs:* $K_1 \cup K_n$ *or* $K_1 \cup K_n \setminus \{\{ux_1\}\}$ *or* $K_1 \cup K_n \setminus \{\{ux_1\},\{ux_2\}\}$ *or* $K_1 \cup K_n \setminus \{\{ux_1\},\{ux_2\},\{ux_3\}\}$ *or .....or* $K_1 \cup K_n \setminus \{\{ux_1\},\{ux_2\},\{ux_3\},.,.,.,\{ux_{n-1}\}\} = 2K_1 \cup K_{n-1}$ *with* u *and* z *are two isolated vertices.*

Proof. If $Z(S) \neq S$, by theorem 1, then $\Gamma(S) \leq AG(S)$ and if $Z(S) = S$, by theorem 2, then z is an isolated vertex in $AG(S)$. Now by theorem 16, the results hold. □

Example 19 *Suppose that* $\Gamma(S)$ *is a complete graph* K_3 *with an end vertex* u *and* $u^2 = 0$. *Also assume that* $V(K_3) = \{x, y, z\}$. *Then* $xy = xz = yz = uz = 0$ *and we have* $ux = uy = z$ *and* $z^2 = 0$. *Moreover we have one of the following three statements.*

(i) $x^2 = 0$ *and* $y^2 = z$ *or* $x^2 = z$ *and* $y^2 = 0$. *In this case if* $Z(S) \neq S$, *by lemma 6, we have* $AG(S) \cong K_4 \setminus \{\{ux\}\}$ *or* $AG(S) \cong K_4 \setminus \{\{uy\}\}$ *and if* $Z(S) = S$, *by lemma 10, we have* $AG(S) \cong K_1 \cup K_3 \setminus \{\{ux\}\}$ *or* $AG(S) \cong K_1 \cup K_3 \setminus \{\{uy\}\}$.

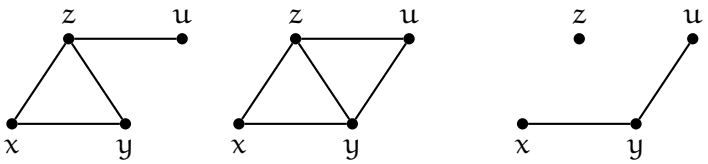

$\Gamma(S)$ $\quad$ $AG(S)$, $Z(S) \neq S$ $\quad$ $AG(Z(S))$

(ii) $x^2 = z$ *and* $y^2 = z$. *In this case if* $Z(S) \neq S$, *by lemma 7, we have* $AG(S) \cong K_4$ *and if* $Z(S) = S$, *by lemma 11, we have* $AG(S) \cong K_1 \cup K_3$.

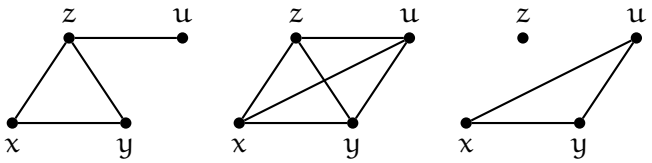

$\Gamma(S)$ $\quad$ $AG(S)$, $Z(S) \neq S$ $\quad$ $AG(Z(S))$

(iii) $x^2 = y^2 = 0$. *In this case if* $Z(S) \neq S$, *by lemma 8, we have* $AG(S) \cong K_4 \setminus \{\{ux\},\{uy\}\} = K_3 + \{uz\}$ *and if* $Z(S) = S$, *by lemma 9, we have* $AG(S) \cong 2K_1 \cup K_2$ *such that* u *and* z *are two isolated vertices in* $AG(S)$.

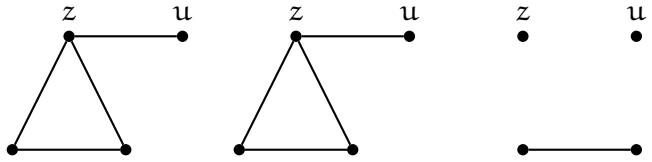

$\Gamma(S)$ $\quad$ $AG(S)$, $Z(S) \neq S$ $\quad$ $AG(Z(S))$

In the following we study the case of $u^2 = z$ and we show that u is adjacent to x, for all $x \in V(K_n) \setminus \{z\}$.

Proposition 20 *Suppose that* $\Gamma(S)$ *is a complete graph* K_n *with an end vertex* u. *Also assume that* $u^2 = z$ *and* $x, y \in V(K_n) \setminus \{z\}$. *Then* $ux = z$, $z^2 = 0$ *and* $x^2 = 0$ *or* $x^2 = z$.

Proof. Since $u^2 = z$, we have $z^2 = u^2z = u(uz) = u0 = 0$ and since u is not adjacent to x in $\Gamma(S)$, we have $ux \neq 0$. If $ux = u$, then $uy = (ux)y = u(xy) = 0$ and if for all $y \in V(K_n)\setminus\{z\}$, we have $ux = y$, then $uy = u(ux) = u^2x = zx = 0$ which are impossible. Thus $ux \notin \{0, u\} \cup V(K_n) \setminus \{z\}$. Therefore $ux = z$. Since $ux = z$, we have $ux^2 = (ux)x = zx = 0$ and so $x^2 \in \mathrm{ann}_S(u) = \{0, z\}$.

□

Lemma 21 *Suppose that* $\Gamma(S)$ *is a complete graph* K_n *with an end vertex* u. *Also assume that* $u^2 = z$ *and* $x \in V(K_n) \setminus \{z\}$. *Then* u *is adjacent to* x *in* $AG(S)$.

Proof. By proposition 20, we have $z^2 = uz = 0$, $ux = z$ and $x^2 = 0$ or $x^2 = z$. Since $z^2 = uz = 0$, we have $\mathrm{ann}_S(z) = Z(S)$. On the other hand, since $u^2 = z$ and $ux = z$, so $u \notin \mathrm{ann}_S(x) \cup \mathrm{ann}_S(u)$ which follows that $\mathrm{ann}_S(x) \cup \mathrm{ann}_S(u) \neq Z(S) = \mathrm{ann}_S(z) = \mathrm{ann}_S(ux)$. Therefore x is adjacent to u in $AG(S)$. □

By the above lemma, we have the following theorem.

Theorem 22 *Suppose that* $\Gamma(S)$ *is a complete graph* K_n *with an end vertex* u *and* $u^2 = z$. *Then the following two statements hold.*

(i) If $Z(S) \neq S$, *then* $AG(S) \cong K_{n+1}$.

(ii) If $Z(S) = S$, *then* $AG(S) \cong K_1 \cup K_n$.

Proof. (i) Since $Z(S) \neq S$ by theorem 1, we have $\Gamma(S) \leq AG(S)$. By lemma 21, for all $x \in V(K_n) \setminus \{z\}$, we have u is adjacent to x in $AG(S)$. Also by lemmas 12 and 13, for all $x, y \in V(K_n)$, we have x is adjacent to y in $AG(S)$. Therefore $AG(S) \cong K_{n+1}$.

(ii) Sincs $Z(S) = S$ by theorem 2, we have z is an isolated vertex in $AG(S)$. Now by lemmas 12, 13, 21, we have $AG(S) \cong K_1 \cup K_n$. □

Example 23 *Suppose that* $\Gamma(S)$ *is a complete graph* K_3 *with an end vertex* u *and* $u^2 = z$. *Also assume that* $V(K_3) = \{x, y, z\}$. *Then* $xy = xz = yz = uz = 0$ *and we have* $ux = uy = z$ *and* $z^2 = 0$. *Moreover we have one of the following three statements.*

(i) $x^2 = 0$ *and* $y^2 = z$ *or* $x^2 = z$ *and* $y^2 = 0$.

(ii) $x^2 = y^2 = z$.

(iii) $x^2 = y^2 = 0$.

In three cases if $Z(S) \neq S$, *by lemma 7, we have* $AG(S) \cong K_4$ *and if* $Z(S) = S$, *by ,lemma 11, we have* $AG(S) \cong K_1 \cup K_3$

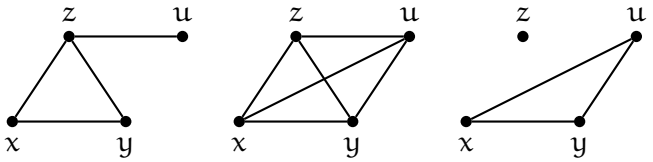

$\Gamma(S)$ $AG(S)$, $Z(S) \neq S$ $AG(Z(S))$

In the following we study the case of $u^2 = u$ and we show that there is at least one vertex $y \in V(K_n)$ such that u is not adjacent to y in $AG(S)$ and so in this case $AG(S)$ is not a complete graph.

Proposition 24 *Suppose that* $\Gamma(S)$ *is a complete graph* K_n *with an end vertex* u. *Also assume that* $u^2 = u$ *and* x, y *are two distincet vertices in* $V(K_n) \setminus \{z\}$. *Then* $z^2 = 0$ *or* $z^2 = z$. *and* $ux \in Z(S) \setminus \{0, z, u\} = V(K_n) \setminus \{z\}$. *Also we have the following two statements.*

(i) If $ux = x$, *then* $x^2 = 0$ *or* $x^2 = x$ *or* $x^2 = y$ *and* $uy = y$.

(ii) If $ux = y$, *then* $uy = y$ *and* $y^2 = 0$ *and also* $x^2 = 0$ *or* $x^2 = z$.

Proof. Since u is not adjacent to x in $\Gamma(S)$, we have $ux \neq 0$. If $ux = z$, then $z = ux = u^2x = u(ux) = uz = 0$ this is impossible and if $ux = u$, then $uy = (ux)y = u(xy) = 0$ which is again impossible. So $ux \notin \{0, z, u\}$ and thus $ux \in Z(S) \setminus \{0, z, u\} = V(K_n) \setminus \{z\}$.

(i) Also suppose that $ux = x$. Then $ux^2 = x^2$. If $x^2 = z$, then $z = uz = 0$ and if $x^2 = u$, then $uy = x^2y = x(xy) = 0$ which are impossible. So $x^2 \notin \{z, u\}$ and thus $x^2 \in Z(S) \setminus \{z, u\} = V(K_n) \setminus \{z\}$. Therefore $x^2 = 0$ or $x^2 = x$ or $x^2 = y$. Also if $x^2 = y$, then $uy = ux^2 = (ux)x = x^2 = y$.

(ii) Now assume that $ux = y$. Then $y^2 = (ux)y = u(xy) = 0$ and $uy = u(ux) = u^2x = ux = y$. Since $ux^2 = (ux)x = yx = 0$, we have $x^2 \in \mathrm{ann}_S(u) = \{0, z\}$ and thus $x^2 = 0$ or $x^2 = z$. □

Let $u^2 = u$. The following lemma states which vertices of $V(K_n) \setminus \{z\}$ are connected to the end vertex u in $AG(S)$.

Lemma 25 *Suppose that* $\Gamma(S)$ *is a complete graph* K_n *with an end vertex* u. *Also assume that* $u^2 = u$ *and* $x, y \in V(K_n) \setminus \{z\}$. *Then the following two statements hold.*

(i) u *is adjacent to* x *in* $AG(S)$ *if and only if* $ux = y$ *and* $x^2 = z$.

(ii) u *is not adjacent to* x *in* $AG(S)$ *if and only if* $ux = x$ *or* $ux = y$ *and* $x^2 = 0$. *Moreover if* $ux = y$, *then in both cases* $x^2 = z$, *and* $x^2 = 0$ *we have* u *is not adjacent to* y *in* $AG(S)$.

Proof.

(i) First suppose that u is adjacent to x in $AG(S)$. Then $ux \neq x$ and by proposition 24, $ux = y$ and $y^2 = 0$ and $x^2 = 0$ or $x^2 = z$. If $x^2 = 0$, then $\mathrm{ann}_S(x) \cup \mathrm{ann}_S(u) = V(K_n) \cup \{0, z\} = V(K_n) \cup \{0\} = \mathrm{ann}_S(y) = \mathrm{ann}_S(ux)$ and so u is not adjacent to x in $AG(S)$ this is impossible. Therefore $x^2 \neq 0$ and so $x^2 = z$.

Conversely, assum that $ux = y$ and $x^2 = z$. Then $x \notin \mathrm{ann}_S(x) \cup \mathrm{ann}_S(u)$ and $x \in \mathrm{ann}_S(y)$ and so u is adjacent to x in $AG(S)$.

(ii) First suppose that u is not adjacent to x in $\Gamma(S)$ and $ux \neq x$. Then by proposition 24, we have $ux = y$, $y^2 = 0$ and also $x^2 = 0$ or $x^2 = z$. If $x^2 = z$, then u is adjacent to x in $AG(S)$ this is impossible. Therefore $x^2 = 0$.

Conversely, if $ux = x$, then u is not adjacent to x in $AG(S)$. Now assume that $ux \neq x$. Then by proposition 24, we have $ux = y$, $y^2 = 0$ and since $x^2 = 0$, we have $\mathrm{ann}_S(x) = \mathrm{ann}_S(y) = \mathrm{ann}_S(ux)$ and so u is not adjacent to x in $AG(S)$.

Moreover if $ux = y$, then $uy = u(ux) = u^2x = ux = y$ and so u is not adjacent to y in $AG(S)$. □

By proposition 24, for all $x \in V(K_n) \setminus \{z\}$, we have $ux \in Z(S) \setminus \{0, z, u\} = V(K_n) \setminus \{z\}$ and $ux = x$ or there is $y \in V(K_n) \setminus \{z, x\}$ that $ux = y$ and $uy = y$. So u is not adjacent to x in $AG(S)$ or u is not adjacent to y in $AG(S)$. Therefore there is at least one vertex $x \in V(K_n) \setminus \{z\}$ that is not adjacent to u in $AG(S)$ and thus $AG(S)$ is not a commplete graph.

Corollary 26 *Suppose that* $\Gamma(S)$ *is a complete graph* K_n *with an end vertex* u. *Also assume that* $u^2 = u$. *Then* $AG(S)$ *is not a complete graph.*

Theorem 27 *Suppose that* $\Gamma(S)$ *is a complete graph* K_n *with an end vertex* u *and* $u^2 = u$. *Also assume that* $Z(S) \neq S$ *and* $V(K_n) = \{x_1, x_2, x_3, ., ., ., x_{n-1}, z\}$. *Then* $AG(S) \cong K_{n+1} \setminus \{\{ux_1\}, \{ux_2\}, \{ux_3\}, ., ., ., \{ux_m\}\}$ *if and only if for all* $1 \leq i \leq m$ *and* $m + 1 \leq j \leq n - 1$, *we have the following two statements.*

(i) either $ux_i = x_i$ *or* $ux_i = x_t$ *and* $1 \leq t \leq m$ *also* ${x_i}^2 = 0$.

(ii) $ux_j = x_i$ *and* ${x_j}^2 = z$

Proof. (i) First suppose that $AG(S) \cong K_{n+1} \setminus \{\{ux_1\}, \{ux_2\}, \{ux_3\}, ., ., ., \{ux_m\}\}$. Then u is not adjacent to x_i in $AG(S)$ and by lemma 25 for all $1 \leq i \leq m$, we have $ux_i = x_i$ or $ux_i = x_t$ and ${x_i}^2 = 0$. Moreover if $ux_i = x_t$, then $ux_t = x_t$ and so u is not adjacent to x_t in $AG(S)$. Thus $1 \leq t \leq m$.

(ii)Since u is adjacent to x_j in $AG(S)$ by lemma 25 for all $m+1 \leq j \leq n-1$, we have $ux_j = x_t$ and ${x_j}^2 = z$. Also if $ux_j = x_t$, then $ux_t = x_t$ and so u is not adjacent to x_t in $AG(S)$. Thus $1 \leq t \leq m$. Therefore $ux_j = x_i$.

Conversely, by lemma 25, if statement (i) holds, then for all $1 \leq i \leq m$, we have u is not adjacent to x_i in $AG(S)$ and if statement (ii) holds, then for all $m + 1 \leq j \leq n - 1$, we have u is adjacent to x_j in $AG(S)$ and so $AG(S) \cong K_{n+1} \setminus \{\{ux_1\}, \{ux_2\}, \{ux_3\}, ., ., ., \{ux_m\}\}$. □

In the above theorem, since $AG(S)$ is not a commplete graph so $m \neq 0$. If $m = 1$ or $m = n - 1$, then we have the following corollary.

Corollary 28 *Suppose that* $\Gamma(S)$ *is a complete graph* K_n *with an end vertex* u *and* $u^2 = u$. *Also assume that* $Z(S) \neq S$ *and* $V(K_n) = \{x_1, x_2, x_3, ., ., ., x_{n-1}, z\}$. *Then the following statements hold.*

(i) $AG(S) \cong K_{n+1} \setminus \{\{ux_1\}\}$ *if and only if* $ux_1 = x_1$ *and for all* $2 \leq i \leq n-1$, *we have* $ux_i = x_1$ *and* ${x_1}^2 = 0$ *and* ${x_i}^2 = z$.

(ii) $AG(S) \cong K_n + \{uz\}$ *if and only if for all* $1 \leq i, j \leq n - 1$, *we have if* $ux_i \neq x_i$, *then* $ux_i = x_j$ *and* ${x_i}^2 = {x_j}^2 = 0$.

The next corollary follows from theorem 27.

Corollary 29 *Suppose that* $\Gamma(S)$ *is a complete graph* K_n *with an end vertex* u *and* $u^2 = u$. *Also assume that* $V(K_n) = \{x_1, x_2, x_3, ., ., ., x_{n-1}, z\}$. *Then the following statements hold.*

(i) If $Z(S) \neq S$, *then* $AG(S)$ *can be one of the graphs:* $K_{n+1} \setminus \{\{ux_1\}\}$ *or* $K_{n+1} \setminus \{\{ux_1\}, \{ux_2\}\}$ *or* $K_{n+1} \setminus \{\{ux_1\}, \{ux_2\}, \{ux_3\}\}$ *or,..... ,or* $K_{n+1} \setminus \{\{ux_1\}, \{ux_2\}, \{ux_3\}, ., ., ., \{ux_{n-1}\}\}$.

(ii) If $Z(S) = S$, *then* $AG(S)$ *can be one of the graphs:* $K_1 \cup K_n \setminus \{\{ux_1\}\}$ *or* $K_1 \cup K_n \setminus \{\{ux_1\}, \{ux_2\}\}$ *or* $K_1 \cup K_n \setminus \{\{ux_1\}, \{ux_2\}, \{ux_3\}\}$ *or,.....,or* $K_1 \cup K_n \setminus \{\{ux_1\}, \{ux_2\}, \{ux_3\}, ., ., ., \{ux_{n-1}\}\} = 2K_1 \cup K_{n-1}$ *with* u *and* z *are two isolated vertices.*

Proof. By corollary 26, $AG(S)$ is not a complete graph. If $Z(S) \neq S$ by theorem 1, we have $\Gamma(S) \leq AG(S)$ and if $Z(S) = S$ by theorem 2, we have z is an isolated vertex in $AG(S)$. Now by theorem 27, the results hold. □

Example 30 *Suppose that* $\Gamma(S)$ *is a complete graph* K_3 *with an end vertex* u *and* $u^2 = u$. *Also assume that* $V(K_3) = \{x, y, z\}$. *Then* $xy = xz = yz = uz = 0$ *and* $z^2 = 0$ *or* $z^2 = z$. *Moreover we have one of the following three statements.*

(i) $ux = y = uy$, $x^2 = z$, $y^2 = z^2 = 0$ *or* $ux = x = uy$, $y^2 = z$ *and* $x^2 = z^2 = 0$,. *In this case if* $Z(S) \neq S$, *by lemma 6, we have* $AG(S) \cong K_4 \setminus \{\{uy\}\}$ *or* $AG(S) \cong K_4 \setminus \{\{ux\}\}$ *and if* $Z(S) = S$, *by lemma 10, we have* $AG(S) \cong K_1 \cup K_3 \setminus \{\{uy\}\}$ *or* $AG(S) \cong K_1 \cup K_3 \setminus \{\{ux\}\}$.

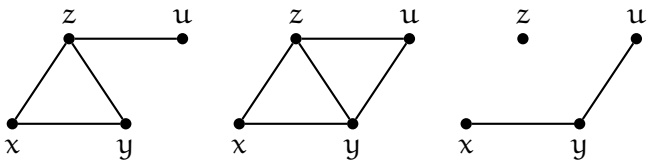

(ii) $z^2 \in \{0, z\}$ *and* $ux = y = uy$, $x^2 = y^2 = 0$, *or* $ux = x = uy$, $x^2 = y^2 = 0$ *or* $ux = y$, $uy = x$, $x^2 = y^2 = 0$. *In this case if* $Z(S) \neq S$, *by lemma 8, we have* $AG(S) \cong K_4 \setminus \{\{ux\}, \{uy\}\} = K_3 + \{uz\}$ *and if* $Z(S) = S$, *by lemma 9, we have* $AG(S) \cong 2K_1 \cup K_2$ *such that* u *and* z *are two isolated vertices in* $AG(S)$.

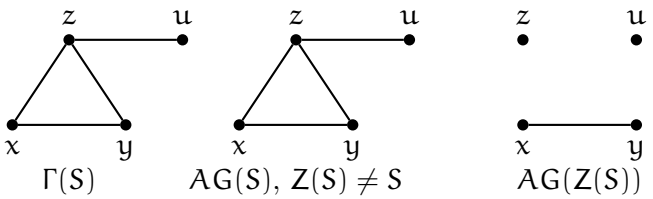

(iii) $z^2 \in \{0, z\}$ *and* $ux = x$, $uy = y$ *and we have the following six cases.*

(1) $y^2 = 0$, *and* $x^2 \in \{0, x, y\}$.

(2) $y^2 = y$,*and* $x^2 \in \{0, x\}$.

(3) $y^2 = x$, *and* $x^2 = 0$.

In this case if $Z(S) \neq S$*, by lemma 8, we have* $AG(S) \cong K_4 \setminus \{\{ux\}, \{uy\}\} = K_3 + \{uz\}$ *and if* $Z(S) = S$*, by lemma 9, we have* $AG(S) \cong 2K_1 \cup K_2$ *such that* u *and* z *are two isolated vertices in* $AG(S)$*.*

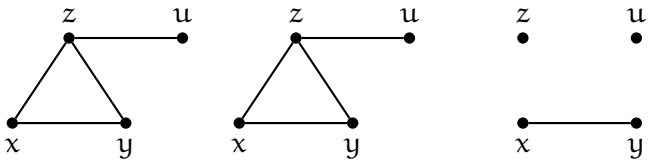

$\Gamma(S)$ $\quad$ $AG(S)$, $Z(S) \neq S$ $\quad$ $AG(Z(S))$

Finally, we study the case of $u^2 \notin \{0, z, u\}$ and so $u^2 = b \in V(K_n) \setminus \{z\}$. we show that u is adjacent to all vertices $y \in V(K_n) \setminus \{z, b\}$ in $AG(S)$ and u is adjacent to b in $AG(S)$ if and only if $ub \neq b$.

Proposition 31 *Suppose that* $\Gamma(S)$ *is a complete graph* K_n *with an end vertex* u*. Also assume that* $u^2 = b \notin \{0, z, u\}$*. Then* $u^2 = b \in V(K_n) \setminus \{z\}$ *and we have the following two statements.*

(i) For all $x \in Z(S) \setminus \{0, z, u, b\}$*, we have* $ux = z$*,* $z^2 = 0$ *and* $x^2 = 0$ *or* $x^2 = z$*.*

(ii) $ub = b$ *and* $b^2 = b$*, or* $ub = z$ *and* $b^2 = 0$ *or* $ub = y \in Z(S) \setminus \{0, z, u, b\}$ *and* $b^2 = z$*,* $y^2 = 0$*.*

Proof. (i) Suppose that $u^2 = b$. For all $x \in Z(S) \setminus \{0, z, u, b\}$, since u is not adjacent to x in $\Gamma(S)$, we have $ux \neq 0$. If $ux = u$, then $ub = (ux)b = u(xb) = 0$ which is impossible. For all $y \in V(K_n) \setminus \{z\}$, if $ux = y$, then $uy = u(ux) = u^2x = bx = 0$ which is again impossible and so $ux \notin \{0, u\} \cup V(K_n) \setminus \{z\}$. Therefore $ux = z$ and $z^2 = (ux)z = u(xz) = 0$.

Since $ux = z$, we have $ux^2 = (ux)x = zx = 0$ and so $x^2 \in \mathrm{ann}_S(u) = \{0, u\}$. Therefore $x^2 = 0$ or $x^2 = z$.

(ii) Clearly $ub \neq 0$ and $ub \neq u$ so $ub \in V(K_n)$ and thus $ub = b$ or $ub = z$ or $ub = y \in V(K_n) \setminus \{z, b\}$. Since $u^2 = b$, if $ub = b$, then $u^3 = uu^2 = ub = b = u^2$ and so $u^4 = u^3 = u^2$. Thus $b^2 = u^4 = u^3 = u^2 = b$ and if $ub = z$ we have $b^2 = bb = u^2b = u(ub) = uz = 0$.

Now assume that $ub = y \in Z(S) \setminus \{0, z, u, b\}$. Then $y^2 = (ub)y = u(by) = 0$. Since $uy = z$, we have $b^2 = bb = u^2b = u(ub) = uy = z$. □

Lemma 32 *Suppose that* $\Gamma(S)$ *is a complete graph* K_n *with an end vertex* u*. Also assume that* $u^2 = b \in V(K_n) \setminus \{z\}$ *and* $x \in V(K_n) \setminus \{z, b\}$*. Then* u *is*

adjacent to x *in* $AG(S)$. *Moreover* u *is adjacent to* b *in* $AG(S)$ *if and only if* $ub \neq b$.

Proof. By proposition 31, For all $x \in V(K_n) \setminus \{z, b\}$, we have $ux = z$. Since $u^2 = b$ so $u \notin ann_S(x) \cup ann_S(u)$ and $u \in ann_S(z) = ann_S(ux)$. Thus u is adjacent to x in $AG(S)$.

Moreover if u is adjacent to b in $AG(S)$, then $ub \neq b$.

Conversely assume that $ub \neq b$. By proposition 31, we have $ub = z$ and $b^2 = 0$ or $ub = y \in Z(S) \setminus \{0, z, u, b\}$ and $b^2 = z$, $y^2 = 0$.

If $ub = z$ and $b^2 = 0$, then $u \notin ann_S(b) \cup ann_S(u)$ and $u \in ann_S(z) = ann_S(ub)$. Thus u is adjacent to b in $AG(S)$. Also if $ub = y \in Z(S) \setminus \{0, z, u, b\}$ and $b^2 = z$, $y^2 = 0$, then $b \notin ann_S(b) \cup ann_S(u)$ and $b \in ann_S(y) = ann_S(ub)$. Therefore u is adjacent to b in $AG(S)$. □

Corollary 33 *Suppose that* $\Gamma(S)$ *is a complete graph* K_n *with an end vertex* u. *Also assume that* $u^2 = b \in V(K_n) \setminus \{z\}$ *and* $Z(S) \neq S$. *Then* $AG(S)$ *is not a commplete graph if and only if* $ub = b$.

Theorem 34 *Suppose that* $\Gamma(S)$ *is a complete graph* K_n *with an end vertex* u *and* $u^2 = b \in V(K_n) \setminus \{z\}$. *Then the following statements hold.*

(i) If $Z(S) \neq S$, *then we have two cases.*

(1) $AG(S) \cong K_{n+1}$ *if and only if* $ub \neq b$.

(2) $AG(S) \cong K_{n+1} \setminus \{\{ub\}\}$ *if and only if* $ub = b$.

(ii) If $Z(S) = S$, *then we have two cases.*

(1) $AG(S) \cong K_1 \cup K_n$ *if and only if* $ub \neq b$.

(2) $AG(S) \cong K_1 \cup K_n \setminus \{\{ub\}\}$ *if and only if* $ub = b$.

Proof. If $Z(S) \neq S$, then $\Gamma(S) \leq AG(S)$. By lemma 32, for all $x \in V(K_n) \setminus \{z, b\}$, we have u is adjacent to x in $AG(S)$ and u is adjacent to b in $AG(S)$ if and only if $ub \neq b$. Thus the statement (i) holds.

(ii) Since $Z(S) = S$, we have z is an isolated vertex in $AG(S)$. Now by lemma 32, the results hold. □

Example 35 *Suppose that* $\Gamma(S)$ *is a complete graph* K_3 *with an end vertex* u *and* $u^2 = x$ *or* $u^2 = y$. *Also assume that* $V(K_3) = \{x, y, z\}$. *Then* $xy = xz = yz = uz = 0$ *and* $z^2 = 0$. *Moreover we have one of the following two statements.*

(i) $ux = z$, $uy = y$, $u^2 = y^2 = y$, *and* $x^2 = 0$ *or* $x^2 = z$ *or* $uy = z$, $ux = x$, $u^2 = x^2 = x$, *and* $y^2 = 0$ *or* $y^2 = z$. *In this case if* $Z(S) \neq S$, *by lemma 6, we have* $AG(S) \cong K_4 \setminus \{\{uy\}\}$ *or* $AG(S) \cong K_4 \setminus \{\{ux\}\}$ *and if* $Z(S) = S$, *by lemma 10, we have* $AG(S) \cong K_1 \cup K_3 \setminus \{\{uy\}\}$ *or* $AG(S) \cong K_1 \cup K_3 \setminus \{\{ux\}\}$.

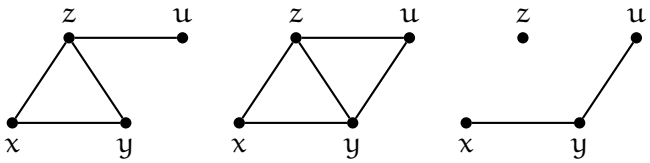

$\Gamma(S)$ $AG(S)$, $Z(S) \neq S$ $AG(Z(S))$

(ii) Also we have the following four cases.

(1) $ux = y$, $uy = z$, $u^2 = x$, *and* $x^2 = y^2 = 0$.
(2) $ux = z$, $uy = x$, $u^2 = y$, *and* $x^2 = 0$, $y^2 = z$.
(3) $ux = uy = z$, $u^2 = y$, $y^2 = 0$ *and* $x^2 = 0$ *or* $x^2 = z$.
(4) $ux = uy = z$, $u^2 = x$, $x^2 = 0$ *and* $y^2 = 0$ *or* $y^2 = z$.

In this case if $Z(S) \neq S$, *by lemma 7, we have* $AG(S) \cong K_4$ *and if* $Z(S) = S$, *by lemma 11, we have* $AG(S) \cong K_1 \cup K_3$ *such that* u *is an isolated vertex in* $AG(S)$.

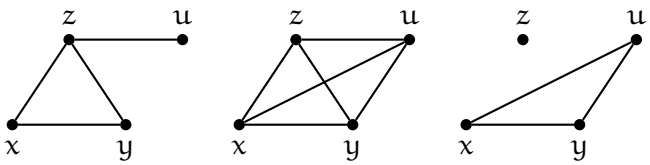

$\Gamma(S)$ $AG(S)$, $Z(S) \neq S$ $AG(Z(S))$

Acknowledgements

The authors are deeply grateful to the referees for careful reading of the manuscript and helpful suggestions.

References

[1] M. Afkhami, K. Khashyarmanesh, M. Sakhdari, On the annihilator graphs of semigroups, *J. Algebra and its Appl.* **1**4 (2015) 1550015 – 1550029. ⇒120, 121, 123

[2] M. Afkhami, K. Khashyarmanesh, M. Sakhdari, Annihilator graphs with four vertices, *Semigroup Forum.* **9**4 (2017) 139 – 166. ⇒120, 121, 122, 123
[3] M. Afkhami, K. Khashyarmanesh, M. Sakhdari, Annihilator graph of a commutative semigroup whose zero-divisor graph is a refinement of a star graph, *Quasigroups and Related Systems.* **2**9 (2021) 157–170. ⇒120
[4] J. A. Bondy and U. S. R. Murty, *Graph Theory with Applications,* American Elsevier, New York, 1976. ⇒121
[5] F. DeMeyer, L. DeMeyer, Zero-divisor graphs of semigroups, *J. Algebra.* **2**83 (2005) 190–198. ⇒120
[6] L. DeMeyer, M. Dsa, I. Epstein, A. Geiser and K. Smith, Semigroups and the zero-divisor graph, *Bull. Inst. Comb. Appl.* **5**7 (2009) 60–70. ⇒120
[7] F. DeMeyer, T. Mckenzie, K. Schneider, The zero-divisor graph of a commutative semigroup, *Semigroup Forum.* **6**5 (2002) 206–214. ⇒120
[8] T. Wu, D. Lu, Subsemigroups determined by the zero-divisor graph, *Discrete Math.* **3**08 (2008) 5122–5135. ⇒120
[9] T. Wu, F. Cheng, The structure of zero-divisor semigroups with graph $\mathsf{K}_n \circ \mathsf{K}_2$, *Semigroup Forum.* **7**6 (2008) 330–340. ⇒120
[10] T. Wu, Q. Liu, L. Chen, Zero-divisor semigroups and refinements of a star graph, *Discrete Math.* **3**09 (2009) 2510–2518. ⇒120

Received: June 6, 2022 • Revised: July 12, 2022

Acta Univ. Sapientiae Informatica **14,** 1 (2022) 137–154

DOI: 10.2478/ausi-2022-0009

Some properties of the closed global shadow graphs and their zero forcing number

M. R. RAKSHA
Department of Mathematics
CHRIST (Deemed to be University)
Bangalore-560029, INDIA.
email:
raksha.mr@res.christuniversity.in

Charles DOMINIC
Department of Mathematics
CHRIST (Deemed to be University)
Bangalore-560029, INDIA.
email:
charles.dominic@christuniversity.in

Abstract. Zero forcing is one of the dynamic vertex coloring problem. Zero forcing number is the minimum cardinality of the zero forcing sets. This parameter is the upper bound for the maximum nullity. A new class of graph where the maximum nullity is equal to the zero forcing number of the graph is defined as closed global shadow graph. Basic properties and zero forcing number of this graph class is analysed.

1 Introduction

All graphs considered in this article are finite, undirected and simple. A graph is a pair $G = (V, E)$. The set V or $V(G)$ is called the vertex set and E or $E(G)$ is called the edge set. $E(G) = \{(u, v) \mid u, v \in V(G) \text{ and } u \neq v\}$. Two vertices are said to be adjacent to each other if there exists an edge between them. If u and v are adjacent vertices in G then we represent this as $u \sim v$.

Computing Classification System 1998: G.2.2
Mathematics Subject Classification 2010: 05C07, 05C38, 05C50, 05C69
Key words and phrases: zero forcing number, zero forcing set, closed global shadow graph, open global shadow graph

A vertex is said to be a neighbour of other if they are adjacent to each other. Open neighbourhood of an arbitrary vertex v in the graph G is the set $N(v)$ containing all the vertices that are adjacent to v. Closed neighbourhood of an arbitrary vertex v is the set $N[v]$ containing the vertices in the open neighbour set $N(v)$ and the vertex v. Degree of the vertex v in the graph G is the number of edges incident to v. The minimum degree among the vertices of a graph G is represented by $\delta(G)$ and the maximum degree among the vertices of a graph G is represented by $\Delta(G)$.

A shadow graph of G is obtained by taking a graph and a copy of it say G and G'. Then making all the neighbouring vertices of u' in G' adjacent to the vertex u in G [17]. Motivated by the definition of shadow graphs the concept of open global shadow graphs were introduced in [14]. In this paper, we introduce a class of graphs which is closely related to the open global shadow graph and is known as the closed global shadow graph. Let G be a graph and G' be a copy of G such that $V(G) = \{v_1, v_2, \ldots, v_n\}$ and $V(G') = \{v_1', v_2', \ldots, v_n'\}$. The closed global shadow graph denoted by $GS[G]$ is obtained by taking two copies of G say, G and G' and joining the vertex v_i to each of the vertex in $\{V(G') \setminus N(v_i')\}$, where $1 \leq i \leq n$.

The closed global shadow graph of the cycle C_5 is depicted in the figure 1. It is evident that C_5 is a graph having vertex set $\{v_1, v_2, \ldots, v_5\}$ and the copy of the graph C_5 that is C_5' has the vertex set $\{v_1', v_2', \ldots, v_5'\}$. The vertex $v_i \in V(C_5)$ is adjacent to each of the vertex in $\{C_5' \setminus N(v_i')\}$, where i takes value between 1 to 5.

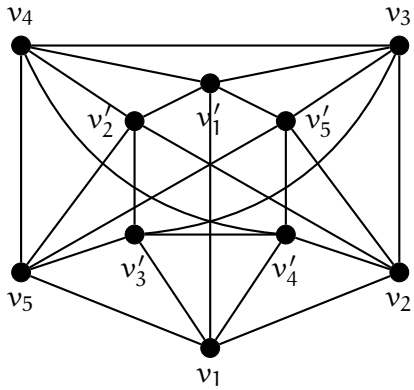

Figure 1: Closed global shadow graph of C_5: $GS[C_5]$

We use the following definitions for the further development of this article.

- Zero forcing set $S \subseteq V(G)$, is a set of black vertices which forces the entire graph black based on the following color change rule.
- Color change rule: A black vertex can force at most one white vertex black, provided it is the only white neighbour of it.
- The derived coloring of a graph G is the result of applying the color-change rule until no more changes are possible.
- Zero forcing number is a minimization problem. The zero forcing number of a graph is the minimum cardinality of the zero forcing set.
- For n number of vertices, the total number of maximum possible edges are $\frac{n(n-1)}{2}$. Let G be a graph, and let u, v be any two vertices which are not adjacent in G. Then we call uv as the missing edge in G.

For basic definitions related to graphs we refer to [18]. The zero forcing was initially introduced independently by AIM work group to bound the minimum rank [1]. Burgarth and Giovannetti introduced the zero forcing to understand the controlability of quantum system [6]. Zero forcing number of different type of graphs are studied in [8, 9, 13, 11]. Since the introduction of zero forcing it has been used in many areas like physics, disease and information spreading model in social network,logic circuit, coding theory and power network monitoring [4, 6, 7, 19, 12, 16].

The following section is intended to discuss about some basic properties of the closed global shadow graph of a given graph G.

2 Results on the closed global shadow graph of a graph

The closed global shadow graph is obtained by taking two copies of the given graph G with n vertices each. Therefore the following observation is obvious.

Observation 1 *Let G be a simple graph of order n. Then the total number of vertices in a closed global shadow graph is twice the number of vertices of the graph G.*

The next theorem gives the total number of edges of the closed global shadow graph of the given graph G with t number edges.

Theorem 2 *Let G be a simple graph of order n. Then $|E(GS[G])| = n^2$.*

Proof. Let t be the total edges present in G, and since G' is a copy of G $|E(G')| = t$. However, the total possible edges for an n vertex simple graph is

$\frac{n(n-1)}{2}$. Let v be a vertex in G and v' be its corresponding vertex in G'. By the definition of closed global shadow graph we know that each vertex v in G is adjacent to the corresponding vertex of its non-neighbours and the vertex v'. Similarly each vertex u' in G' is adjacent to the corresponding vertex of its non-neighbours and the vertex u'.

$$|E(GS[G])| = t + t + n + 2(\frac{n(n-1)}{2} - t) = n(n-1) + n = n^2$$

□

Theorem 3 *Let* G *be a simple graph of order* n*. Then the closed global shadow graph of* G*,* $GS[G]$ *is a connected* n *regular graph.*

Proof. To prove that $GS[G]$ **is a connected graph:** Let G be a connected graph. The graph $GS[G]$ will have the graph G and copy of G that is G' and the edges connecting each vertex in G to its corresponding vertices in G'. since G and G' are connected, the closed global shadow graph $GS[G]$ is connected.

Let G be a disconnected graph. Let u and v be the vertices in two different components of G. Clearly v is not adjacent to u in G, then v is made adjacent to u' and u is made adjacent to v' in $GS[G]$. Hence for each missing edge uv in G, there exists a path u, u', v or v, v', u between u, v in $GS[G]$. Due to which $GS[G]$ cannot be disconnected.

To prove that $GS[G]$ **is an** n **regular graph:** By the definition of closed global shadow graph each of the vertices v will be adjacent to $N(v)$ and the corresponding vertices of $V(G) \setminus N(v)$ that is $V(G') \setminus N(v')$. Which make the total degree of v as n. Similarly each vertex u' will be adjacent to $N(u')$ and the corresponding vertices of $V(G') \setminus N(u')$ that is $V(G) \setminus N(u)$. Making the total degree of u' as n. Therefore it is clear that in $GS[G]$, degree of each of the vertices is n. Hence $GS[G]$ is an n-regular graph. □

Theorem 4 *Let* G *be a simple graph of order* $n > 1$*. Then the closed global shadow graph of graph* G *has no cut edge or cut vertex.*

Proof. Case 1 Let us first prove that $GS[G]$ has no cut edge. On contrary let us assume that $GS[G]$ has a cut edge for $n > 1$.

Subcase 1.1 Assume that G has no cut edge. Clearly removal of any edge $E(G)$ or $E(G')$ cannot disconnected the graph $GS[G]$. According to the definition of closed global shadow graph, $GS[G]$ will have all the vertices in G

adjacent to their corresponding vertices in G'. Hence removal of any edge between $V(G)$ and $V(G')$ still keeps the graph $GS[G]$ connected. Therefore a contradiction.

Subcase 1.2 Assume that G has a cut edge let uv be the cut edge. Now removal of the edge uv from the graph G will lead to at least two disconnected components. In the graph $GS[G]$, the vertex u is adjacent to the vertex u', similarly the vertex v is adjacent to the vertex v'. Since there exists edge uv in $GS[G]$, u' and v' will also have an edge between them. Clearly removal of any edge uv will not disconnected the graph $GS[G]$. The only possibility for a cut edge to exists is in between G and G' but since all the vertices of G are adjacent to its corresponding vertices in G', the graph is connected even after the removal of the edge vv'. Hence a contradiction.

Case 2 Let us prove that $GS[G]$ has no cut vertex.

Subcase 2.1 Suppose G is a graph with no cut vertex. This implies that G' has no cut vertex. Clearly for each missing vertex in the graph G a pair of edges are added in $GS[G]$, hence the graph $GS[G]$ doesn't have cut vertex.

Subcase 2.2 Suppose G is a graph with a cut vertex. Let v be a cut vertex in G and K and H be the components of the graph $G - v$. Let K' and H' be the graphs corresponding to K and H respectively in $GS[G]$. Clearly in $GS[G]$ all the vertices in the component H will be adjacent to all the vertices in K' similarly all the vertices in the component K are made adjacent to all the vertices in H'. Therefore we cannot find any cut vertex. □

Theorem 5 *Every pair of vertices in a simple graph* G*, induces a cycle* C_4 *in* $GS[G]$ *with their corresponding vertices in* G'*.*

Proof. Let G be any simple graph, v and u be any two vertices in G. Then for v and u there are two possibilities that is $v \sim u$ or $v \nsim u$.

Case 1 Assume that v and u are adjacent in G ($v \sim u$). In the graph $GS[G]$, v is adjacent to v', u is adjacent to u'. Since G' is a copy of G, v' and u' are also adjacent in $GS[G]$. Therefore, the vertices v, v', u' and u forms a cycle C_4 in $GS[G]$.

Case 2 Assume that v and u are not adjacent in G ($v \nsim u$). Clearly by the definition of closed global shadow graph, v is adjacent to u' in $GS[G]$ as v and u are not adjacent in G. Similarly u is adjacent to v'. The vertices u, u' and v, v' are adjacent in $GS[G]$, since u' and v' are the vertices corresponding to u and v in $GS[G]$. Hence the vertices v, u', u and v' forms a cycle C_4 in $GS[G]$. □

Theorem 6 [15] *Subgraph of a bipartite graph is bipartite.*

Theorem 7 *Let* G *be a simple graph of order* n*. Then* $GS[G]$ *is a complete bipartite graph* $K_{n,n}$ *if and only if either* G *is a null graph of order* n *or* G *is a complete bipartite graph of order* n*.*

Proof. Let G be a null graph of order n. All the vertices of graph G forms an independent set. In the closed global shadow graph of G, $\forall\ v \in V(G)$, v is adjacent to all the vertices in $V(G')$ and $\forall\ u' \in V(G')$, the vertex u' is adjacent to all the vertices in the set $V(G)$. This makes the graph $GS[G]$ as a complete bipartite graph.

Let graph G is a complete bipartite graph $K_{p,q}$ such that $p + q = n$. Let P and Q be the partite sets having p and q number of vertices respectively. Clearly the subgraph induced by the vertices in set P and Q independently forms a null subgraphs. In the closed global shadow graph of the graph $K_{p,q}$, each of the vertices in the set P are adjacent to all the vertices in the set P'. Similarly each of the vertices in the set Q are adjacent to all the vertices in the set Q'. Where P' and Q' are the vertex set of the partite set of G'. Clearly the set P and Q' forms one of the partite set and the set Q and P' forms another partite set of the complete bipartite graph $K_{n,n}$.

To prove the converse part let us assume the contrary, suppose there is a graph G other than the null graph and complete bipartite graph for which $GS[G]$ forms a complete bipartite graph. It can be seen that the graph G is a subgraph of the graph $GS[G]$ with $V(G)$ as the vertex set. The theorem 6 shows that the subgraph induced by a complete bipartite graph is either a null graph or complete bipartite graph. Hence a contradiction. □

Definition 8 *A graph is said to be hamiltonian, if there exist a closed walk such that all the vertices are in the walk and an edge is visited only once.*

Theorem 9 [10] *If* G *is a simple graph of order* $n \geq 3$ *and the degree of every vertex in* G *is greater than or equal to* $\frac{n}{2}$*, then* G *is Hamiltonian.*

Theorem 10 *Every closed global shadow graph of a graph is Hamiltonian.*

Proof. Total number of vertices in the graph $GS[G]$ is $2n$, where n is the order of graph G. Further from theorem 3, $GS[G]$ is a n regular graph. Meaning every vertex in $GS[G]$ has a degree $d(v) = d(v') = n \geq \frac{2n}{2}$, $\forall v \in V(G)$ and $v' \in V(G')$. From dirac's theorem (theorem 9) it can be seen that $GS[G]$ is Hamiltonian. □

Definition 11 *A dominating set is a set of vertices* $D \in V(G)$ *such that a vertex not in the set* D *is adjacent to at least one vertex in the set* D.
The minimum cardinality among the dominating set is called the domination number and is denoted by $\gamma(G)$.

Definition 12 *If subgraph formed by the dominating set is connected, then such a set is called the connected dominating set.*
The minimum cardinality among the connected dominating set is called the connected domination number and is denoted by $\gamma_c G$.

Theorem 13 *Let* $GS[G]$ *be a simple graph of order n. Then the domination and connected domination number is respectively given by* $\gamma(GS[G]) = \gamma_c(GS[G]) = 2$.

Proof. Any two vertex v and v', ($v \in V(G)$ and $v' \in V(G')$) can dominate the entire graph. That is v can dominate $N(v)$ and $V(G') \setminus N(v')$. Similarly v' can dominated $N(v')$ and $V(G) \setminus N(v)$. Also it is clear that any one vertex in $GS[G]$ is not sufficient to force the entire graph $GS[G]$. Hence $\gamma(G) = 2$. Also the subgraph induced by v and v' are connected $\gamma(G) = \gamma_c(G) = 2$. □

Definition 14 *Matching in a graph is a set of edges such that no two edges in the set are incident to the same vertex.*
Perfect matching in a graph is a matching that matches all the vertices in the graph.

Theorem 15 *The closed global shadow graph has perfect matching.*

Proof. In the closed global shadow graph all the vertices are adjacent to their corresponding vertices. Hence each of the edge vv' ($\forall v \in V(G)$ and $\forall v' \in V(G')$) form a perfect matching. □

3 Zero forcing number of closed global shadow graph

In this section we find the zero forcing number of closed global shadow graph and give some upper bounds. Also we provide the relation between the chromatic number and zero forcing number of the closed global shadow graph.

Theorem 16 [5] *The zero forcing number of any graph* G *is given by* $Z(G) \geq \delta(G)$.

Theorem 17 *The zero forcing number of closed global shadow graph is bound by the order of graph* G, $Z(GS[G]) \geq n$.

Proof. From theorem 16 we know that $Z(G) \geq \delta$. It can be seen from theorem 3 that $\delta(GS[G]) = n$. Hence $Z(GS[G]) \geq n$. □

Theorem 18 [3] *The zero forcing number of a graph* G *of order* n *is bound by* Δ *as,* $Z(G) \leq \frac{\Delta}{\Delta+1}n$.

Theorem 19 *Let* G *be a simple graph of order* $n \geq 2$ *and* $GS[G]$ *be its closed global shadow graph of order* $2n$. *Then the zero forcing number of* $GS[G]$ *is given by* $2 \leq Z(GS[G]) \leq 2n-2$.

Proof. From theorem 17, $Z(GS[G]) \geq n$. When the order of G is 2, $Z(GS[G]) \geq 2$. On the other hand the upper bound can be found by using theorem 18.

$$Z(G) \leq \tfrac{\Delta}{\Delta+1}n$$

$$Z(GS[G]) \leq \tfrac{n}{n+1}2n$$

$$Z(GS[G]) \leq \tfrac{2n^2}{n+1}$$

The above equation can be factorised as

$$\tfrac{2n^2}{n+1} = 2n - 2 + \tfrac{2}{n+1}.$$

Since $n \geq 2$, $\frac{2}{n+1}$ is never a whole number. Hence $2 \leq Z(GS[G]) \leq 2n-2$. □

Theorem 20 *Let* G *be a simple graph with two connected components* K_m, K_n, *that is* G *is isomorphic to* $K_m \cup K_n$. *Then the zero forcing number* $Z(GS[G]) = m+n$.

Proof. From theorem 17 it is known that $Z(GS[G]) \geq m+n$. It is left to show that $Z(GS[G]) \leq m+n$. Let G be the graph with two components K_m and K_n as cliques. Similarly let G' be the graph with two components K'_m and K'_n as cliques. In $GS[G]$, all the vertices of K_m are adjacent to all the vertices of K'_n and all the vertices of K_n are adjacent to all the vertices in K'_m. By taking $V(K_m)$ and $V(K'_n)$ as the black vertices each vertex in K_m can force its corresponding vertex in K'_m. Similarly all vertices in K'_n can force its corresponding vertex in K_n as black. Thereby forcing the entire graph black. This implies that $Z(GS[G]) \leq m+n$. □

Theorem 21 *Let* G *be the complete graph* K_n *of order* $n \geq 2$*. Then* $Z(GS[G]) = n$*.*

Proof. If G is the complete graph, then closed global shadow graph of G, $GS[G]$ contains two copies of K_n and the corresponding vertices in each copy are adjacent. By taking all the n vertices of G in $GS[G]$ as black we can force the entire graph $GS[G]$ as black. Once all the n vertices of G are taken black, each black vertex is left with exactly one corresponding white vertex which can be forced black. Hence $Z(GS[G]) \leq n$. From theorem 17 we know that $Z(GS[G]) \geq n$. Hence the proof. □

Theorem 22 [13] *The zero forcing number of complete bipartite graph is given as* $Z(K_{m,n}) = n + m - 2$*.*

Theorem 23 *The zero forcing number* $Z(GS[G]) = 2n-2$ *if and only if* $GS[G]$ *is the complete bipartite graph* $K_{n,n}$*, where* n *is the number of vertices in* G*.*

Proof. If $GS[G]$ is a complete bipartite graph, then according to theorem 22 the zero forcing number, $Z(GS[G]) = n + n - 2 = 2n - 2$.

When $Z(GS[G]) = 2n - 2$, we need to show that the graph $GS[G]$ is the complete bipartite $K_{n,n}$. If there are just 2 vertices in G, it can be seen in figure 2 that $Z(GS[G]) = 2$ and both the graph are complete bipartite. Hence the theorem is true when $n = 2$.

For graph G with more than 2 vertices, let us assume that $Z(GS[G]) = 2n-2$ but $GS[G]$ is not a complete bipartite graph.

Claim *For a connected graph of order* $n \geq 2$*, the only bipartite closed global shadow graph of* G *is the complete bipartite graph.*

Proof of the Claim Assume that $GS[G]$ is a bipartite graph but not a complete bipartite graph. Since the subgraph of a bipartite graph is a bipartite graph, the graph G which is the subgraph of $GS[G]$ is also a bipartite graph. If G is a complete bipartite graph, then $GS[G]$ is also a complete bipartite graph from theorem 7, this is a contradiction.

Hence G is a bipartite graph but not a complete bipartite graph. If K and H are the two partite set of the graph G then there exist a vertex $v \in K$ and $u \in H$, such that $v \nsim u$. Let K' and H' be the partite set of G' and there exist a vertex $v' \in K'$ and $u' \in H'$ such that $v' \nsim u'$. Clearly in $GS[G]$, $v \sim u'$, $u \sim v'$. Since $v \sim v'$ and $u \sim u'$. The only possibility to divide these four vertices into two partite set is by taking G and G' as the two partite sets. However G and G' are not null graph. Hence a contradiction.

Now it is evident that $GS[G]$ is not a bipartite graph. Let v_i, v_j and v_k be three arbitrary vertices in $V(GS[G])$.

Case 1 If the vertex v_i is not adjacent to the vertex v_j, both the vertices v_i and v_j are adjacent to the vertex v_k. Clearly the induced graph formed by vertices $v_i, v_j, v_k, v_i', v_j'$ and v_k' forms a complete bipartite graph with v_i, v_j, v_k' in one partite set and v_i', v_j', v_k in other partite set. Since $GS[G]$ is not a complete bipartite graph, there exist v_t such that v_t is adjacent to v_i and not adjacent to v_j. Now by taking v_i as the initial black vertex along with $n-1$ of its neighbour v_i can force remaining one white neighbour black. From the above construction clearly v_t is adjacent to at least two black vertices (v_i and v_j') so clearly we need to choose at most $n-3$ of its neighbours to force the remaining white neighbour of v_t black. At this stage either the entire graph is forced black with at most $1+n-1+n-3 = 2n-3$ black vertices or the forcing process continues. If the forcing process continues, then there will be at least one more white vertex which gets forced hence there will be at most $2n-3$ black vertices, so the zero forcing number will be at most $2n-3$. Hence a contradiction.

Case 2 If the vertex v_i is not adjacent to the vertex v_j, the vertex v_i is adjacent to the vertex v_k and the vertex v_j is not adjacent to the vertex v_k. Now consider v_i and $n-1$ neighbours of v_i to be black, so that v_i can force the remaining one white neighbour of v_i black. From the construction v_k is adjacent to at least 2 black vertices v_i and v_j'. By taking at most $n-3$ of its neighbours black the remaining white neighbour of v_k can be forced. At this stage either the entire graph is forced black with at most $1+n-1+n-3 = 2n-3$ black vertices or the forcing process continues. If the forcing process continues there there will be at least one more white vertex which gets forced hence there will be at most $2n-3$ black vertices, so the zero forcing number will be at most $2n-3$. Hence a contradiction.

Case 3 If the vertex v_i is adjacent to the vertex v_j, both the vertices v_i and v_j are adjacent to the vertex v_k. Now consider v_i and $n-1$ neighbours of v_i to be black so that v_i can force the remaining one white vertex black. From the construction v_k is adjacent to at least 2 black vertices v_i and v_j. By taking at most $n-3$ of its neighbours black the remaining white neighbour of v_k can be forced. At this stage either the entire graph is forced black with at most $1+n-1+n-3 = 2n-3$ black vertices or the forcing process continues. If the forcing process continues there there will be at least one more white vertex which gets forced hence there will be at most $2n-3$ black vertices, so the zero forcing number will be at most $2n-3$. Hence a contradiction.

Case 4 If the vertex v_i is adjacent to the vertex v_j, both the vertices v_i and v_j are not adjacent to the vertex v_k. Clearly the induced graph formed by vertices $v_i, v_j, v_k, v_i', v_j'$ and v_k' forms a complete bipartite graph with the vertices v_i, v_j', v_k' in one partite set and the vertices v_i', v_j, v_k in other partite set. Since $GS[G]$ is not a complete bipartite graph, there exist the vertex v_t such that v_t is adjacent to v_i and not adjacent to v_j'. Now by taking v_i as the initial black vertex along with $n-1$ of its neighbour v_i can force remaining one white neighbour black. From the above construction clearly v_t is adjacent to at least two black vertices (v_i and v_j) so clearly we need to choose at most $n-3$ of its neighbours to force the remaining white neighbour of v_t. At this stage either the entire graph is forced black with at most $1+n-1+n-3 = 2n-3$ black vertices or the forcing process continues. If the forcing process continues there there will be at least one more white vertex which gets forced hence there will be at most $2n-3$ black vertices, so the zero forcing number will be at most $2n-3$. Hence a contradiction. □

Theorem 24 *If* G *is a path* P_n *where* $n > 2$*, then the zero forcing number of closed global shadow graph* $Z(GS[P_n]) = n+1$.

Proof. From theorem 17 we know that $Z(GS[G]) \geq n$. We need to show that n initially colored black vertices are not sufficient to force the whole graph black. Let G be a path P_n with vertex set $\{v_1, v_2, \ldots, v_n\}$. Without loss of generality let vertex v_1 and v_n be the two vertices in the graph P_n having degree one and remaining v_i, $2 \leq i \leq n-1$ be $n-2$ vertices in the graph P_n having degree 2.

Let G' be the path P_n' with vertex set $\{v_1', v_2', \ldots, v_n'\}$. Without loss of generality let v_1' and v_n' be two vertices in the graph P_n' having degree one and remaining v_j', $2 \leq j \leq n-1$ be $n-2$ vertices in the graph P_n' having degree 2.

Case 1 When a degree 1 vertex in P_n is taken initially black:

Let v_1 be the initially colored black vertex. In $GS[P_n]$, vertex v_1 is adjacent to v_2, v_1', v_j', where $3 \leq j \leq n$. That is $| N(v_1) | = n$, by taking $n-1$ of its neighbours to be initially black v_1 can force the remaining one white neighbour black. The forcing process stops as the black vertices v_1', v_j', where $3 \leq j \leq n$ have more than two white neighbours and vertex v_2 has exactly two white neighbours. Therefore it is not possible to force the entire graph black by taking a degree 1 vertex in P_n as initially black.

Case 2 When a degree 1 vertex in P_n' is taken initially black. Same as Case 1 is followed.

Case 3 When a degree 2 vertex in P_n is taken initially black:

Let v_2 be the initially colored black vertex. In $GS[P_n]$, v_2 is adjacent to v_1, v_3, v_2', v_j' where where $4 \leq j \leq n$. Totally v_2 has n neighbours, by taking

$n-1$ of its neighbour to be initially black v_2 can force the remaining one white neighbour black. The forcing process stops as v_1 has two white neighbours, v_3 has three white neighbour (in case when G is P_3, v_3 will have 2 white neighbours) and v_2', v_j', where $4 \leq j \leq n$ have two or more white neighbours. Therefore it is not possible to force the entire graph black by taking a degree 2 vertex in P_n as initially black.

Case 4 When a degree 2 vertex in P_n' is taken initially black. Same as Case 3 is followed.

Clearly from the above cases we can conclude that $Z(GS[G]) > n$. Now we are left to show that $Z(GS[G]) \leq n+1$.

Consider all the vertices in G' and one of the end vertex in G (v_1 or v_n) say v_1 to be black. Then v_1 can force v_2 black, v_2 can force v_3 black, ...this process continues till all the vertices are forced black. Hence $Z(GS[G]) \leq n+1$. □

In the above theorem when $n = 2$, that is when graph G is P_2. $GS[G]$ is a cycle C_4 and $Z(GS[G]) = Z(C_4) = 2$.

Theorem 25 *If G is a cycle C_n, then the zero forcing number of closed global shadow graph of C_n is*

$$Z(GS[G]) = \begin{cases} 3 & \text{if } n = 3 \\ 6 & \text{if } n = 5 \\ n+2 & \text{if } n = 4 \text{ and } n > 5 \end{cases}$$

.

Proof. Let the graph G be a cycle C_n with n number of vertices. When $n = 3$, C_3 is same as the complete graph K_3. Hence from theorem 21, 3 black vertices are enough to force the entire graph black. When $n = 4$, C_4 forms a complete bipartite graph according to theorem 7 and theorem 23 $Z(GS[C_4]) = 4+2 = 6$. When $n = 5$, let the graph $GS[C_5]$ have vertex set $V(GS[G]) = \{V(G), V(G')\}$ ($V(G) = \{v_1, v_2, v_3, v_4, v_5\}$ and $V(G') = \{v_1', v_2', v_3', v_4', v_5'\}$). By taking v_1 and 4 of its neighbours say v_2, v_5, v_3', v_4' as black v_1 can force v_1' black. Clearly, all the black vertices have 2 white neighbours. we know from theorem 17 $Z(GS[G]) \geq n$, but here with 5 black vertices it is not possible to force the entire graph black. By taking one more black vertex say v_5', then v_5' can force v_3 and v_3' can force v_2' and further v_3 can force v_4 black. There by forcing the entire graph black.

It is clear from the theorem 17 that $Z(GS[G]) \geq n$. Now we need to show that with $n+1$ black vertices it is not possible to force the entire graph black

when $n > 5$. On contrary let us assume that $n+1$ vertices are enough to force the whole graph $GS[G]$ black. Since G or G' is a regular graph(cycle C_n where $n \geq 6$), choosing any vertex as the initial black vertex makes no difference. Let v_1 be the initial black vertex. Now, v_1 is adjacent to n other vertices of $GS[G]$ (v_2, v_n, v'_1, v'_j where $3 \leq j \leq n-1$). By choosing any of the $n-1$ neighbours black the remaining white neighbour of v_1 can be forced black.

Clearly v_2 and v_n have three white neighbours (v'_2, v'_n and v_3 or v_{n-1} respectively). Hence we need to select at least two of them as black in order for v_2 or v_n to continue forcing, a contradiction.
v'_1 has $n-1$ black neighbours this implies that $n-2$ of its neighbours should be taken as black, contradiction.
Finally for the black vertices v'_j,$3 \leq j \leq n-1$ either $n-3$ or $n-5$ white vertices are left.
Case 1 If $n-3$ white vertices are left it is evident that $n-3 > 2$ for all $n \geq 6$. Hence the forcing process stops.
Case 2 If $n-5$ white vertices are left, then the following subcases follows

Subcase 2.1 When $n = 6$, $n-5$ is one hence this vertex v'_j (in particular v'_4) can force its only white neighbour (v_4) black. However at this stage the black vertex has two or more white neighbour. That is v_4 has v_3, v_5, v'_2 and v'_n as its white neighbours Hence the process stops.

Subcase 2.2 When $n = 7$, $n-5$ is two this vertex v'_j (in particular v'_4 or v'_5) having $n-5 = 7-5 = 2$ white vertex, can force one of the white neighbour black by taking the other white neighbour as initially black. Say v_4 and v_3 are the white neighbours of v'_4, by taking one of them black other vertex can be forced black. Now clearly any black vertices has either no white neighbour or two or more white neighbour. Hence the process stops.

Subcase 2.3 It can be observed that for $n > 7$, $n-5$ take values more than 2. Hence it becomes a contradiction to our assumptions.

Form the above cases we can conclude that we need at least $n+2$ initial black vertices in order to force the entire graph black.

In the graph $GS[G]$, by taking all the n vertex of G' to be black, the graph $GS[G]$ reduces to C_n. In other words by taking all the n vertices of G' to be black, the only white vertices left is from G. Hence by taking two out of n vertices in G whole graph $GS[G]$ can be forced black. This forcing process shows that $Z(GS[G]) \leq n+2$. □

Definition 26 *Join of two graphs* K *and* H *is the graph obtained by taking a copy of* K *and a copy of* H *and making each of the vertices in the graph* K *to be adjacent to each of the vertices in the graph* H. *The join of* K *and* H *is denoted by* $K+H$.

Theorem 27 *Let* G *be an* n *order simple graph and* G^1 *be the join of* G *and* K_1 *that is* $G^1 = G + K_1$. *Then* $Z(GS[G^1]) \geq Z(GS[G]) + 1$.

Proof. Let G be a graph of order n with vertex set $\{v_1, v_2, \ldots, v_n\}$. Let $Z(GS[G]) = z$ and the zero forcing set be S. Clearly G^1 is a graph of order $n+1$ such that v_{n+1} is adjacent to all the other n vertices. In $GS[G^1]$ all the vertices in S will be adjacent to either v_{n+1} or v'_{n+1}. That is degree of each of the vertices in $GS[G]$ is increased by one. $Z(GS[G^1])$ cannot be z as every vertex in the set S will have at least 2 white neighbours. Thereby increasing the zero forcing number of $GS[G^1]$, $Z(GS[G^1]) \geq Z(GS[G]) + 1$. □

Theorem 28 *Let* G *be a wheel graph* $W_{1,n}$. *Then the zero forcing number of closed global shadow graph of* $W_{1,n}$ *is*

$$Z(GS[G]) = \begin{cases} 4 & \text{if } n = 3 \\ n+3 & \text{if } n \geq 4. \end{cases}$$

Proof. Wheel graph $W_{1,n}$ is obtained by adding a central vertex to a cycle which is adjacent to all the other vertices of the graph C_n. When $n = 3$, the wheel graph is similar to that of a complete graph K_4 hence by theorem 21 the zero forcing number is 4. When $n \geq 4$, by taking all the vertices in the set $V(W_{1,n})$ and two of the vertices in the set $V(W'_{1,n})$ other than v'_{n+1} to be initially black, the graph $GS[W_{1,n}]$ can be completely forced black. Hence $Z(GS[G]) \leq n + 3$.
Clearly when $n = 4$ and $n > 5$, from the theorem 27, we know that

$$Z(GS[W_{1,n}]) \geq Z(GS[C_n]) + 1 = n + 2 + 1 = n + 3$$

For graph when $n = 5$, $Z(GS[W_{1,5}]) \geq Z(GS[C_5]) + 1 = 6 + 1 = 7$. But it can be shown that with 7 black vertices it is not sufficient to force the entire graph black. Let $v_1, v_2, \ldots, v_6$ be the vertices of the graph $W_{1,5}$ such that v_6 is the central vertex. In $GS[W_{1,5}]$, by taking v_1 and 5 of its neighbours black, the remaining one white neighbour of v_1 is forced black. Further the forcing stops as all the black vertices except v_1 that is $v'_1, v_2, v_5, v_6, v'_3, v'_4$ have three white neighbour. In order for any of $v'_1, v_2, v_5, v_6, v'_3$ or v'_4 vertices to force their neighbour, two of their neighbours must be taken initially black. There by forcing the entire graph black. It is clear that with 7 black vertices it is not possible to force the graph black. Hence $Z(GS[W_{1,5}]) = 8 = n + 3$. □

Theorem 29 *The zero forcing number* $Z(GS[G]) = 2$ *if and only if* G *is either* K_2 *or* $\overline{K}_2$.

Proof. If G is either K_2 or $\bar{K_2}$, then $GS[G]$ is cycle C_4.We know that the zero forcing number of cycle is 2. Hence $Z(GS[K_2]) = Z(GS[\bar{K_2}]) = Z(C_4) = 2$.

If $Z(GS[G]) = 2$, from theorem 17 it evident that $n = 1$ or 2. Clearly when $n = 1$, $GS[G]$ is P_2 implies $Z(GS[G]) = Z(P_2) = 1$. Hence G is either K_2 or $\bar{K_2}$. In both the cases $GS[G]$ is a cycle C_4 as shown in the figure 2. Hence $Z(GS[G]) = 2$. □

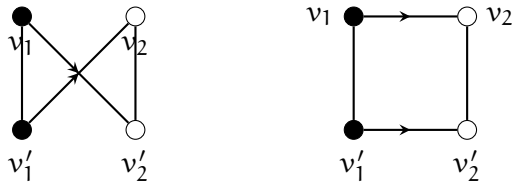

$G = 2K_1$, $Z(GS[G]) = 2$ | $G = K_2$ or P_2, $Z(GS[G]) = 2$

Figure 2: All the possible closed global shadow graph of graph when n=2.

Theorem 30 *The zero forcing number* $Z(GS[G]) = 3$ *if and only if* G *is either* K_3 *or* $\bar{P_3}$.

Proof. When G is K_3, from theorem 21 it can be concluded that $Z(GS[K_3]) = 3$. When G is $\bar{P_3}$, the forcing process is depicted in the figure 3 (since $Z(GS[G]) \geq n = 3$, 3 black vertices are enough to force the entire graph).
Let the zero forcing number of closed global shadow graph is $Z(GS[G]) = 3$, this implies that $n = 1, 2$ or 3 from theorem 3. But from theorem 29 there exist no graph when $n = 1, 2$ that has the zero forcing number of its closed global shadow graph to be 3. Hence $Z(GS[G]) = 3$ is possible only when $n = 3$. There are 4 possible graphs G when $n = 3$. null graph $\bar{K_3}$, complete graph K_3, $\bar{P_3}$ and path P_3. When G is complete graph K_3 and $\bar{P_3}$ it can be seen in figure 3 that $Z(GS[G]) = 3$. Where as when G is null graph from theorem 23 we known that $Z(GS[G]) = 2n - 2 = 2 * 3 - 2 = 4$ and when G is path P_3 it can be seen from the theorem 24 that $Z(GS[G]) = n + 1 = 3 + 1 = 4$. □

Theorem 31 [1] *If* G *is a Hamiltonian graph and* $M(G)$ *is the maximum nullity of graph* G*, then the zero forcing number is related to maximum nullity of the graph as* $Z(G) = M(G)$.

Theorem 32 *Let* G *be any simple graph of order n, then* $Z(GS[G]) = M(GS[G])$.

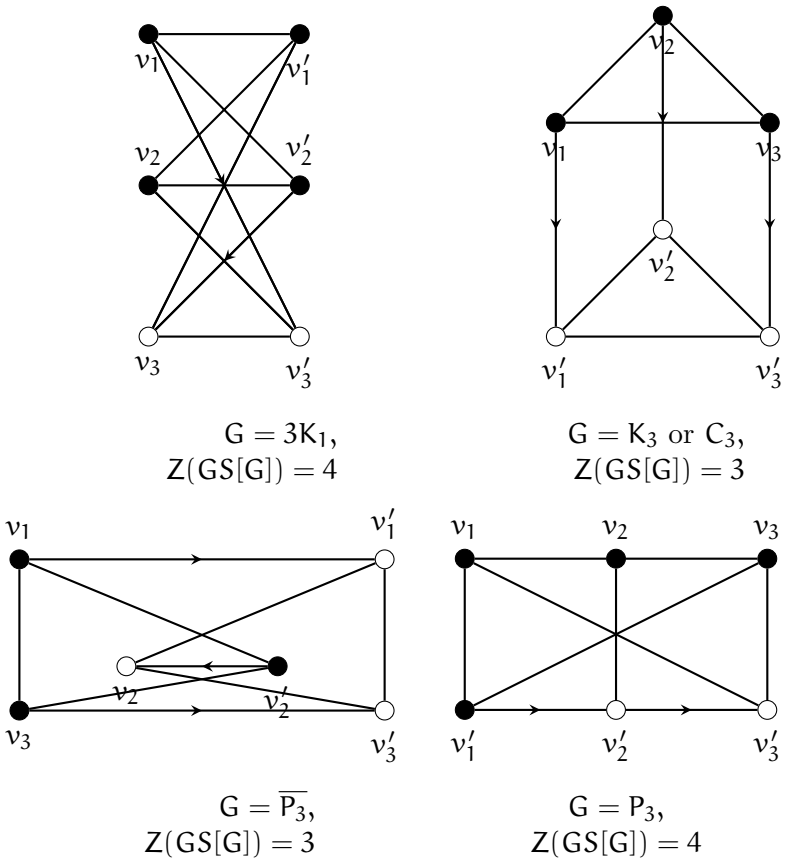

Figure 3: All the possible closed global shadow graph of graph when n=3.

Proof. It is proved in theorem 10 that closed global shadow graph is Hamiltonian. From the above theorem 31 we conclude that $Z(GS[G]) = M(GS[G])$. □

Theorem 33 [2] *Let* G *be any graph, then* $\chi(G) \leq Z(G) + 1$.

Theorem 34 (Brook's) *For any connected undirected graph* G*, the chromatic number of* G *that is* $\chi(G) \leq \Delta$*. Where* Δ *is the maximum degree of graph* G*. Provided* G *is not a complete graph or odd cycle.*

Theorem 35 *Let* G *be simple graph, then* $\chi(GS[G]) \leq n$.

Proof. The graph $GS[G]$ is always connected n-regular graph. $GS[G]$ can never form a complete graph or odd cycle. Hence according to brook's theorem $\chi(GS[G]) \leq n$. □

Theorem 36 *Let* G *be any graph, then* $\chi(GS[G]) < Z(GS[G]) + 1$.

Proof. The graph $GS[G]$ is n-regular graph and clearly $Z(GS[G]) \geq n$. According to theorem 35, $\chi(GS[G]) \leq n$. Therefore the theorem 33 can be rewritten as $\chi(GS[G]) < Z(GS[G]) + 1$. □

Theorem 37 *If* G *is a complete graph, then* $\chi(GS[G]) = Z(GS[G])$.

Proof. According to theorem 21, $Z(GS[G]) = n$ if G is a complete graph. From theorem 35, $\chi(GS[G]) \leq n$ is known. It is left to show that $\chi(GS[G]) \geq n$. G being a complete graph on n vertices is a subgraph of $GS[G]$ and $\chi(G) = n$. The chromatic number of $GS[G]$ will be at least that of its subgraph (G). Therefore $\chi(GS[G]) \geq n$. □

4 Conclusion

The natural and intrinsic characterisation of the closed global shadow graph is provided. This includes some of the characterisation like hamiltonicity, perfect matching, regularity, etc., The zero forcing number of various classes of closed global shadow graph are studied. In few cases, the necessary and sufficient condition for equality of certain zero forcing number is analysed. The closed global shadow graph $GS[G]$ has a subgraph graph $G\Box K_2$. It can be seen that $Z(GS[G]) = Z(G\Box K_2)$ when G is a complete graph K_n. It is an open problem to solve when the zero forcing number of $GS[G]$ becomes equal to the zero forcing number of $G\Box K_2$. The relation between chromatic number and zero forcing number of $GS[G]$ is understood. One may still find the characterisation for $\chi(GS[G])$ to be equal to $Z(GS[G])$.

Acknowledgement

We authors, thank the anonymous referees for their constructive comments and suggestions which helped in improving this article.

References

[1] AIM Minimum Rank–Special Graphs Work Group, Zero forcing sets and the minimum rank of graphs, *Linear Algebra and its Applications* **428**, 7 (2008) 1628–1648. ⇒139, 151

[2] F. Alinaghipour Taklimi, *Zero forcing sets for graphs*, PhD thesis, The University of Regina (2013). ⇒152

[3] D. Amos, Y. Caro, R. Davila, R. Pepper, Upper bounds on the k-forcing number of a graph, *Discrete Applied Mathematics*, **181**, (2015) 1–10. ⇒144
[4] F. Barioli, W. Barrett, S. M. Fallat, H. T. Hall, L. Hogben, B. Shader, P. van den Driessche, H. Van Der Holst, Parameters related to tree-width, zero forcing, and maximum nullity of a graph, *Journal of Graph Theory*, **72**, 2 (2013) 146–177. ⇒139
[5] A. Berman, S. Friedland, L. Hogben, U. G. Rothblum, B. Shader, An upper bound for the minimum rank of a graph, *Linear Algebra and its Applications*, **429**, 7 (2008) 1629–1638. ⇒143
[6] D. Burgarth, V. Giovannetti, Full control by locally induced, *Physical Review Letters*, **99**, 10 (2007) 100501. ⇒139
[7] D. Burgarth, V. Giovannetti, L. Hogben, S. Severini, M. Young, Logic circuits from zero forcing, *Natural computing* **14**, 3 (2015) 485–490. ⇒139
[8] B. Chacko, C. Dominic, K. Premodkumar,On the zero forcing number of graphs and their splitting graphs, *Algebra and Discrete Mathematics*, **28**, 1 (2009) 29–43. ⇒139
[9] R. Davila, M. A. Henning, ero forcing in claw-free cubic graphs, *Bulletin of the Malaysian Mathematical Sciences Society*, **43**, 1 (2020) 673–688. ⇒139
[10] G. A. Dirac, Some theorems on abstract graphs,Proceedings of the London Mathematical Society, **3**, 1 (1952) 69–81. ⇒142
[11] C. Dominic, Zero forcing number of degree splitting graphs and complete degree splitting graphs, Acta Universitatis Sapientiae Mathematica, **11**, 1 (2019) 40–53. ⇒139
[12] T. W. Haynes, S. M. Hedetniemi, S. T. Hedetniemi, M. A. Henning, Domination in graphs applied to electric power networks, SIAM Journal on Discrete Mathematics, **15**, 4 (2002) 519–529. ⇒139
[13] L. S. Mays, The Zero Forcing Number Of GraphsBipartite, (2013). ⇒139, 145
[14] M. R. Raksha, C. Dominic, Open global shadow graph and it's zero forcing number (2022) Communicated. ⇒138
[15] J. Salvatore, *Bipartite graphs and problem solving*, University of Chicago, 2007, pp. 8. ⇒141
[16] M. Trefois, J. C. Delvenne, Zero forcing number, constrained matchings and strong structural controllability, *Linear Algebra and its Applications*, **484**, 1 (2015) 199–218. ⇒139
[17] S. Vaidya, B. Lekha, New families of odd gracefull graphs *International Journal of Open Problems in Computer Science and ,Mathematics.* **3**, 5 (2010). ⇒138
[18] D. B. West, *Introduction to Graph Theory. vol 2.*, Prentice Hall, Upper Saddle River, 2001. ⇒139
[19] M. Zhao, L. Kang, G. J. Chang, Power domination in graphs, *Discrete Mathematics*, **306**, 15 (2006) 1812–1816. ⇒139

Received: March 14, 2022 • Revised: July 18, 2022

Acta Universitatis Sapientiae

The scientific journal of Sapientia Hungarian University of Transylvania publishes original papers and surveys in several areas of sciences written in English.
Information about each series can be found at
http://www.acta.sapientia.ro.

Acta Universitatis Sapientiae, Informatica

Each volume contains two issues.


Sapientia University


Sciendo by De Gruyter


Scientia Publishing House

ISSN 1844-6086

http://www.acta.sapientia.ro

Information for authors

Acta Universitatis Sapientiae, Informatica publishes original papers and surveys in various fields of Computer Science. All papers are peer-reviewed.

Papers published in current and previous volumes can be found in Portable Document Format (pdf) form at the address: http://www.acta.sapientia.ro.

The submitted papers should not be considered for publication by other journals. The corresponding author is responsible for obtaining the permission of coauthors and of the authorities of institutes, if needed, for publication, the Editorial Board is disclaiming any responsibility. Submission must be made by email (acta-inf@acta.sapientia.ro) only, using the LaTeX style and sample file at the address http://www.acta.sapientia.ro. Beside the LaTeX source a pdf format of the paper is necessary too.

Prepare your paper carefully, including keywords, ACM Computing Classification System codes (http://www.acm.org/about/class/1998) and AMS Mathematics Subject Classification codes (http://www.ams.org/msc/).

References should be listed alphabetically based on the Intructions for Authors given at the address http://www.acta.sapientia.ro.

Illustrations should be given in Encapsulated Postscript (eps) format.

Contact address and subscription:
Acta Universitatis Sapientiae, Informatica
RO 400112 Cluj-Napoca
Str. Matei Corvin nr. 4.
Email: acta-inf@acta.sapientia.ro

Printed by F&F INTERNATIONAL
Director: Enikő Ambrus

Supported by:

ISSN 1844-6086
http://www.acta.sapientia.ro